

THESIS

DETERMINING RAINFALL THRESHOLDS FOR LANDSLIDE INITIATION A CASE STUDY IN WADASLINTANG WATERSHED WONOSOBO, CENTRAL JAVA PROVINCE

Thesis submitted to The Graduate School, Faculty of Geography, Gadjah Mada University in partial fulfillment of the requirements for the degree of Master of Science in Geo-information for Spatial Planning and Risk Management

By:

EMBA TAMPANG ALLO

08/276579/PMU/5627

SUPERVISORS:

Dr. H. A. Sudibyakto, M.S.

Dr. Dhruva Pikha Shrestha



**DOUBLE DEGREE M.Sc. PROGRAM
GEO-INFORMATION FOR SPATIAL PLANNING AND RISK MANAGEMENT
GMU, JOGJAKARTA – ITC, ENSCHEDE**

2010



THESIS

DETERMINING RAINFALL THRESHOLDS FOR LANDSLIDE INITIATION A CASE STUDY IN WADAS LINTANG WATERSHED WONOSOBO, CENTRAL JAVA PROVINCE



UGM



ITS

By:

Emba Tampang Allo

08/276579/PMU/5627

Has been approved in Yogyakarta

On ... February 2010

By Team of Supervisor:

Dr. H. A. Sudibyakto, M.S.
Supervisor 1

Dr. Dhruva Pikha Shrestha
Supervisor 2

Certified by:

Program Director of Geo-Information for Spatial Planning and Risk Management
Graduate School, Gadjah Mada University

Dr. H. A. Sudibyakto, M.S.

dedicated to:

Naomi Yulitha Sambe

Jessica Christania Elmerillia Sambe Tampang Allo

Jericho Christanto Eusizwageri Sambe Tampang Allo

.....my constant inspiration.....

DISCLAIMER

This document describes work undertaken as part of a program of study at The Double Degree International Program of Geo-information for Spatial Planning and Risk Management, a Joint Educational Program of ITC, the Netherlands, and UGM, Indonesia. All views and opinions expressed therein remain the sole responsibility of the author, and do not necessarily represent those of the institute.

Emba Tampang Allo

ABSTRACT

Landsliding is one of the most damaging natural disasters in tropical countries, such as Indonesia, especially on the mountainous and hilly terrain area. The study area, Wadas Lintang Watershed in Wonosobo District, experiences landslide in yearly basis. Due to landslide, the area has been facing the loss of human lives and damages to properties. The landslide events commonly occur in rainy season, thus the rainfall can be regarded as the main trigger in the area. The condition has been being problematic due to lack of availability of information pertaining correlation between rainfall and persistent landslide events in this area. This research intends to determine rainfall thresholds for landslide initiation in the Wonosobo area.

The result suggests that the initiation of landslide events in the study area is governed by formula of $I = 63.683D^{-0.336}$ where I: rainfall intensity (mm); and D: rainfall duration (days). Furthermore, the research indicates that rainfall events up to five days prior to the day of failure also influence slope stability leading to landsliding in the study area, and the recurrence of excessive rainfall event causing landsliding ranges from 1 to 2.42 years.

To get better understanding about the landslide initiation in the study area, terrain hydrological assessment also was conducted comprising infiltration rate measurement, soil texture and permeability analysis. The result shows that infiltration capacity is categorized as low to medium indicating that the area is prone to landslide. This is due to presence of highly clay content (30-70%) in the soil material throughout the study area.

Slope stability assessment also has been performed using SINMAP analysis. The result reveals the degree of susceptibility of the area to landsliding that 66.76% of the total area categorized as stable, 9.14% as low susceptible, 9.91% as medium susceptible, 12.34% as high susceptible, and 1.86% as very high susceptible. The result cannot be verified due to limited data; however it can be used as preliminary tool for identification of hazardous and safe area in this study area.

Keywords: landslide, rainfall thresholds, infiltration, slope stability, SINMAP.

ACKNOWLEDGEMENT

Above all, I want to glorify My Savior, Jesus Christ, for the grace, peace, protection, guidance, and permission so that I can finish my study.

It is very difficult to list and thank to all persons who have contributed to my study, especially in constructing and writing my thesis, since it is impossible for me to finish it without the invaluable inputs and comments. Herewith I want to acknowledge and extend my gratitude to them:

To Bappenas and Netherlands Education Centre, for providing me the scholarship to continue my study in Gadjah Mada University (GMU), Jogjakarta and International Institute for Geo-information Science and Earth Observation (ITC), Enschede.

To Government of Tolitoli District, for giving me permission to continue my study, especially to my employer, Dinas Kehutanan (Forest Service), and my officemate for their support.

To my supervisors: Dr. Sudibyakto, for his attention and support between his busy schedule; and Dr. Dhruba Pikha Shrestha, for the very intensive long distance guidance. Their immeasurable assistances, suggestions, inputs and comments allow this work to come to the end.

To all lecturer and staff members of GMU and ITC: Dr. Junun Sartohadi, Dr. Muh. Aris Marfai, Dr. Danang Srihadmoko, Nugroho Christanto, M.Sc., Drs. Robert Voskuill, Drs. Michel Damen, Dr. David G. Rossiter, and all the lecturers that I could not mention individually.

To Government of Wonosobo District, especially to Badankesbanglinmaspol that provides data for my research and to all of Wadaslintang residents for their warmth and hospitality during my fieldwork in their area.

To Geo-info batch IV, my classmate, Bona, Dewi, Fetty, Diah, Wahyu, Zein, Ganda, Tandang, Eka, Komang, Sigit, Toto, Jaswadi, Andi, and Nina; for the invaluable and unforgettable help, cooperation, friendship, warmth, care, and support during my study. My special thanks flows to Bona, my co-worker, for the help and share during my fieldwork and thesis writing, especially for the guidance in GIS software; thanks for the constructive discussion; and thanks for being my brother in all situations, let this remains forever.

To my soulmate: Naomi Yulitha Sambe, for the prayers, patience and long distance companion. My sweet princess: Chika and my little brave prince: Chiko, thanks for being source of my inspirations giving me the strength to complete this study.

To my family: my parents, my sisters, and my brothers, for their eternal encouragement, hope, and love accompanying me to the end of my study. All of these make me strong to go through this one of the hard periods in my life.

**Emba Tampang Allo
Kota Gudeg, January 2010**

TABLE OF CONTENTS

COVER PAGE	i
APPROVAL PAGE	ii
ABSTRACT	v
ACKNOWLEDGEMENT	vi
TABLE OF CONTENTS	vii
LIST OF TABLES	viii
LIST OF FIGURE	x
ABBREVIATIONS	xi
1. INTRODUCTION.....	1
1.1. Background.....	1
1.2. Problem Statement.....	3
1.3. Aim and Objectives	3
1.4. Research Questions.....	3
1.5. Research Benefit.....	3
2. LITERATURE REVIEW	4
2.1. Landslide.....	4
2.2. Rainfall Thresholds and Landslide.....	7
2.3. Land use	8
2.4. Slope Stability	9
3. MATERIALS & METHODS.....	12
3.1. Available Data and Software's Used in the Research.....	12
3.2. Methods Applied.....	13
3.3. Data Collection	20
3.4. Data Processing	23
3.5. Reporting.....	26
4. STUDY AREA	27
4.1. Wonosobo District	27
4.2. Wadaslintang Watershed	28
5. RESULT AND DISCUSSION	35
5.1. Landslide Inventory	35
5.2. Rainfall Data.....	38
5.3. Rainfall Thresholds.....	40
5.4. Effect of Antecedent Rainfall	42
5.5. Rainfall Recurrence.....	47
5.6. Terrain Hydrological Condition	50
6. CONCLUSIONS, LIMITATIONS, AND RECOMMENDATIONS.....	68
6.1. Conclusion	68
6.2. Research Limitations.....	69
6.3. Recommendations	69
REFERENCES	
APPENDIXES	

LIST OF TABLES

Table 1: Historical Data of Landslide in Indonesia in year 1998 - 2007	1
Table 2: Landslide Events in Wonosobo District, Year 2001 - 2008	2
Table 3: Gumbel Data Analysis Method Based on Kaliwiro Station Data	48
Table 4: Recapitulation Infiltration and Cumulative Infiltration Model in the Study Area.....	50
Table 5: Recapitulation of soil moisture content equation and the developed relationship of soil moisture content - infiltration rate.....	58
Table 6: Classes of slope stability based on value of the Stability Index (SI).....	62
Table 7: Predicted State for Various Landuse in the Study Area	65

LIST OF FIGURES

Figure 1:	Schematic view and of photo a Rockfall and in Colorado, USA, in 2005. (Highland et al., 2008).....	4
Figure 2:	Schematic view and photo of a rotational slide in New Zealand (Highland et al., 2008) .	5
Figure 3:	Schematic view and photo of a translational slide in Canada (Highland et al., 2008)	5
Figure 4:	Schematic view and photo of a lateral spreads in California, USA, in 1989 (Highland et al., 2008).....	5
Figure 5:	Schematic view and photo of debris flow in 1999 in Venezuela (Highland et al., 2008) ..	5
Figure 6:	Schematic view and photo of debris avalanche in Philippine in 2006 (Highland et al., 2008).....	6
Figure 7:	Schematic view and photo of an earthflow Canada in 1993 (Highland et al., 2008).....	6
Figure 8:	Schematic view and photo of slow earthflow (creep) in UK (Highland et al., 2008).....	6
Figure 9:	Various Rainfall Thresholds proposed in literature: (a) Intensity – duration (ID) (Dahal et al., 2008); (b) Antecedent 3 days Rainfall (A(d)) (Kuthari, 2007); (c) Total Cumulative Rainfall (E) against Event Duration (D) (Sengupta et al., 2009); and (d) Normalized Intensity – Duration (Dahal et al., 2008).....	8
Figure 10:	Diagram illustrating the geometry of the assumed infinite-slope stability model and parameters involved in the safety factor in Equation (8) (Deb et al., 2009).	17
Figure 11:	Schematic flows of fieldwork preparation	21
Figure 12:	Fieldwork activities.....	22
Figure 13:	Administrative Map of Central Java Province (not scaled), Wonosobo District and the Research Site	27
Figure 14:	3 D View of the Study Area (not scaled)	28
Figure 15:	Land use types in the study area.....	29
Figure 16:	Elevation variety of the study area	30
Figure 17:	Landform classification of the study area	31
Figure 18:	Monthly Precipitation in Period of 1980 - 2008.....	31
Figure 19:	Drainage Map showing the main river, the tributaries and the rain gauges.....	32
Figure 20:	Dadap Gede landslide, showing position, profile and its overview.	33
Figure 21:	Dadap Gede landslide profile based on transect lines	34
Figure 22:	Structure of the disaster report of Wonosobo District (Anonymous, 2009b).....	35
Figure 23:	Traces of landslides in the study area.	36
Figure 24:	Example of unreported landslide, showing appearance before and after failure, remained scarp, and its position in the study area.	37
Figure 25:	Distribution of verified landslide in the study area.	38
Figure 26:	Distribution of rainfall in the study area over the years of 1980 to 2008	38
Figure 27:	Distribution of monthly average precipitation and number of landslide in years of 2001 to 2008 in Wonosobo District.....	39
Figure 28:	Relationship between monthly number of landslides and monthly precipitation in period of 2001 to 2008.....	40
Figure 29:	Rainfall intensity – duration thresholds curve for landsliding in Wadas Lintang watershed.	41
Figure 30:	Rainfall and landslide data in Wadaslintang watershed.	42
Figure 31:	Three Days antecedent rainfall thresholds curve for landsliding in Wadas Lintang watershed.	43
Figure 32:	Five Days antecedent rainfall thresholds curve for landsliding in Wadas Lintang watershed	44
Figure 33:	Ten Days antecedent rainfall thresholds curve for landsliding in Wadas Lintang watershed	44
Figure 34:	Fifteen Days antecedent rainfall thresholds curve for landsliding in Wadas Lintang watershed	45
Figure 35:	Relationship between daily rainfalls at failure with antecedent rainfall before failure, with correlation coefficient values.	46
Figure 36:	Recurrence Curve, Equation, and coefficient of correlation	49

Figure 37:	Predicted Infiltration Rate (left side) and Cumulative Infiltration Model (right side) Curves for Various Land Uses in the study area. Number in bracket is the order number of the land use in the Table 4.	51
Figure 38:	Comparisons of infiltration rate and cumulative infiltration model among the various landuse types.....	54
Figure 39:	Comparisons of Actual Infiltration Rate and Predicted Infiltration Rate Curves for Various Land Uses in the study area. Number in bracket is the order number of the land use in the Table 4.	55
Figure 40:	Variation of k values based on land use type and landform unit.....	56
Figure 41:	Curves of Soil Moisture Change in Respect to Time for Various Land Uses in the study area. Number in bracket is the order number of the land use in the Table 5.	59
Figure 42:	Soil Textures in the Study Area	61
Figure 43:	Comparison of SINMAP Modeling Results for Various DEM Resolutions	63
Figure 44:	Contribution of landuse types in high to very high susceptibility regions and ration of susceptibility level for various landuse types.....	66
Figure 45:	3D View Plotting Distribution of Susceptibility Levels and Landslide Locations (not scaled)	67

ABBREVIATIONS

Badan Kesbanglinmaspol	:	Badan Kesatuan Bangsa, Perlindungan Masyarakat & Politik (Nation Unity, Society Protection, and Politics Agency)
Bappeda	:	Badan Perencanaan Pembangunan Daerah (Spatial Planning Agency)
BNPB	:	Badan Nasional Penanganan Bencana (National Disaster Management Agency)
Dinas PU	:	Dinas Pekerjaan Umum (Public Work Service)
GIS	:	Geographical Information System
SINMAP	:	Stability Index Mapping

1. INTRODUCTION

1.1. Background

Landslides can be defined as the movement of a mass of rock, debris or earth down a slope (Cruden, 1991). Landsliding is one of the most damaging natural disasters in tropical countries, such as Indonesia, especially on the mountainous and hilly terrain area. The incidences of this disaster cannot be avoided, however understanding this hazard can stimulate proper mitigation which will reduce the impacts significantly (Daag, 2003). Landslide data from National Disaster Management Agency (BNPB, 2009) presented in Table 1 below, shows that in the period of 1998 to 2007, there were 569 landslide occurrences in Indonesia. These landslides caused 1,362 fatalities, 315 people injured, around 1,100 people missing, and around 170,000 people evacuated. Moreover, these landslides also damaged around 42,000 houses, 290 public facilities, 420 km road, and around 387,000 hectares of crops, plantation, and forest.

Table 1: Historical Data of Landslide in Indonesia in year 1998 - 2007

Year	Landslide Number	Victims (People)				Damages			
		Deaths	Injured	Evacuated	House (Unit)	Public Facilities (Unit)	Roads (Km)	Crops, Plantation, Forest (Ha)	
1998	19	41	32	-	380	4	2	138	
1999	9	58	-	-	365	10	-	-	
2000	94	167	-	-	1,386	-	-	780	
2001	29	15	3	-	175	4	-	3	
2002	44	136	21	12,908	3,603	2	56	5,322	
2003	103	311	92	95,799	13,968	32	225	363,023	
2004	53	139	8	44,997	4,788	169	31	15,515	
2005	41	209	29	6,113	13,997	35	110	1,331	
2006	73	196	52	9,489	2,392	12	3	491	
2007	104	90	78	1,271	974	24	-	654	
Total	569	1,362	315	170,577	42,028	292	427	387,257	

Source: National Disaster Management Agency (2009)

Java Island is one of areas in Indonesia that experiences landslides in a yearly basis. Study by Marfai *et al.* (2008), reveals that between 1990 and 2005 1,112 people died and 395 people were wounded due to landslides in this region. Furthermore, landslide events in this area tend to increase year by year both in number and the number of fatalities affected. The study also states that the increase is due to deforestation, excavation for construction materials (rock and soil), and expansion of settlement in unstable area.

Many factors are affecting landslides. The factors consist of environmental/ natural factors which include slope, soil, geomorphology, geology, and rainfall. The human induced factors are undercutting of steep slopes for road construction and expansion of settlement areas, deforestation, land use changes, and construction of reservoirs (dams). Slope failures are caused by above mentioned two factors or combination of them (Highland et al., 2008).

Rainfall can be considered as the main triggering factor in case of landslides in Indonesia, since most of the landslides were reported to occur during the rainy season (October to March). Prolonged rainfall will increase infiltration and create a saturated soil which reduces shear strength thus it leads to slope failure. Besides, (Smith et al., 2008) state that the presence of water in the soil or rock supplements the overall weight of the slope, which increases the shear forces causing the slope less stable.

Rainfall has long been well known as the main cause of landslides. However, the relationship between landslide and rainfall (intensity and duration) in many areas is still unclear. The relation, especially about the precise amount and duration of rainfall that triggers landslide has not been studied well. The correlation over a large area will be different since it's influenced by spatial distribution of rainfall and other controlling factors in the area, such as elevation.

Table 2: Landslide Events in Wonosobo District, Year 2001 - 2008

Year	Jan.	Feb.	Mar	Apr	Mei	Jun	Jul	Agust	Sep	Okt	Nop	Des	Total
2001	-	2	2	-	1	-	-	-	1	-	2	2	10
2002	1	1	1	3	-	-	-	-	-	-	5	11	22
2003	7	3	6	2	-	-	-	1	-	9	5	8	41
2004	17	1	2	4	-	-	1	1	-	1	3	15	45
2005	2	5	2	11	2	-	-	-	-	2	7	6	37
2006	9	5	4	13	2	2	1	1	-	2	8	11	58
2007	5	15	7	14	1	1	-	-	4	-	17	20	84
2008	5	6	17	7	-	-	-	-	-	8	17	7	67
Total	46	38	41	54	6	3	2	3	5	22	64	80	364
Avg.	5.75	4.75	5.13	6.75	0.75	0.38	0.25	0.38	0.63	2.75	8.00	10.00	
Perc.	12.64	10.44	11.26	14.84	1.65	0.82	0.55	0.82	1.37	6.04	17.58	21.98	

Source: Badan Kesbanglinmaspol of Wonosobo, 2009.

Historical data (see Table 2 above) shows that Wonosobo, one of regencies in Central Java Province, has stricken by landslides frequently which result in serious impacts; damaging houses and infrastructures even fatalities. The last landslides occurred on 23th/24th January 2009 and on 26th/27th February 2009. According to local people, the landslides occurred after prolonged high rainfall intensity (Anonymous, 2009c). The condition has been being problematic due to lack of availability of information pertaining

correlation between rainfall and persistent landslide events in this area. Therefore, research focus on studying this phenomenon is important for landslide mitigation. This research intends to determine rainfall thresholds for landslide initiation in the Wonosobo area.

1.2. Problem Statement

Landslides commonly occur in Wonosobo area, during the rainy season. Due to landslides, the area has been facing the loss of human lives and damages to properties. To minimize the losses due to landsliding, it is important to develop early warning system for which understanding the relation between landsliding and rainfall intensity and duration, especially the precise amount of rainfall that triggers landslides.

1.3. Aim and Objectives

This research aims to determine rainfall thresholds for landslide initiation in Wadas Lintang Watershed - Wonosobo, Central Java Province. The specific objectives are as follows:

- a. To determine the influence of rainfall prior to the day of landslide occurrence
- b. To determine the return period of excessive rainfall events which trigger landslides
- c. To study the terrain hydrological properties in the study area
- d. To assess the land use type under which condition is susceptible to landsliding

1.4. Research Questions

- a. What are the critical rainfall amounts that can trigger landslides in the study area?
- b. What is the influence of the number of rainy days just before the landslide occurrence?
- c. What is the return period of excessive rainfall events causing landslide?
- d. What are the terrain hydrological properties in the study area?
- e. What type of land uses under which condition are more susceptible to landslide?

1.5. Research Benefit

The research will provide information about the critical intensity or duration of rainfall that can trigger landslide in the study area. The data can be useful in landslide mitigation task which is conducted in the area. The rainfall thresholds data can be used also for establishing landslide early warning system (Guzzetti *et al.*, 2007; Dahal *et al.*, 2008)

2. LITERATURE REVIEW

2.1. Landslide

Generally, landslide can be defined as movement of a mass of rock, debris or earth down a slope (Cruden, 1991; Dai *et al.*, 2002) when the shear stress of the material is higher than its shear strength (Van Westen *et al.*, 2009). This movement is influenced by various factors, such as slope gradient, soil properties, ground water table, geomorphology, land use, rainfall and also by human intervention such as deforestations, undercutting of slope for road construction or expansion of settlement areas. In addition to these, landslide also occurs as an effect of other natural disasters, such as earthquake and volcanic activity. Landslides normally occur on steeper area especially in the mountainous and hilly region.

According to Highland *et al.* (2008) there are four main types of landslides which are described as follows:

Falls is movement of soil or rock, or both, from a steep slope due to the steepness of the slope. Type of movement is commonly by falling, bouncing, or rolling.

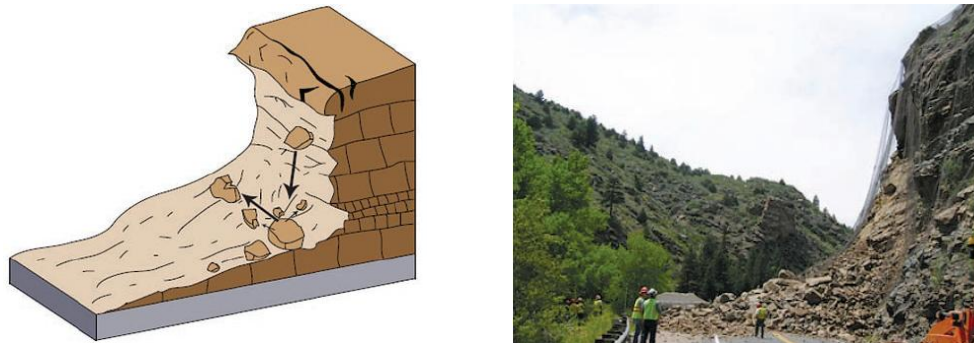


Figure 1: Schematic view and of photo a Rockfall and in Colorado, USA, in 2005. (Highland *et al.*, 2008)

Slide is the movement of soil, debris or rock along a distinct surface of rupture which separates the slide material from the more stable underlying material. This type of landslide is divided into two: rotational and translational slide.



Figure 2: Schematic view and photo of a rotational slide in New Zealand (Highland *et al.*, 2008)

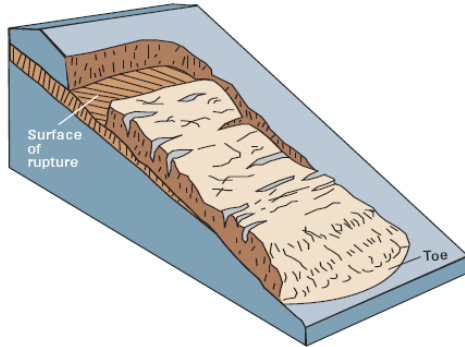


Figure 3: Schematic view and photo of a translational slide in Canada (Highland *et al.*, 2008)

Spread is an extension of a cohesive soil or rock mass combined with the general subsidence of the fractured mass of cohesive material into softer underlying material. Spreads may result from liquefaction or flow (and extrusion) of the softer underlying material. Types of spreads include block spreads, liquefaction spreads, and lateral spreads.

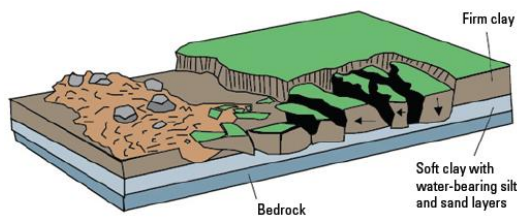


Figure 4: Schematic view and photo of a lateral spreads in California, USA, in 1989 (Highland *et al.*, 2008)

Flow is downslope movement of fluidized soil or rock due to heavy rainfall.

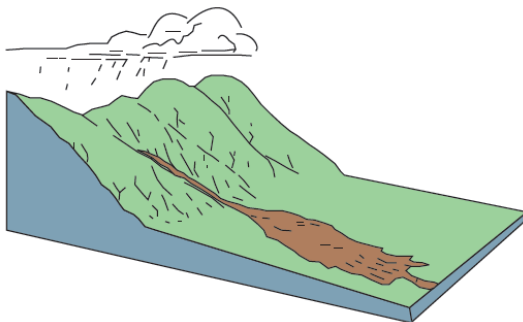


Figure 5: Schematic view and photo of debris flow in 1999 in Venezuela (Highland *et al.*, 2008)

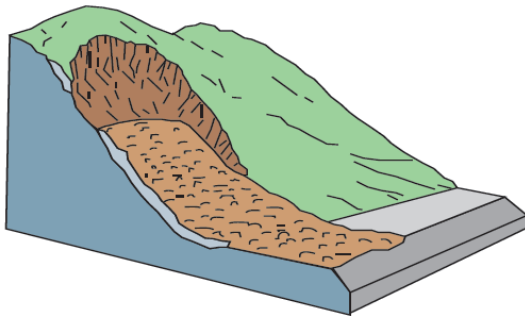


Figure 6: Schematic view and photo of debris avalanche in Philippine in 2006 (Highland et al., 2008)

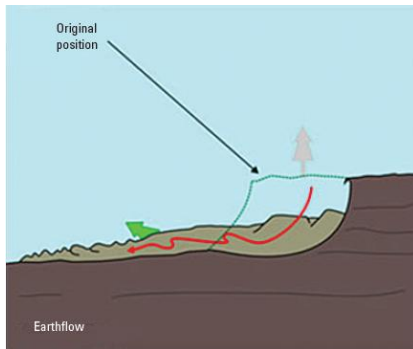


Figure 7: Schematic view and photo of an earthflow in Canada in 1993 (Highland et al., 2008)

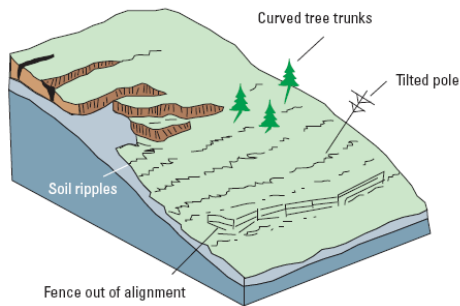


Figure 8: Schematic view and photo of slow earthflow (creep) in UK (Highland et al., 2008)

2.2. Rainfall Thresholds and Landslide

Guzzetti *et al.* (2007), defined a threshold as the minimum or maximum level of some quantity needed for a process to take place or a state to change. A minimum threshold defines the lowest level below which a process does not occur. A maximum threshold represents the level above which a process always occurs.

In terms of landslide, a rainfall threshold is the minimum intensity or duration of rainfall to cause landslide. Generally, there are two ways to obtain the rainfall threshold; empirical thresholds and physical thresholds (Guzzetti *et al.*, 2007; Dahal *et al.*, 2008).

The empirical thresholds can be obtained by statistically analyzing the rainfall event that causes landslide. These thresholds are divided into four sub categories: intensity-duration (ID) thresholds, total rainfall event thresholds, rainfall event-duration (ED) thresholds, and rainfall event-intensity (EI) thresholds (Guzzetti *et al.*, 2007). Intensity-duration (ID) thresholds are the most common thresholds proposed in the literature (Guzzetti *et al.*, 2007; Dahal *et al.*, 2008; Sengupta *et al.*, 2009). The thresholds calculate the total amount of precipitation (intensity) in a period, commonly in millimeters per hour and the range of durations between 1 and 100 h. Total rainfall thresholds take into account the amount of precipitation during the landslide event. The thresholds use different rainfall variables: daily rainfall (R), antecedent rainfall (A(d)), cumulative event rainfall (E), and normalized cumulative event rainfall (EMAP) expressed as a percentage of Mean Annual Precipitation (MAP). The last type of thresholds is used when some landslide events occurred during very low amount of rainfall corresponding to the nearest rainfall station which contradicts the thresholds relation (Dahal *et al.*, 2008). Rainfall event-duration (ED) thresholds measure the event of rainfall causing landslide based on different variables: cumulative event rainfall, the critical rainfall, and the corresponding normalized variables. Figure 9 below shows various rainfall thresholds proposed in literature.

Physical thresholds are determined based upon relationship between hydrological and slope stability. This method requires wide knowledge and detailed information on hydrological, lithological, morphological, and soil characteristics that control the initiation of landslide in an area (Guzzetti *et al.*, 2007; Dahal *et al.*, 2008). According to Guzzetti *et al.* (2007), this model is capable of determining the amount of precipitation to trigger slope failure and the location and time of expected landslide. This model also performs best for only shallow landslides. However, it is impractical for a large area since it is difficult to obtain all the necessary parameters.

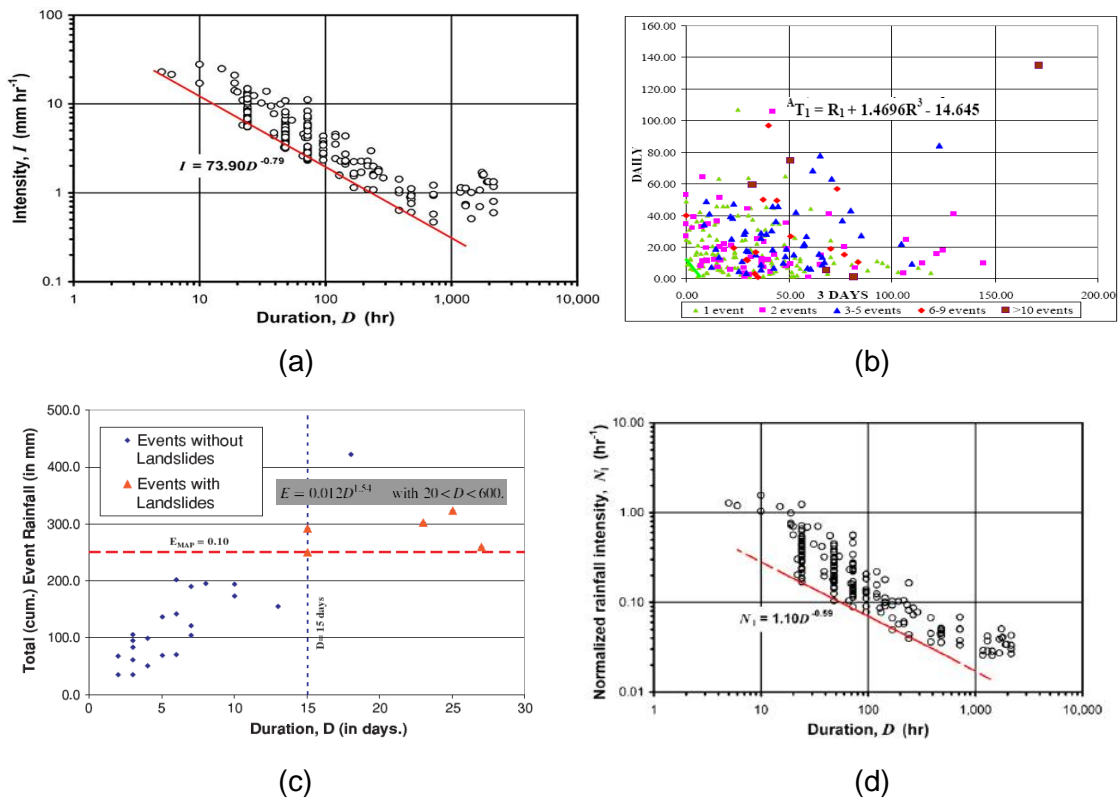


Figure 9: Various Rainfall Thresholds proposed in literature: (a) Intensity – duration (ID) (Dahal et al., 2008); (b) Antecedent 3 days Rainfall (A(d)) (Kuthari, 2007); (c) Total Cumulative Rainfall (E) against Event Duration (D) (Sengupta et al., 2009); and (d) Normalized Intensity – Duration (Dahal et al., 2008)

2.3. Land use

Land use is the interaction between humans and the biophysical environment. The interaction gives impacts on the structure, function, and dynamics of ecosystems at the various levels of ecological organizations, including local, regional, and global levels. Human activities on environment that produce changes in land cover such as agriculture, mining, and urban development influence the functioning of ecological systems. The influence has resulted in global climate change, soil and hydrological degradation, and increased biological extinctions (Aspinall et al., 2008).

According to Karsli et al. (2008) landuse change have been recognized as the most important factor influencing the occurrence and re-activation of landslides triggered by rainfalls. In a heavily rainy environment, the relation between landslide and vegetation cover is extremely important and it should not be underestimated, since vegetation can influence the slope stability parameters, such as cohesion, internal friction angle, weight of the slope-forming material and pore-water pressure. Vegetation can both enhance effective soil cohesion due to root matrix reinforcement and soil suction or negative water

pressure through evapotranspiration and interception. Due to these effects, vegetation can increase soil shear-strength up to 60% depending on the tree species, on the other hand it was found that landslide activity increases up to 15% in places where the original land cover has been removed or altered.

2.4. Slope Stability

The 'slope stability' and its corollary 'slope instability' are defined as the propensity for a slope to undergo morphologically and structurally disruptive landslide processes. Slow, distributed forms of mass movement such as soil creep are generally considered not sufficiently disruptive to be included in this definition. From a hazard and engineering perspective, assessments of slope stability are generally intended to apply to periods ranging from days to decades, or in some cases to specified periods relating to the design-life of a potentially affected structure. However, slope stability may also be treated as a factor in landform evolution and therefore its significance in this role has to be measured over much longer time scales (Glade *et al.*, 2005).

Landslides are always associated with a disturbance of the equilibrium relationship which exists between stress and strength in material resting on the slopes. The relationship is determined by factors such as the height and steepness of the slope and the density, strength cohesion and friction of the materials making up the slope. Instability arises when the shear strength or maximum resistance of the material comprising the slope to shear stress is exceeded by a downslope stress (Yalcin, 2007).

In general, there are two ways of assessing slope stability: geophysical method and hydrological method. The geophysical method analyzes slope stability based on internal structure and the mechanical properties of the soil or rock mass of the slope, meanwhile the hydrological model simulates saturated and unsaturated flow in slopes due to distribution of pore water pressures, both positive and negative, as the main aspect in rainfall-triggered landslides. Both methods are described in turn below.

According to Hack (2000), geophysical methods that are frequently used in slope stability investigation are: seismic, geo-electric, electromagnetic, and gravity methods. Seismic methods are based on the measuring of an elastic wave (also: seismic, shockwave, or acoustic wave) traveling through the sub-surface. The wave is reflected or refracted on boundaries characterized by different densities and/or deformation properties. Seismic methods can nearly always be used to determine the internal structure of materials in a slope. Sometimes logistics and practical problems as how and where geophones and sources can be placed may make the method impractical. Electromagnetic methods investigate slope stability based on penetration of

electromagnetic field. The penetration depends on the electric conductivity and dielectric constant of the materials in the sub-surface and on the frequency of the transmission field. The measurements can then be correlated with the borehole information to obtain the electromagnetic properties to analyze the stability. Geo-electrical or resistivity measurements are based on the difference in resistivity between different sub-surface materials. The measuring equipment consists of two current electrodes and two measuring electrodes, a DC current source, and a measuring device. The measurements are analyzed using computer software in terms of two and three-dimensional 'resistivity-imaging' or 'resistivity tomography'. Gravimetric surveys investigate the difference in densities between different subsurface materials. The gravity measured at the surface of the earth is compared with a theoretical value (normal gravity) corresponding to an earth model in which only radial density variation is present. The applications to slope stability studies are rare and require an accurate topographic map to correct the effect of irregular topographic relief on the gravity measurements. Potentially, gravimetry can give 'in-situ' estimate of the density of slope material using methods that correlate elevation with gravity differences.

Dahal *et al.* (2009), summarizes hydrological modeling commonly used in assessing slope stability. HYSWASOR proposed by Van Genuchten, (1980) in Dahal *et al.*, (2009) and Combined Hydrology and Slope Stability Model (CHASM) which was used by Anderson & Lloyd, (1991); Collision & Anderson (1996) in Dahal *et al.*, (2009) are two models that accurately simulate the slope stability condition during rainfall. In the TOPMODEL which was established by Beven and Kirkby in 1979 (Dahal *et al.*, 2009), the influence of topography on slope material saturation behavior is computed, in the form of topography index which simulated runoff hydrographs. The Antecedent Soil Water Status Model (ASWSM) (Crozier, 1999) accounted for the draining of early rainfall and accumulation of late rainfall. This model provides an equation for estimating the probability of landslide occurrence as a function of daily intensity and previous water accumulation. A coupled SEEP/W–SLOPE/W analysis proposed by GeoStudio (2005) in Dahal *et al.*, (2009) is another example of a coupled hydrological-slope stability modeling software. The SEEP/W package analyses seepage problems with a numerical discretization technique, whereas SLOPE/W can be used as a limit equilibrium slope stability model. SEEP/W adopts an implicit numerical solution to solve Darcy's equation for saturated and unsaturated flow conditions, describing pore water pressure and movement patterns within porous materials over space and time. SHALTAB is a contour- or polygon-based hill slope hydrological model proposed by Dietrich *et al.* (1995) and Montgomery & Dietrich

(1994) in Dahal *et al.*, (2009). This model also considered some of the index properties of slope materials, and can be implemented as an extension of commercially available GIS software (ArcView). SINMAP (Pack *et al.*, 1998; Pack *et al.*, 2001) is another approach suitable for modeling slopes that have a shallow soil depth and impermeable underlying bedrock. It is similar to SHALSTAB, but uses cohesion and root cohesion (for forested slopes) in the calculations. Thus, SINMAP may be viewed as an advanced version of SHALSTAB.

SINMAP is an ArcView extension which computes and maps slope stability index based on geographical data, especially digital elevation data. The stability index refers to the infinite slope stability model that is determined by analyzing the ratio of destabilizing parameter of gravity and stabilizing parameters of friction and cohesion on a sliding plane.

To derive the terrain stability, SINMAP requires several inputs: slope, wetness index, gravity, soil density, ratio of transmissivity to recharge rate, cohesion, and angle of friction. The first two inputs are automatically computed from digital elevation model (DEM). The rest variables are uncertain which range from lower to upper bounds. These variables have default value that can be adjusted by user. (Pack *et al.*, 1998)

3. MATERIALS & METHODS

3.1. Available Data and Software's Used in the Research

Several data are needed in this research. They are listed as follows:

Landslide Data

Landslide data are needed to perform the thresholds analysis. Each landslide event can be characterized by its location (geographic coordinates), type, and time of failure (date and time) which can be correlated with rainfall data.

Landslide data was collected from available reports, from year 2001 – early 2009 (Badan Kesbanglinmaspol). This can be considered the most reliable available data since it is a compilation of report from lower governmental institution levels (sub districts and villages). Landslide data was also collected by interviewing the people in the area.

Rainfall Data

Rainfall database was prepared from Dinas PU in Wonosobo. Daily rainfall data are available throughout the area. Hourly rainfall data is only available at the rainfall station located on the dike of the dam. The dam is located outside of the study area, thus the data cannot be used for the analysis. The geographic locations of the rainfall stations also have been obtained using handheld GPS receiver to perform the rainfall thresholds analysis.

Administrative Map

Administrative map was obtained from Bappeda of Wonosobo District. The administrative map was used as guide in fieldwork activities, especially to locate the landslide position based on village names.

Land use Map

Land use map was collected from Bappeda of Wonosobo District. Combined with images interpretations, the land use then verified during the fieldwork activities.

Topographic Map

Digital topographic map scale 1:25,000 from Bakosurtanal was used as base map for building DEM, building hill shade map, delineating watershed boundary, and also for SINMAP slope stability analysis.

Satellite Image/Aerial Photo

Satellite Image which was used in the research was SPOT Image year 2006. The Aerial Photo 1994 sheet number 93A/W22/1/22 taken on 23rd April 1994 with scale of 1:50.000 was provided by Bakosurtanal.

✦ Soil hydrologic properties

Soil hydrologic properties taken during the field work are infiltration tests and soil sampling for laboratory test. The results were used for studying the terrain hydrological properties in the study area.

Computer software applied in this research consists of GIS software, soil data analysis, word processing, spreadsheet data processing, and presentation preparation. The software's are listed below:

✦ ILWIS 3.3

✦ ArcView 3.3 and ArcGIS 9.3

✦ Soil Water Characteristics version 6.02.74

✦ MS Excel 2007

✦ MS Word 2007

✦ MS Power Point 2007

3.2. Methods Applied

To address the research objectives, several methods have been applied in the research. The methods are described as follows:

✦ Determining rainfall threshold, influence of previous rainfall to landsliding, and recurrence of excessive rainfall events

To determine the precise rainfall needed to trigger landsliding, in this research intensity – duration thresholds (intensity in mm and duration in days) was used, based on landslide data which are reported to occur in the study area. The influence of previous rainfall events to landsliding was assessed using Antecedent Rainfall Threshold analysis for 3-, 5-, 10-, and 15-day antecedent rainfall. Gumbel Distribution Model known as Extreme Value Distribution Type I, was used to determine the return period of excessive rainfall events causing landslide.

✦ Studying terrain hydrological properties

Hydrological properties also play role in slope failure. To obtain the terrain hydrological properties in the study area, infiltration measurements were conducted in various land units as combination of landuse and landform in the study area. In the same location soil samples (disturbed and undisturbed) were taken to analyze its texture, initial soil moisture content, and permeability.

☛ Determining the landslide susceptibility for various landuses

Landslide susceptibility for various landuse types in the study area was assessed using SINMAP analysis. This is one of hydrological methods in modeling the slope stability (Dahal *et al.*, 2009). The main inputs for this analysis are digital elevation data, and landslide distribution map (a point map).

3.2.1. Rainfall Distribution, Frequency and Threshold Analyses

☛ Rainfall Distribution

Rainfall distribution was analyzed in GIS based on rainfall station positions and landslide locations which were used to perform rainfall threshold analysis. To select the rainfall station corresponding to a particular landslide, spatial distributions of landslide locations was analyzed using GIS software, and the nearest stations were selected. The total 24-hour rainfall (mm) or continued precipitation of many days at a station was considered the event rainfall for the corresponding landslide event (Dahal *et al.*, 2008).

☛ Rainfall Frequency

To determine the excessive rainfall causing more slope failures, Gumbel Distribution model, known as extreme value distribution type I, was used to determine the recurrence of extreme rainfall events in the study area. This method calculates return period of particular rainfall intensity, or vice versa, based on yearly maximum precipitation in a certain period. The resulted formula from linear trend line is used to derive the intended return period or rainfall intensity.

In Gumbel method the recurrence is obtained based on the following equation (Wilson, 1969):

$$T = \frac{1}{1-P'} \quad (1)$$

P' is determined by formula:

$$P' = e^{-e^{-y}} \quad (2)$$

and y is calculated from:

$$y = -\ln(-\ln(1 - \frac{1}{t})) \quad (3)$$

where:

T: Return period of an event X in years

e: Natural logarithm base

P': probability of non occurrence of an event X in T years

t: probability of occurrence of an event X in T years

☛ Rainfall Threshold Analyses

Rainfall thresholds analysis which is used in this study are intensity – duration (*ID*) thresholds and antecedent rainfall thresholds calculated empirically. *ID* thresholds are used to define the lowest boundary of rainfall intensity (mm/day) and the minimum duration that triggers landslide. The relationship between rainfall and landslide in this study can be obtained by processing the data in Microsoft Excel by means of simple power law method.

In intensity – duration (*ID*) thresholds, a database consisting of rainfall intensity (mm/day) and rainfall duration (day) of landslide events is made in Microsoft Excel. The two data sets were then used to generate a scattered graph, in which rainfall intensity is used as y-axis and duration as x-axis. By choosing simple power law method, a trend line is added and the graph shows the equation of rainfall threshold. Generally, intensity – duration (*ID*) thresholds is presented by equation $I = aD^b$, where I: intensity, D: Duration, and a and b: constants.

To study the effect of previous rainfall intensity, antecedent rainfall thresholds of 3, 5, 10, and 15 days is determined for the study area. The approximate minimum antecedent threshold, defined by the equation $T = R_0 + aR_c - b$, where *T*: thresholds, *R₀*: rainfall intensity of failure day, a & b: constants, and c: cumulative rainfall of 3, 5, 10, and 15 days before failure. The constants (a and b) are visually identified after constructing a scatter plot showing daily precipitation amounts and cumulative rainfall amounts (3, 5, 10, and 15 days).

3.2.2. *Terrain Susceptibility to Landslide Analysis*

☛ Terrain hydrological condition

Terrain hydrological condition was studied in this research including infiltration rate, cumulative infiltration, permeability, soil moisture content, and soil texture. As stated previously, infiltration test was carried out in the field and soil properties were analyzed in the laboratory.

The measured infiltration rate is used to generate predicted infiltration rate (*f*) using Horton formula and to generate cumulative infiltration (*F*). The cumulative infiltration (*F*) shows how much water is infiltrated into the ground, as well as the soil thickness affected by the infiltrated rainfall. These conditions are related with the increase in unit weight by which in contrast decreases the shear strength of a particular slope. The equation for predicted infiltration rate and cumulative infiltration are given below in turn.

Predicted infiltration rate (f) (Wanielista *et al.*, 1997):

$$f = f_c + (f_n - f_c)e^{-kt} \quad (4)$$

where:

f : infiltration rate (cm min⁻¹)

f_c : constant infiltration rate (cm min⁻¹)

f_0 : initial infiltration rate (cm min⁻¹)

t : time (minute)

k : constant value

f_c is estimated from actual infiltration rate curve

k is determined with the equation (Wanielista *et al.*, 1997):

$$k = \frac{1}{(t_{n+1} - t_n)} \ln \left[\frac{(f_n - f_c)}{(f_{n+1} - f_c)} \right] \quad (5)$$

k value is chosen from several substitutions into infiltration rate (f) formula which gives the best fit between predicted infiltration curve and measured/actual infiltration curve.

Cumulative infiltration (F) (Wanielista *et al.*, 1997):

$$F(t) = \int_0^t f(t) dt = (f_c)t - \left(\frac{f_n - f_c}{k} \right) (1 - e^{-kt}) \quad (6)$$

Soil moisture change (θ)

$$\theta(t) = \theta_s - (\theta_s - \theta_0)e^{-kt} \quad (7)$$

where:

θ : soil moisture content

θ_s : maximum soil moisture content (saturated condition)

θ_0 : initial soil moisture content

t : time (minute/s)

Terrain stability index

This research employs SINMAP (Pack *et al.*, 1998; Pack *et al.*, 2001) to calculate the slope stability in the study area. The parameter is set at default value since there is no specific test/measurement taken due to limited time. The default parameters are:

Gravity: 9.81m/s².

Soil density: 2,000 kg/m³.

Water density: 1000 kg/m³.

Ratio of transmissivity to recharge rate: 2,000 (lower) and 3,000 (upper)

Dimensionless Cohesion: 0.0 (lower) and 0.25 (upper)

Soil friction angle: 30° (lower bounding) and 45° (upper bounding)

3.2.3. Landslide Initiation Assessment

Stability index resulted from SINMAP analysis is a combination of several analysis performed previously. The main inputs for the SINMAP are DEM, landslide inventory map, soil properties, and hydrological parameters. The two latter parameters are changeable; otherwise the user can use the default value provided by the software.

SINMAP underlies its theory based on the infinite slope stability model that balances the destabilizing components of gravity and the stabilizing components of friction and cohesion. The pore pressure due to soil moisture reduces the effective normal stress, which through the angle of friction is related to shear strength (Pack *et al.*, 2001). The model calculates the safety factor (SF) expressing the ration of stabilizing forces (shear strength) to destabilizing forces (shear stress) on a failure plane parallel to the surface (Deb *et al.*, 2009). The safety factor calculation in SINMAP is:

$$SF = \frac{C_r + C_s + \cos^2 \theta [\rho_s g (D - D_w) + (\rho_s g - \rho_w g) D_w] \tan \phi}{D \rho_s g \sin \theta \cos \theta} \quad (8)$$

where C_r is root cohesion ($N\ m^{-2}$), C_s is soil cohesion ($N\ m^{-2}$), θ is slope angle ($^\circ$), ρ_s is wet soil density ($kg\ m^{-3}$), ρ_w is the density of water ($kg\ m^{-3}$), g is gravitational acceleration ($9.81\ m\ s^{-2}$), D is the vertical soil depth (m), D_w is the vertical height of the water table within the soil layer (m), and ϕ is the internal friction angle of the soil ($^\circ$). θ is the arc tangent of the slope S , expressed as a decimal drop per unit horizontal distance.

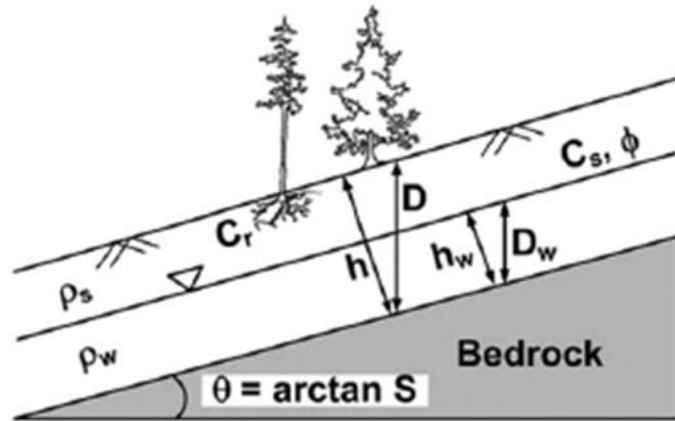


Figure 10: Diagram illustrating the geometry of the assumed infinite-slope stability model and parameters involved in the safety factor in Equation (8) (Deb *et al.*, 2009).

Figure 10 above showing the geometry used in Equation (8) and used in SINMAP to modify the equation by combining the steady state hydrological model (Pack *et al.*, 1998). Based on the figure, the soil thickness (h) and soil depth (D) are related as $h = D \cos \theta$ to form the dimensionless of infinite-slope stability model:

$$SF = \frac{C + \cos \theta (1 - wr) \tan \phi}{\sin \theta} \quad (9)$$

where $w=D_w/D=h_w/h$ is the relative wetness defining the relative depth of perched water table within the soil layer, $C=(C_r+C_s)/(h\rho_s g)$ is the combined cohesion (root and soil) showing the relative contribution of the cohesive forces to slope stability, and $r=\rho_w/\rho_s$ is the water-to-soil density ratio.

SINMAP governs the hydrological model assuming that the areas in which the soil cover has higher water content (and degree of saturation) tend to occur in convergent hollow areas of the hillslopes, and landslides usually originate in such areas (Deb *et al.*, 2009). The model also assumes that the discharge at any point is equivalent with the effective steady state recharge, thus the lateral discharge q , is estimated by $q=Ra$ ($\text{m}^2 \text{day}^{-1}$), and the capacity of lateral flux at any point is termed by soil transmissivity and slope angel, $T\sin\theta$. Thus the relative wetness is expressed as:

$$w = \min\left(\frac{Ra}{T \sin \theta}, 1\right) \quad (10)$$

By incorporating the Equation (10) into Equation (9), the equation of Safety Factor becomes:

$$SF = \frac{C + \cos \theta \left[1 - \min\left(\frac{Ra}{T \sin \theta}, 1\right) r\right] \tan \phi}{\sin \theta} \quad (11)$$

The a and θ , the topographic variables, are obtained from Digital Elevation Model (DEM), whereas C , $\tan\phi$, r , and R/T are user input. The parameter r is treated constant (0.5) but the rest are uncertain allowing specification of lower and upper boundaries. Where $R/T=x$, and $\tan\phi=t$, the probability of Stability Index, the probability of slope to be stable, is evaluated over range of C , x , and t . The smallest C and t (i.e. C_1 and t_1) combined with the largest x (i.e. x_2) defines the worst-case scenario. Areas under the worst-case scenario having SF greater than 1 are identified as unconditional stable, and defined as minimum deterministic SF :

$$SI = SF_{min} = \frac{C_1 + \cos \theta \left[1 - \min\left(x_2 \frac{a}{\sin \theta}, 1\right) r\right] t_1}{\sin \theta} \quad (12)$$

When the minimum safety factor is less than 1, there exists a probability of slope to fail. If the value of cohesion and friction of angel are highest combined with the lowest R/T , SI is defined by maximum SF :

$$SI = SF_{max} = \frac{C_2 + \cos \theta \left[1 - \min\left(x_1 \frac{a}{\sin \theta}, 1\right) r\right] t_2}{\sin \theta} \quad (13)$$

SINMAP implements mathematically the computation and mapping of a slope-stability index based on surface topography to route flow downslope. The flow is assumed that the subsurface hydrologic boundary (or bedrock-drift boundary) parallels the surface and the soil hydraulic conductivity is uniform. The flow model predicts relative levels of the perchedwater table for the whole of a watershed area implying subsurface flow through the colluviums or regolith, then is used to assess slope stability (Pack *et al.*, 1998; Deb *et al.*, 2009).

In performing the calculation, SINMAP requires a DEM, a point map of landslides, and the values of calibration parameters. The model calibration parameters include the range of cohesion values, soil-density values, range of internal friction-angle values, and range of T/R ratios. The T/R can be derived from the permeability rates observed during the fieldwork and the recharge rate from the rainfall thresholds of the previous analysis. Unfortunately, the soil thickness was not measured during the fieldwork, thus the transmissivity T value cannot be calculated. For the same reason, no comprehensive analyses have been done for the rest calibration parameters. Based on this condition, the calibration parameter values are set to SINMAP default.

By default, SINMAP divides slope stability into six classes: Stable, Moderately Stable, Quasi Stable, Lower Threshold, Upper Threshold, and Defended. According to Pack *et al.* (2001), the first three terms classify the region that, according to the model, should not fail with the most conservative range of the specified parameter ranges. These regions need external factors for instability. The terms “Lower Threshold” and “Upper Threshold” characterize the regions where the probability of instability is less than and greater than 50% respectively. External factors are not required for instability in these regions, but it’s simply by a combination of parameter values within the uncertainty limits specified. “Defended slope” is the term used to characterize region where slope should be unstable for any parameter combination within the given parameter ranges. Such slopes occur in the field are influenced by forces not represented in the model, or the model is inappropriate. Deb *et al.* (2009) reclassifies the predicted state of the slopes set by SINMAP (see Table 6 below) and is used in this research. As proposed by Deb *et al.* (2009), the stability index is redefined into degree of susceptibility of a slope region to landslide. They reclassified predicted state of SINMAP which ranges from stable slope zone to defended slope zone into degree of susceptibility of slope to landslide which ranges from safe area to very high susceptibility.

3.3. Data Collection

3.4.1. Preparation

This stage includes collecting supporting data for field work, obtaining research permit from local government (province, district, and sub-district levels), and preparing materials and equipments for fieldwork purposes.

Fieldwork preparation conducted for preparing materials consists of several activities. The preparation is explained in turn below and followed by schematic figures (Figure 11).

- a. Building DEM from digital topographic map (scale 1:25,000) using ArcGIS 9.3. The resulted a 10-m DEM covered whole area of Wonosobo District.
- b. Preparing watershed boundary of the Wadaslintang area (automatic delineation) using DEM Hydroprocessing in ILWIS 3.3. The resulting watershed boundary map was used to clip the area of the study watershed.
- c. Building hillshade map based on DEM of the watershed to delineate landform in the study area.
- d. Modifying existing land use map based on imagery interpretation. The modified land use map then overlaid with landform map to assign the soil sampling and infiltration test points.
- e. Tabulating landslide events based on combination with administrative map (villages) and watershed boundary. Landslide events occurring in the villages located outside of the watershed were excluded.

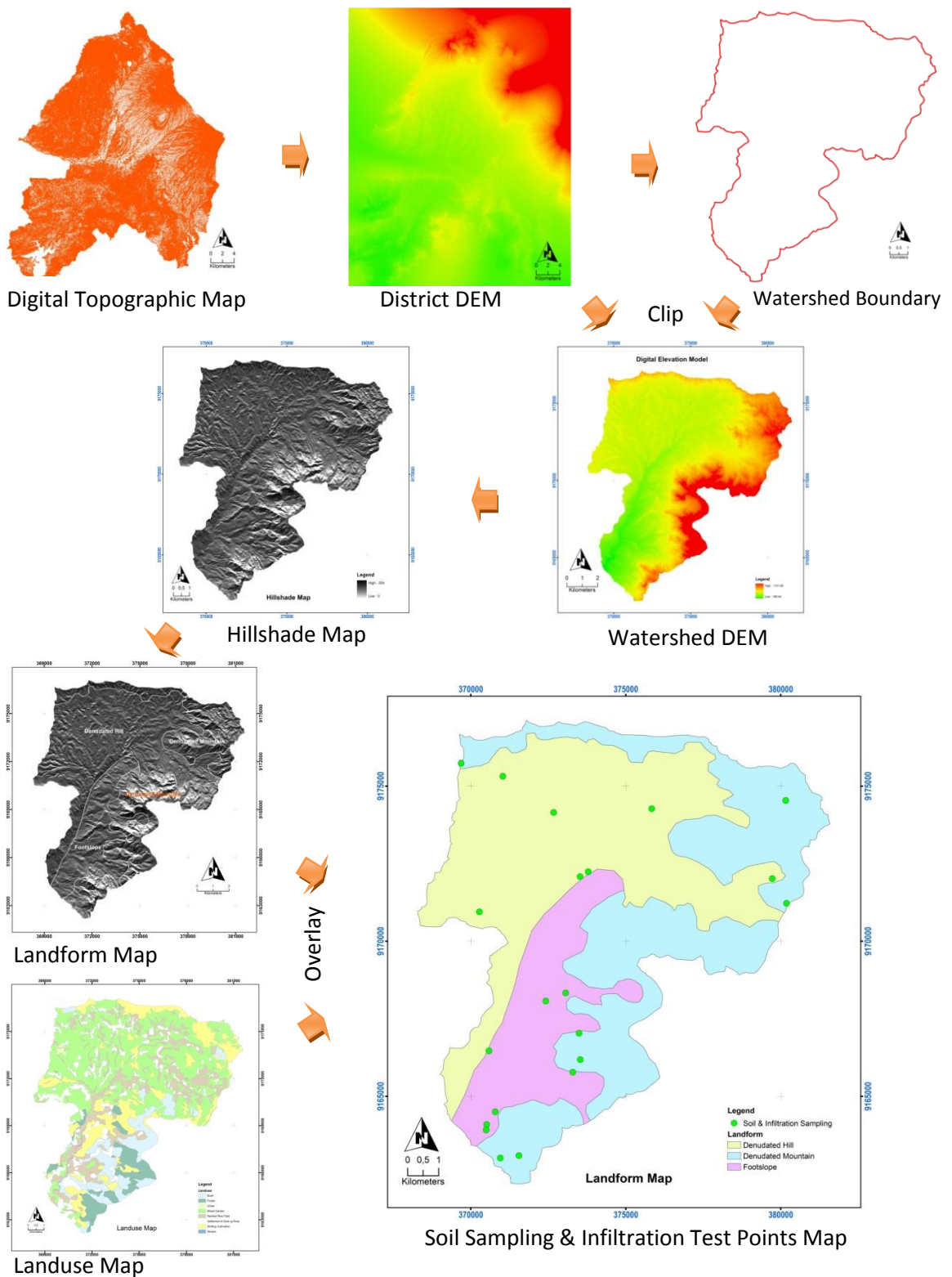


Figure 11: Schematic flows of fieldwork preparation

3.4.2. Fieldwork and Data Collecting

Basically, data collecting during field work can be separated into two main activities: direct collection of field data (e.g. landslide locations, land use verification, soil data collection, infiltration test and collecting data on rainfall and gauging locations); and collection of data by conducting interviews with local people (e.g. time of landslide occurrences, trend of the landslide occurrences year by year, etc). The interview was addressed to the people who know well the area and the time and location of landslide events, such as the head of a village, since the landslide occurrences in their area will be reported to them. Figure 12 below shows some fieldwork activities conducted in the study area.

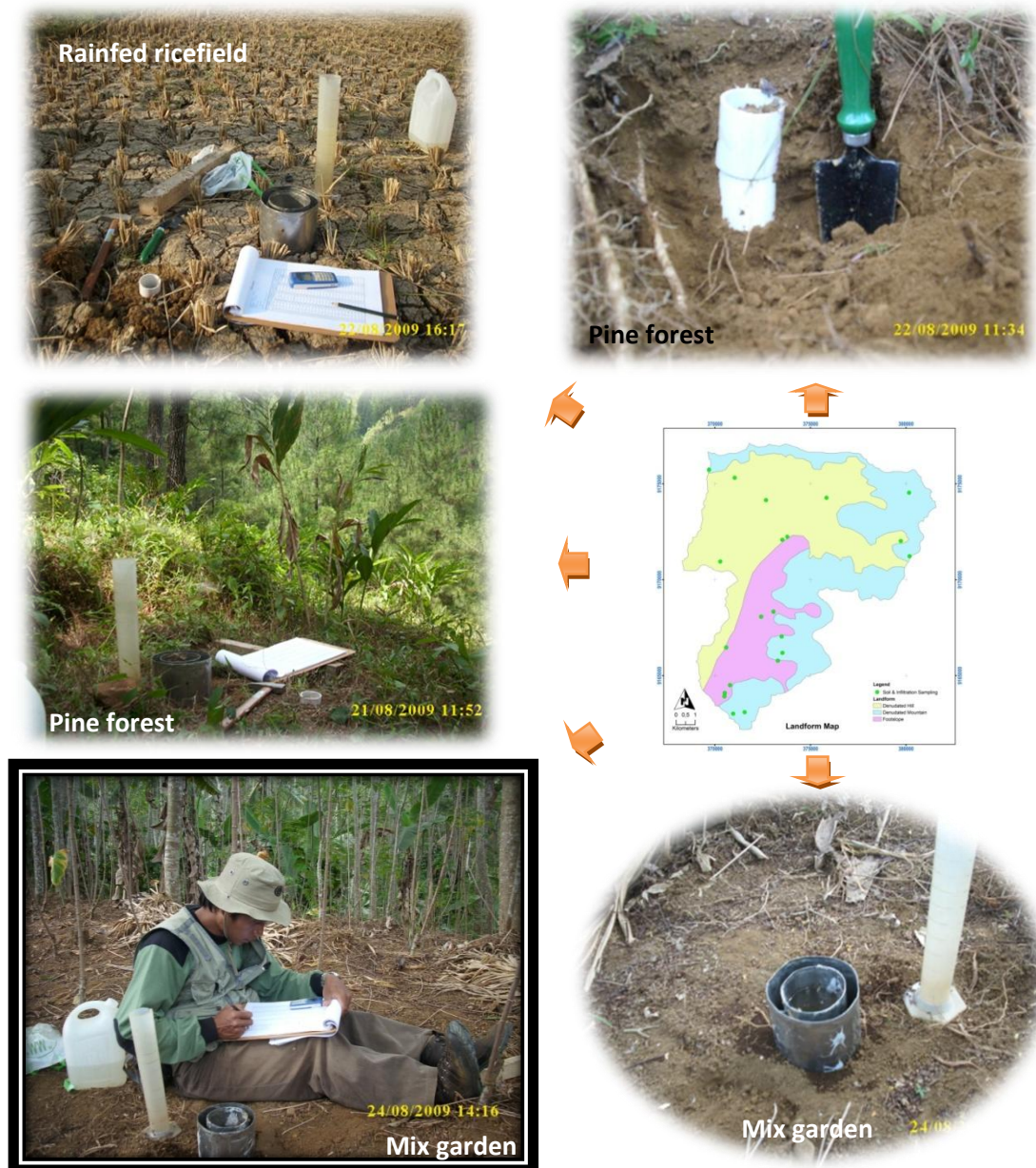


Figure 12: Fieldwork activities

Figure 12 above presents example of fieldwork activities, especially soil sampling and infiltration tests in various land uses. Soil sampling and infiltration test were conducted in the same location. Disturbed and undisturbed soil samples were collected from the location. Disturbed soil sampling was done by collecting soil bulks around the location, used for texture soil analysis, and undisturbed soil sampling, used for initial moisture and permeability analysis, was done using 2 tubes. Sampling was carried out using a tube which was pushed into the soil. The other tube was used to push the lower tube. The lower tube with undisturbed soil was wrapped with plastic cover and tape to prevent evaporation, and then the samples were brought to laboratory for analysis.

In the same location, infiltration measurement was carried out. The test employed Horton method using *double-ring infiltrometer*. Length of test varies as it depends on how long the constant infiltration rate is reached.

Visually interpreted image interpretation was combined with existing land use map from governmental institution. The result was verified in the field through direct observation.

Available landslide historical data (report & personal) was collected and classified. Landslide types being used in this research are deep-seated rotational landslides and creep based on landslide occurrences caused by environmental factors, meanwhile the other, human induced landslide (road cutting, settlement) were left out. Fieldwork was conducted to verify the types of landslide (environment or human induced) and also to define the geographical position using GPS. Head of landslide scarp was mapped as point of geographic coordinates (Kuthari, 2007).

Available daily rainfall data was collected from rainfall gauges maintained by Dinas PU. The rainfall gauge locations also were mapped during the fieldwork for GIS analysis of rainfall distribution for rainfall thresholds purpose.

3.4. Data Processing

3.4.1. Generating landslide database and point map

Landslide database was built consisting of type of landslide, landslide id (to be easily operated in GIS), date of failure and geographic coordinates. Landslide point map was generated based on fieldwork result. This map was used to localize the landslide locations (based on landslide id) for rainfall threshold analysis.

3.4.2. Generating rainfall database and spatial distribution map

Rainfall database was built based upon data from rainfall stations in the study area, consisting of time (refers to time of slope failures), rainfall intensity (mm/day), duration (day), and cumulative rainfall of 3, 5, 10, and 15 days before failure. Intensity (mm/day)

and duration (day) were used for Intensity – Duration Thresholds, and the cumulative rainfalls were used to study the role of antecedent rainfall in triggering the landslides.

The rainfall station regarded corresponding to a landslide event was analyzed in GIS laid on spatial distribution of landslide locations and rainfall gauges. The nearest stations were selected.

3.4.3. *Rainfall thresholds analysis*

Intensity-duration Rainfall Threshold

Intensity-duration rainfall threshold was calculated by referring to date of landslide events occurring in the study area. By extracting the dates and locations from the landslide database, rainfall data for a particular date from the nearest rainfall stations are tabulated into MS Excel spreadsheet. During the data tabulation, it's found that the rainfall duration corresponding to landslide occurrences in study area range from 1 to 19 consecutive rainfall days. The rainfall data was averaged then plotted into a scatter graph. The averaged rainfall (mm) and the duration (day) were plotted into Y axis and X axis of the scatter graph respectively. A power trend line and its equation were added into the graph. The power trend line equation is used as the equation for intensity-duration rainfall threshold for landslide occurrence in the study area. Value resulted from this equation shows the approximate minimum rainfall intensity (mm) of a certain duration (days) or vice versa needed to trigger landsliding in Wadaslintang watershed.

Antecedent Rainfall Threshold

Antecedent rainfall thresholds were calculated based upon the dates of slope failure which were extracted from the verified landslide in the area. Differ from the previous rainfall threshold above, the antecedent rainfall threshold using cumulative rainfall of previous days before the day of failure. Cumulative rainfalls were calculated for 3-, 5-, 10-, and 15-days before day of failure. The cumulative rainfall prior to day of failure and rainfall at the day of failure were plotted into X axis and Y axis of a scatter graph respectively. Antecedent rainfall threshold equation was derived from equation of linear trend line added to the scatter graph. The approximate lower bound precipitation threshold was visually identified on the scatter plot (Chleborad, 2003; Kuthari, 2007). The calculation was performed separately for the four cumulative rainfall durations prior to day of failure.

3.4.4. *Rainfall Recurrence*

To calculate the rainfall recurrence, a series (29 years) of annual maximum daily rainfall was constructed, sorted and ranked in ascending order of magnitude. The recurrence interval (*TR*) corresponding to the rank was computed after Left Probability

(LP) (=P' in equation (2)) and Right Probability (RP) was calculated using following formula:

$$LP=n/(m+1) \quad RP=1-LP \quad TR=1/RP \quad Y=-\ln(-\ln(LP))$$

where n is the number of years on record, and m represents the event rank in order of magnitude. Y indicates value in Y axis of scatter plot for this analysis. All these calculation were performed in tabular of MS Excel spreadsheet.

After completing the calculations above, a scatter plot was constructed where sorted rainfall (mm) was plotted to X axis and Y value to Y axis. A linier trend line was added to obtain the linear equation which will be used to calculate return period of particular rainfall or vice versa by involving equations (1), (2), and (3) above. A chi-square test was performed to compare the tabular value and the calculated value using the equations (1), (2), and (3).

3.4.5. Terrain Hydrological Condition

Infiltration rate and cumulative infiltration

Data from field measurement (actual infiltration) was arranged into MS Excel spreadsheet. The equation (4) was used to determine the predicted infiltration, in which the f_n is the actual infiltration rate (cm min^{-1}) of corresponding time step (minute) and f_c is constant actual infiltration rate (cm min^{-1}). k values were determined using equation (5) and was chosen by substituting into equation (4) which gave the best fit between actual and predicted infiltration rates. The actual and predicted infiltration rates were plotted into Y axis of a scatter graph and time step (minute) into X axis.

Cumulative infiltration was computed using equation (6). Again, the f_n is the actual infiltration rate (cm min^{-1}) of corresponding time step (minute) and f_c is constant actual infiltration rate (cm min^{-1}). The k value involved in this equation is the same value of predicted infiltration rate. The cumulative infiltration also was plotted into Y axis and the corresponding time step into X axis in a scatter graph.

Soil moisture change, permeability, and texture

As stated previously, several soil properties were determined in laboratory by analyzing the disturbed and undisturbed soil samples taken from field. The soil properties included initial moisture content, soil permeability, and soil texture.

Soil moisture change in the particular location of the study watershed was calculated using equation (7). Initial soil moisture (%), θ_o , was determined in laboratory, whereas the maximum soil moisture content (%), θ_s , was derived from Soil Water Characteristics software version 6.02.74. The time step corresponding to soil moisture content and the k value used in this equation was the same with of involved in calculation of predicted

infiltration rate and cumulative infiltration. After finishing the calculation, a model was developed correlating soil moisture and infiltration rate. By arranging in a scatter plot the series of soil moisture content into X axis and the series of infiltration rate into Y axis, an equation of linear trend line was obtained showing their relationship. This equation then can be used to predict the infiltration rate at various soil moisture contents.

Soil permeability at several locations in the study area also was derived from undisturbed soil samples; meanwhile the soil texture for each location was analyzed based upon disturbed soil sample. The soil textures then were plotted on a graph using *DPlot*, an add-ins of MS Excel 2007 (see Figure 42).

3.4.6. *Terrain stability index*

Terrain stability index of the study area was computed using SINMAP, an ArcView extension. After installing this extension, a "Sinmap" menu will appear on ArcView toolbar and used to perform the stability analysis. This extension uses Spatial Analyst extension from ESRI to run geographic analysis.

Stability indexes are output by the analysis that represent the stability of terrain and hence the likelihood of landsliding. These indices are not intended to be interpreted as numerically precise and are most appropriately interpreted as indications of "relative" hazard (Pack *et al.*, 2001).

There are 4 steps involved in this analysis: 1) Pit filling corrections, 2) Computation of slopes and flow directions; 3) Computation of specific catchment area; and 4) Computation of the SINMAP stability index. To perform this analysis, SINMAP used a 10-m DEM of the study area built from digital topographic map scale 1: 25,000 and landslide point map based on verified landslide in the study area. The landslide inventory map is used to verify the result of SINMAP analysis. The constant infiltration rate, soil depth, and rainfall threshold can be used to determine T/R ratio. However, the soil depth in the study area was not obtained during the fieldwork, that's way the analysis was run under the default parameters.

3.5. Reporting

In this phase, results of the research were delivered into result, discussion, conclusion and recommendation. This phase is the latest step in this research and as a media of communicating the research result with other people.

4. STUDY AREA

4.1. Wonosobo District

Wonosobo, district in Central Java Province, is located at 7°11" - 7°36" S and 109°43" - 110°04" E and the elevations varies from 120 – 3,350 m (msl). The area extent is 98,468 ha, divided into four parts according to its slope: gently sloping (3-8%), 54.4 Ha; sloping (8-15%), 7,769.1 Ha; Moderate Steep (15-40%), 42,173.6 Ha; and Steep slope (> 40%), 31,829.9 Ha. In general, the northern part of the area is mountainous region, followed by hilly area in the middle, and flat area in the southern part. The area composed of various soil types: Andosol (10,778 Ha), Regosol (19,302 Ha), Latosol (62,815), Organosol (758 Ha), Mediterranean Red-Yellow (3,043 Ha), and Gromosol (1,772 Ha) (Anonymous, 2008).

Wonosobo is bordered with several regencies; in the northern part with Kendal and Batang, in the Eastern part with Temanggung and Magelang, in the Western part with Banjarnegara and Kebumen, and in the Southern part with Kebumen and Purworejo. Wonosobo district consists of fifteen sub-districts: Kejajar, Watumalang, Garung, Mojitengah, Sukoharjo, Wonosobo, Kertek, Leksono, Kalikajar, Selomerto, Kaliwiro, Sapuran, Kalibawang, Wadaslintang, and Kepil. Figure 13 below shows the administrative map of Wonosobo District and the research site.

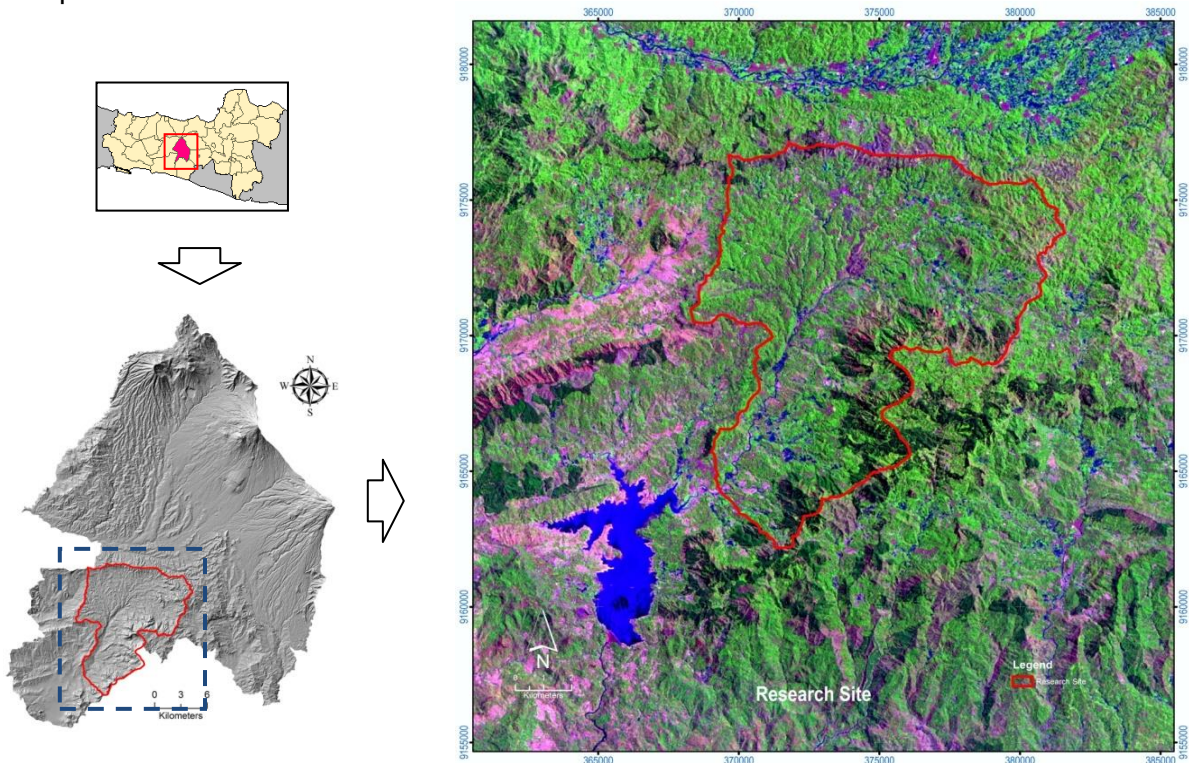


Figure 13: Administrative Map of Central Java Province (not scaled), Wonosobo District and the Research Site

4.2. Wadaslintang Watershed

Research site is located in a watershed in Wonosobo District lying in two Sub Districts: Wadaslintang and Kaliwiro with total extent of 11,183 Ha, and being the main catchment for a dam downstream used for hydro-electricity power. The watershed is located geographically in zone 49S UTM, from 366590 – 381562 X and 9177182 – 9162181 Y. As shown in Figure 14 below, the study area consists of mountainous region in eastern part and northeastern part of the catchment and gently sloping to hilly/undulating region in most of the area. The catchment is split by a fault line indicated by the nearly-straight main river. The landsliding is problematic almost in the whole catchment.

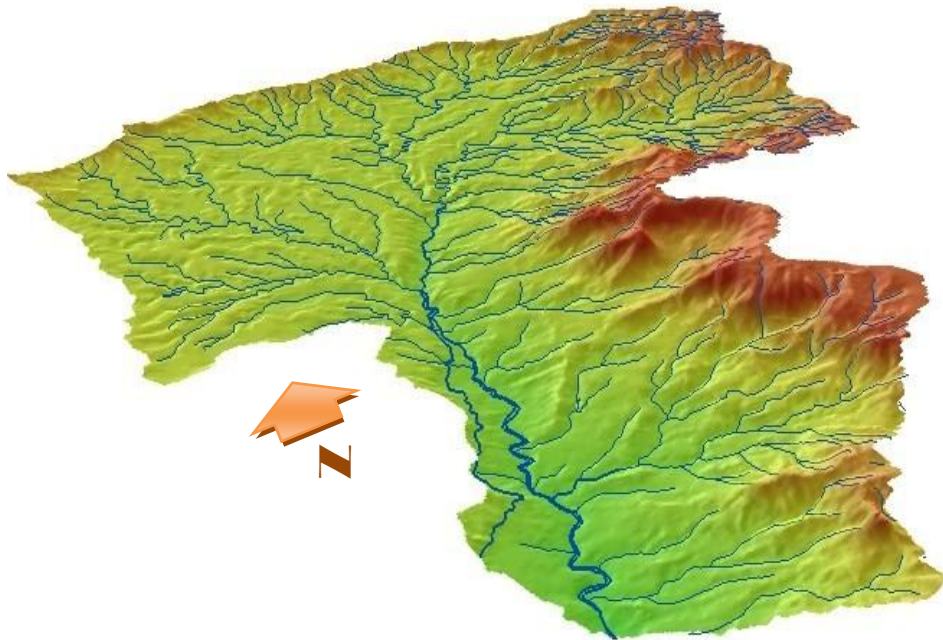


Figure 14: 3 D View of the Study Area (not scaled)

Land use

There are five main land use types in the study area: Rice field (rainfed and irrigated) in the surrounding main river and tributaries, mix garden, shifting cultivation on the steeper slope, forest on the mountainous region, and settlement which is clustered, mainly near the road. Mix garden occupies the largest area spreading throughout the catchment. The main crop of this land use is Sengon tree (*Albizia falcataria*), mixed with seasonal crops, such as cassava and banana, or with low-lying crops, such as coffee and kapulaga (*Amomum cardamomum*). The Sengon tree can be found throughout the study area, even in the backyard of the houses of the local people. The trees have been widely planted

since the “Sengonisasi” terms (Sengon movement) introduced by The Ministry of Forestry around 1990s. Since the tree is categorized as fast-growing tree, the tree can be harvested when it of 5 years old to be used for utensils or furniture. After harvested, the tree will be replanted again. The trees provide extra income for the local people.

By means of GIS, the percentage of each land use can be derived, as follows: Rice field (14.85%), Mix Garden (44.04%), shifting cultivation (13.49%), forest (6.80%), and settlement (10.40%). The subsequent figures show the land use types in the study area.



Forest (Pine Forest)



Mix Garden



Irrigated Rice Field

Rainfed Rice Field

Figure 15: Land use types in the study area.

Altitude

The elevation of the study area varies from 185 – 1,100 m above sea level, and the terrain morphology ranges from plain to mountainous. The Figure 16 below presents the elevation classes in the study area. Above the elevation 925 m msl the area is inaccessible.

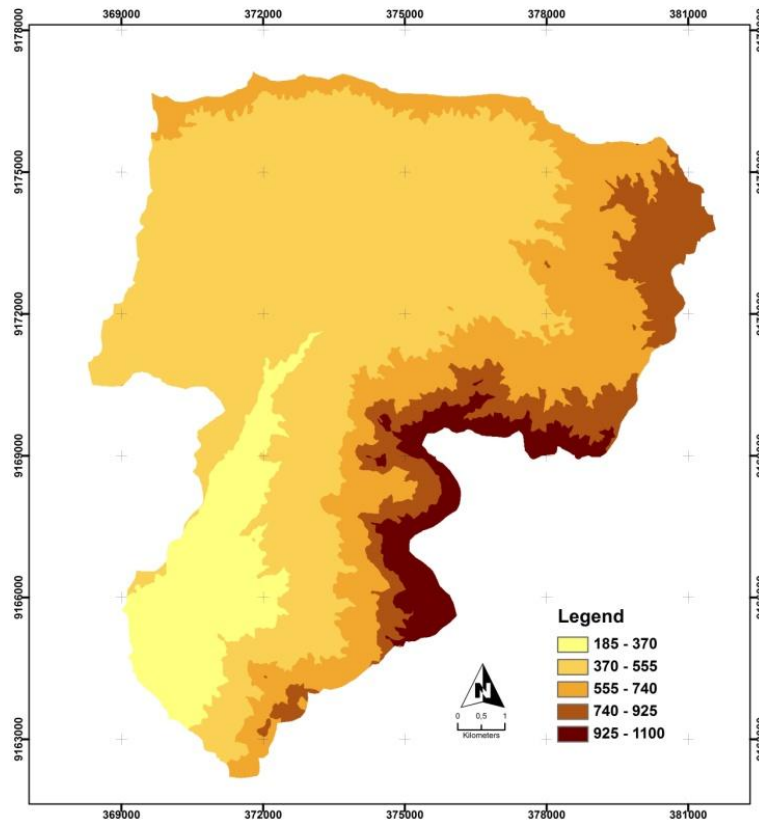


Figure 16: Elevation variety of the study area

Geomorphology (Landform)

The study area consists of three land form types based on Verstappen classification. The landform types were delineated from hillshade map derived from DEM of the study area. The three land form types are: denudated mountains, denudated hills, and foot slopes (see Figure 17 below). The denudated mountain is located on the higher and steeper area then followed by the foot slope. The denudated hills occupy plain to gentle slope below the denudated mountain landform and separated from foot slope landform by a fault line.

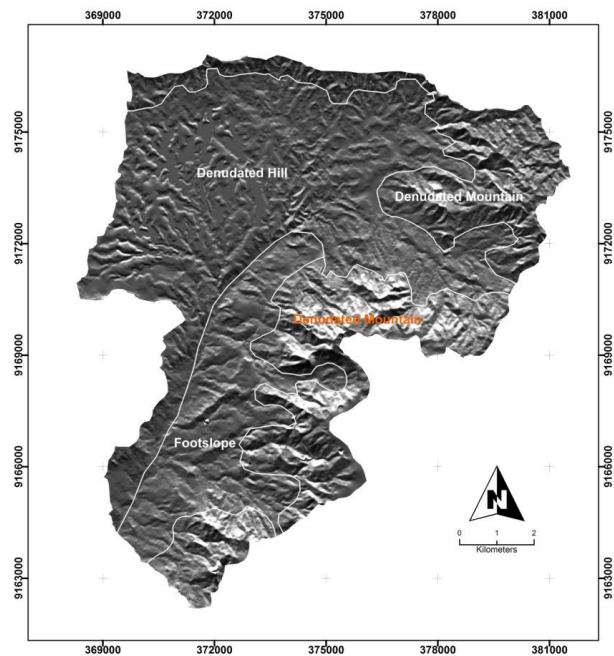


Figure 17: Landform classification of the study area

Climate

Observation of 29-year recorded daily rainfall data (year 1980 – 2008) from 2 main rainfall stations in the study area as shown in the figure below shows that monthly precipitation in the study area can range from 34 – 511 mm with mean annual rainfall of around 3.520 mm. The data also shows general pattern of rainfall distribution in a year. It can be noted that rainy season begins in October continuous to April in the following year. About 50 % of annual rainfall is received in January to April and 30 % in October to December.

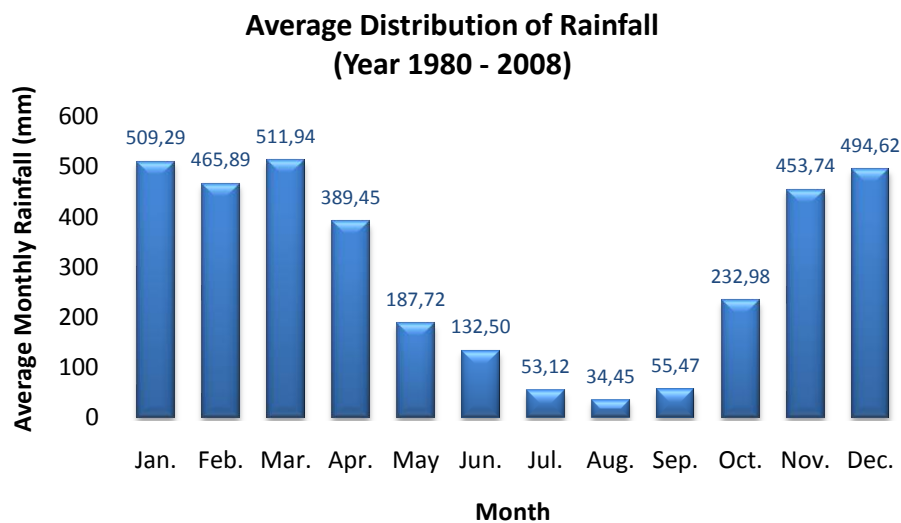


Figure 18: Monthly Precipitation in Period of 1980 - 2008

Drainage

Medono river is the main river in the study area which flows along the fault line in the study area. The river is being very important as it's the main inlet for the dam downstream and also for the agricultural and other human activities along the river. The reservoir is not only used for generating hydro-electricity power but also utilized for other sectors, such as recreation (kayaking, camping, and fishing), and river-fishery. River-fishery developed in the dam is Karamba (floating fish basket) which gives extra income to the people, since it meets the fish (fresh water fish) demand for the local people and for the nearby big cities (Semarang, Jogjakarta).

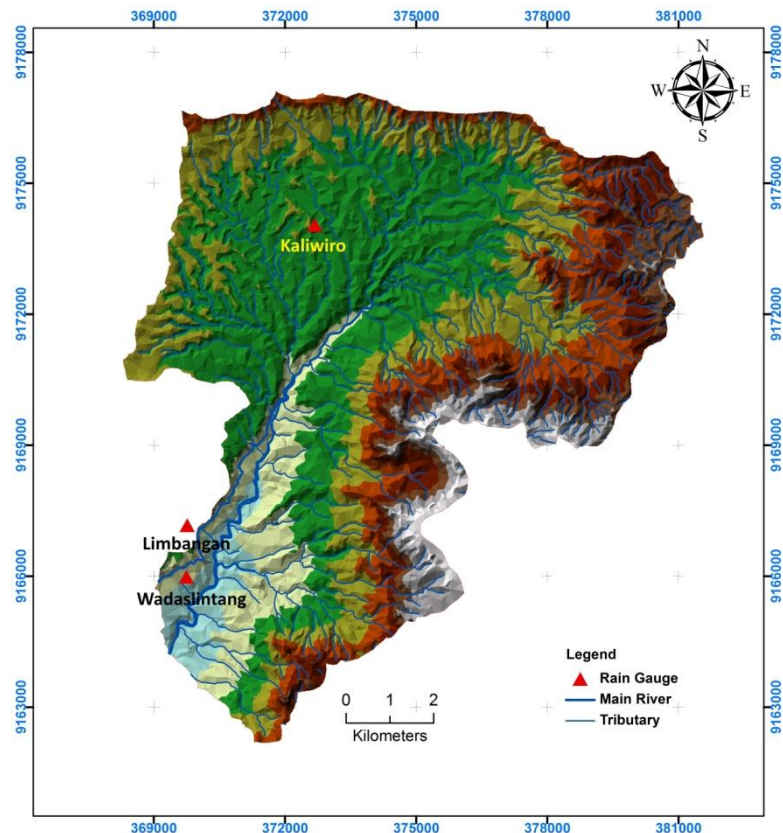


Figure 19: Drainage Map showing the main river, the tributaries and the rain gauges.

Landslides in the study area

Observation during fieldwork reveals that the study area experiences various types of landsliding. Rotational landslide is the most common type found in the area. The other types are creep in very gentle slope to plain area, and debris flow on the steeper mountainous area. The scarps of older landslide, especially shallow landslides, can hardly be identified in the field, due to natural resilience and human intervention. Scarp of the landslide will be covered immediately by pioneer plants, such as shrubs or grasses, since the area is located in the fertile volcanic area. Besides, the scarp will be replanted again

by the farmer if the landslide occurred in their agricultural area. Subsequent figures show schematic profile of a newer deep-seated rotational landslide from Dadap Gede Sub-village which is located in the study area.

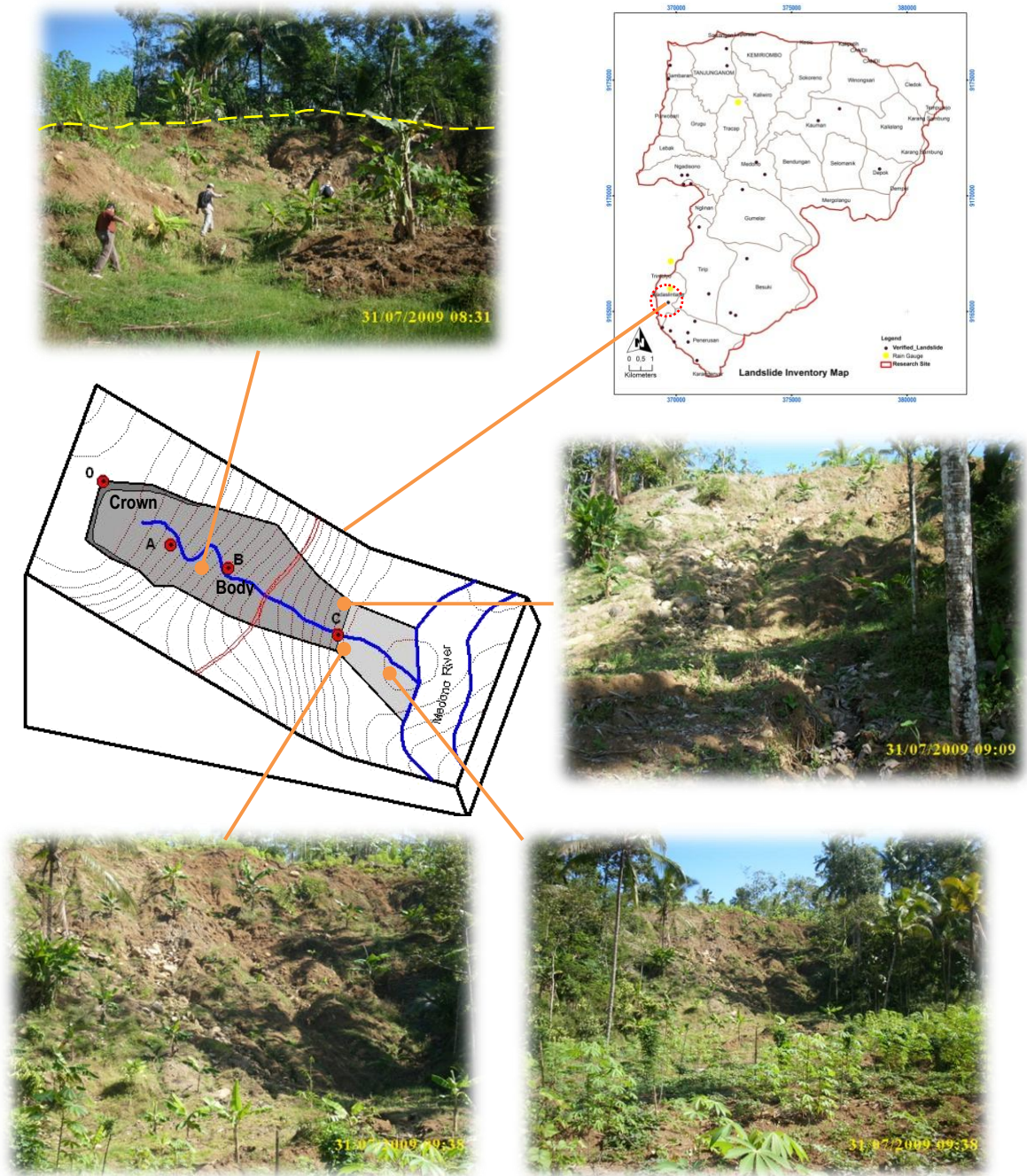


Figure 20: Dadap Gede landslide, showing position, profile and its overview.

To depict the landslide scar in the upper-left most photo in Figure 20, it can be estimated by comparing with the people in the picture above. Another approach to get the better depiction about the dimensionless of the Dadap Gede landslide is by profile schema based on transect lines across the landslide body, as presented in the figure below.

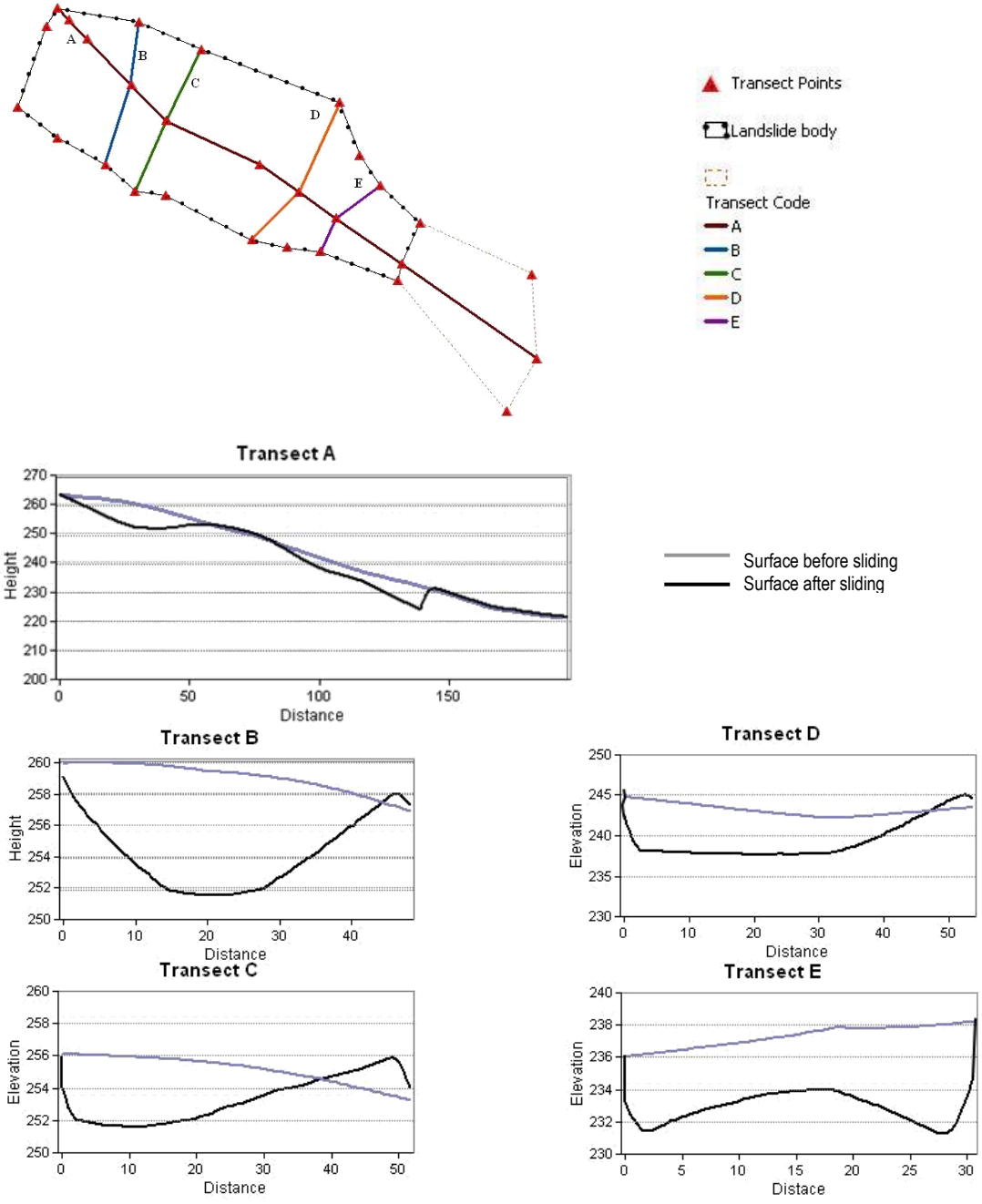


Figure 21: Dadap Gede landslide profile based on transect lines

5. RESULT AND DISCUSSION

5.1. Landslide Inventory

The research is based on the official disaster report of Badan Kesbanglinmaspol of Wonosobo District, Indonesia (Anonymous, 2009b). The report compiles all disasters occurring (floods, fires, landslides, and hurricanes) in Wonosobo District since 2001 to early 2009 where the type of disaster, date and time of occurrence, location (sub-district, village, and sub-village), damage to property (house or infrastructure), victims (death and injured), estimation of loss, and financial compensation received by the victim (house owner) are shown (see Figure 22 below).

The research relies on the report, since it is officially verified and provides data needed for the research analysis. The data provided in this report is based on officially reported disasters from lower governmental institutions (sub-village, village, and sub-district chronologically) directed to regent through Badan Kesbanglinmaspol, a governmental institution at district level. In response to the reported disaster, the regent represented by Badan Kesbanglinmaspol verifies the disaster's effect at the site in order to assess the degree of damage and to estimate the loss as basis for financial compensation from district government to the victim.

**DATA KEJADIAN BENCANA
BULAN JANUARI S/D DESEMBER 2003**

No	JENIS BENCANA	TANGGAL	TEMPAT KEJADIAN	MACAM / TAKSIRAN KERUGIAN	BANTUAN APBD (Rp)	BANTUAN PROPINSI (Rp)
1	Tanah Longsor	01 - 01 - 2003 JAM 14.00 WIB	Bp. WAGINO dan RIBUT Sumberan selatan Rt.01 Rw.21 Kel. Wonosobo Kec. wonosobo	Kerugian ± Rp 3.000.000,-	Rp 1.000.000,-	-
2	Tanah Longsor & bergeser	03 - 01 - 2003 23.00 WIB	Gedung SDN I (4 lokal Ambles & bergeser) Dusun Lamuk Desa Kalibening Kecamatan Sukoharjo	Kerugian ± Rp 50.000.000,-	-	-
3	Tanah Longsor	04 - 01 - 2003 JAM 21.00 WIB	Ny. KODIM Bugangan Rt.01 Rw.VI Kalurahan Kalianget Kecamatan Wonosobo	Kerugian ± Rp 2.000.000,-	Rp 500.000,-	-
4	Tanah Longsor	04 - 01 - 2003 JAM 14.00 WIB	Serambi Masjid Kembaran Dusun Kembaran Desa Kembaran Kec. Kalikajar	Kerugian ± Rp 30.000.000,-	Rp 5.000.000,-	-
5	Angin ribut/Topan	05 - 01 - 2003	MASJID Wulungsari Dsn Blindeng Ds Wulungsari Kec. Selomerto	Atap masjid dan tembok belakang hancur 7 x 10 m	Rp 3.000.000,-	-
6	Tanah Longsor	05 - 01 - 2003	Bp. AHMADI, KUSNUDIN dan HADI SUWITO Dusun Depok Desa Depok Kec. Kaliwiro.	Kerugian ± Rp 3.000.000,-	Rp 1.500.000,-	-

Figure 22: Structure of the disaster report of Wonosobo District (Anonymous, 2009b).

To locate and to map the landslide position, I met the head of the villages or sub-villages then they showed me the location. During the fieldwork observation, it's found that some of the reported landslides occurred caused by slope cutting for settlement and road. Kind of these landslides, human induced landslide, were left out and didn't be tallied for analysis.

Of the total 56 landslide events reported and then verified in the study area, there are 28 of them categorized as natural induced landslides which are used for the research analysis. Commonly, there are two types of landslide observed among the verified landslides: deep-seated rotational landslide and creep. As the creep is frequently reoccur in the same location, only the most damaging event that recorded in the disaster report. The following photos (Figure 23) show the example of landslide types in the study area. Crack in the house wall (shown by yellow arrows) as impact of creep (left photo) and the dotted yellow line shows the crown of a deep-seated rotational landslide (right photo). Other documentations of landslides in the study area are presented in Appendix....



Figure 23: Traces of landslides in the study area.

Despite the valuable data provided by the official disaster report above, it's noted that it has some drawbacks based on fieldwork observation. One of the drawbacks is incomplete inventory. As presented in Figure 22 previously, mainly the recorded landslides are the damaging events, either to the houses (sometimes resulted in death) or to infrastructures, thus landslides which have minor damage effect or small scale landslide events will be neglected. Because of that, the recorded landslides are commonly located in settlement area which lays only on 10.40 % of the total area. Big event landslides located in inaccessible area or in locations far away from daily human activities will be perceived not as threat. This opinion was gotten during fieldwork activities and is held both by local people and by government. Deep-seated rotational landslide in Figure 23 above is an example of unreported landslides. Figure 24 below also displays one of unreported big landslides in the study area. In the 1994 aerial photo provided by Bakosurtanal (upper left picture), the location is still forest area but in the 2006 SPOT Image (upper right picture) the area is bare land, interpreted as landslide body. The interpretation is proven by the photo taken in August 2009 during fieldwork. The landslide is located on the very steep slope, on the upper part of pine forest. The scarp is still can be recognized visually.

Another drawback is that process of reporting process to the upper governmental level might be subjective. During the fieldwork I found house owner that has not received financial compensation although he has moved his house to another location. His previous house has been demolished due to creep that hit the house frequently. His home also was not listed in the landslide report.

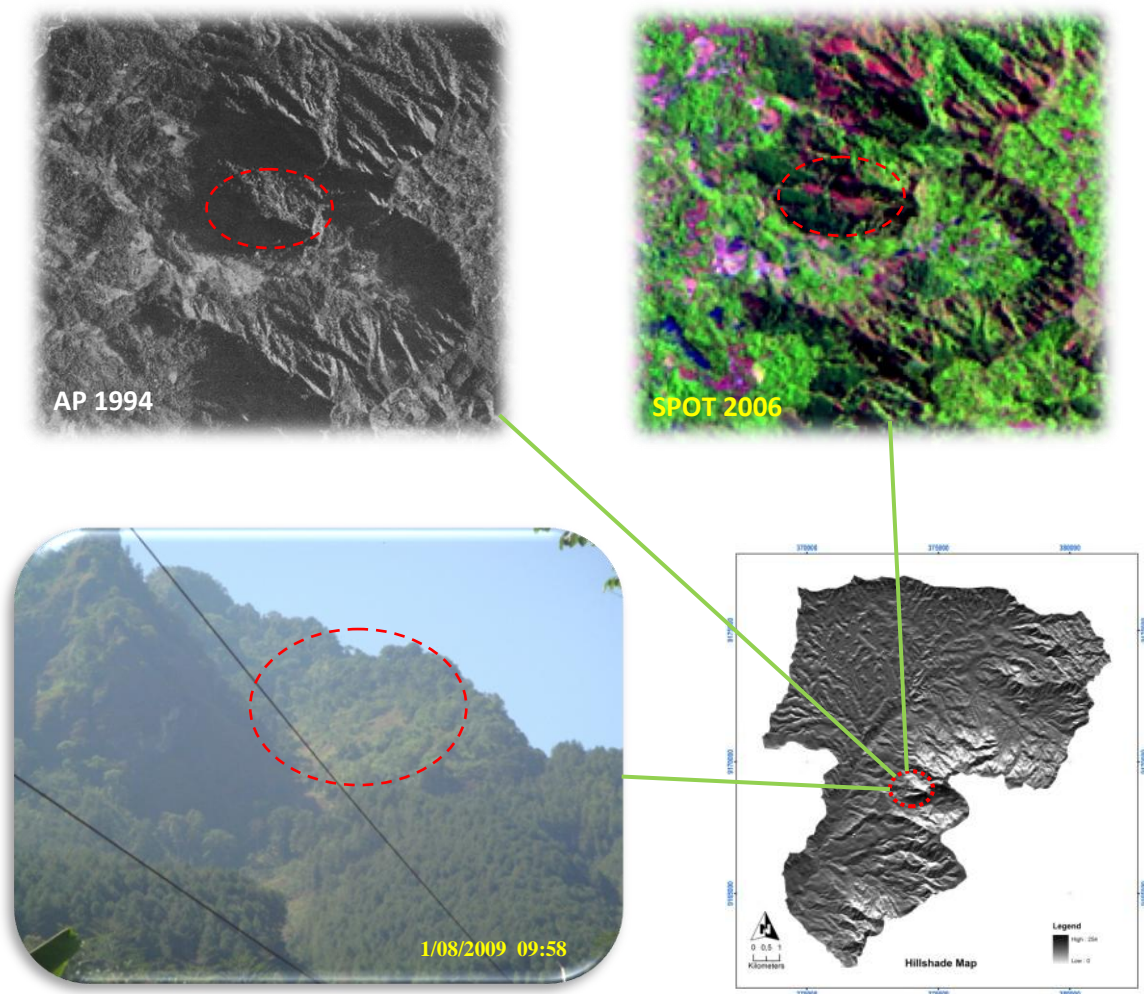


Figure 24: Example of unreported landslide, showing appearance before and after failure, remained scarp, and its position in the study area.

Figure 25 below exhibits completely verified reported landslide in the study area which is laid on official record. Since the research analysis is highly data depending in terms of date of failure, the observed remained landslides such as presented in Figure 23 & Figure 24 above cannot be tallied into landslide data base. Interview with local people also doesn't give sufficient data as they only remember bigger and recent event in their area. Moreover, their approximate remembrance (around early of rainy season, around early of December, etc) can lead to misinterpretation which will finally result in bias of the data.

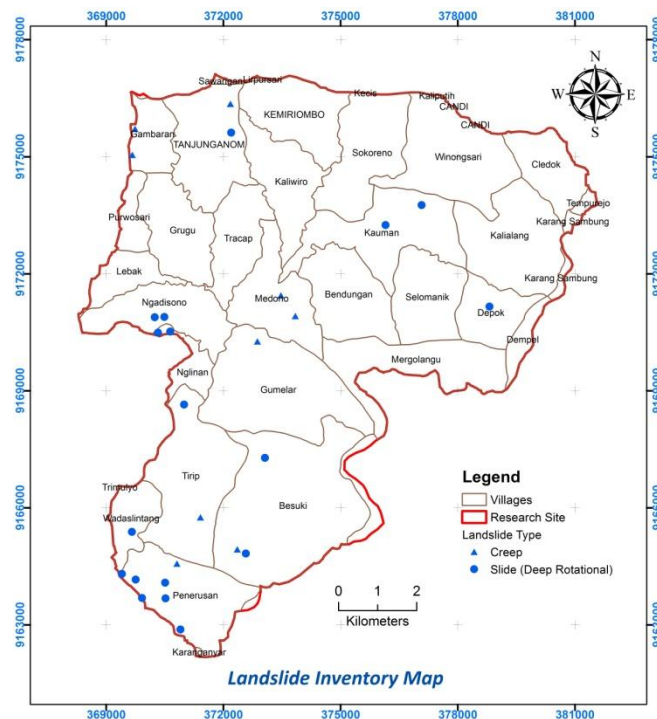


Figure 25: Distribution of verified landslide in the study area.

5.2. Rainfall Data

Rainfall data was collected from Public Work of Wonosobo District. There are 3 rain gauges in the research site (see Figure 19): Kaliwiro, Limbangan, and Wadaslintang. Rainfall data from Limbangan Station is incomplete due to gauge malfunction for 5 years (year 2003 to 2008), thus the data was involved limitedly in the analysis.

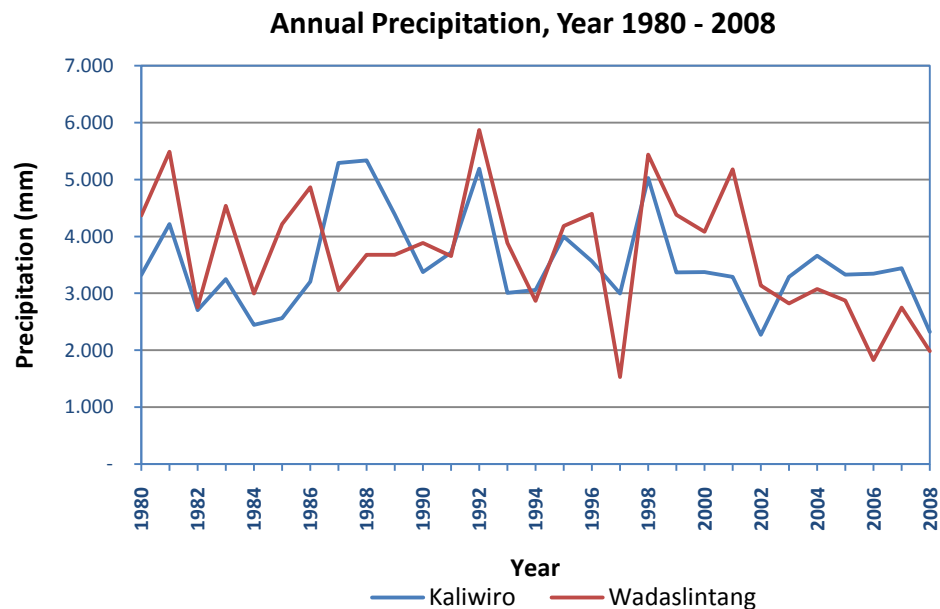


Figure 26: Distribution of rainfall in the study area over the years of 1980 to 2008

Annual rainfall data presented in Figure 26 indicates that rainfall in the study area is quietly high. In period of 29 years the rainfall in the study area ranges from 2.000 mm year⁻¹ to 6.000 mm year⁻¹. The rainfall period also shows a decline trend with some fluctuations.

In relation with landslide incidences in this area, precipitation is can be regarded as the main triggering factors. Information found during the field visit shows that the relationship between precipitation and landsliding in the area is well known by the local people as they confirmed that landslide season is begun at early of rainy season. They also experienced that cracks in soil produced during summer as preliminary guide to slope failure in the rainy season.

The Figure 27 below presents distribution of monthly precipitation and landslide events in years of 2001 to 2008. The data for the whole district was used for statistical reason. The figure indicates that landslide incidences fit with the rainfall pattern, by which confirms that maximum landslides occurred during the wet season. Based on the statistic for the years of 2001 to 2008, 179 landslide incidences occurred in January to April which is about 49 % of the total recorded landslide. Again, in period of October to December, there were 166 (45 %) landslide events occurred. The maximum landsliding incidence occurred in December, in which 550 mm monthly precipitation is recorded.

To assess the degree of correlation of amount of precipitation and landslide incidence, a relationship graph of them was performed in Excel spreadsheet (Figure 28). The relationship has a coefficient correlation as $r^2 = 0.8985$. It suggests that a high correlation exists between the precipitation and the landslide event.

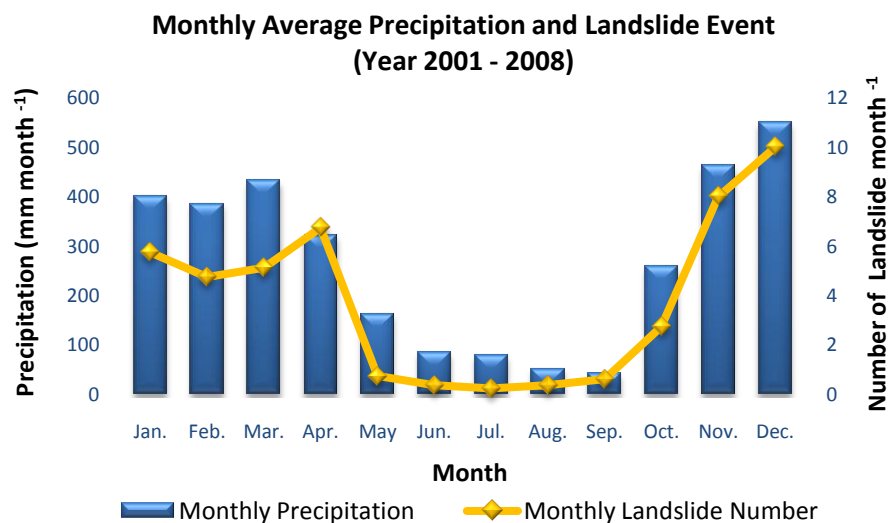


Figure 27: Distribution of monthly average precipitation and number of landslide in years of 2001 to 2008 in Wonosobo District.

Similar to probability of landslide incidence per month, December holds the highest probability, then followed by November, April, January, March, and February, with probability consecutively of 0.22, 0.18, 0.15, 0.13, 0.11, and 0.10. The rest months have probability below 0.10. December has the highest probability as this is the peak rainy season every year.

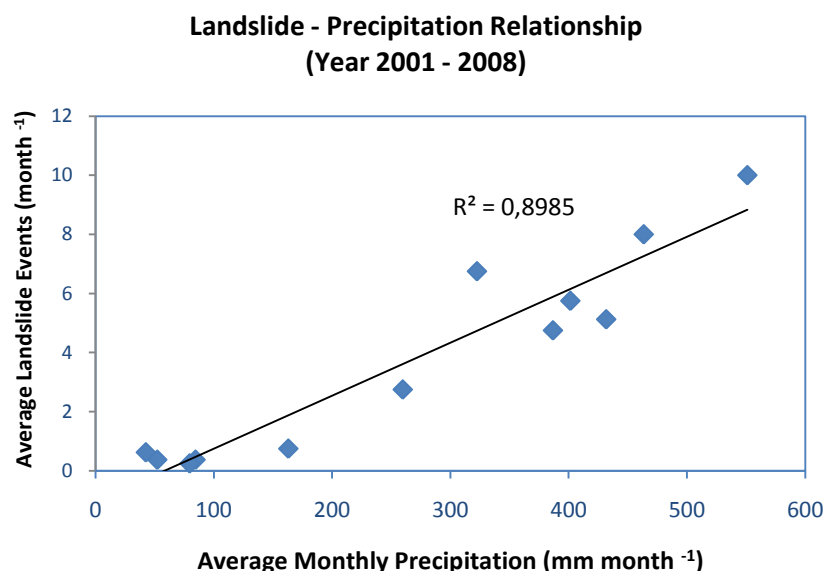


Figure 28: Relationship between monthly number of landslides and monthly precipitation in period of 2001 to 2008

5.3. Rainfall Thresholds

Rainfall data from three rain gauges in the research site was used to analyze rainfall thresholds for the landslide occurrences. Rainfall data from the nearest rain gauge is regarded corresponding with the surrounding landslide events. Using the rainfall data corresponding with the 28 landslide events, an intensity-duration rainfall threshold for landslide initiation was established (Figure 29). The threshold duration is day because only the daily rainfall data available for analysis. The hourly rainfall station is located outside of the research site, thus can't be used for analysis due to bias in data recording.

The relationship between rainfall intensity and duration for landsliding in the study area is defined by the following formula:

$$I = 63.683D^{-0.336} \quad (14)$$

where I is the rainfall intensity in mm day^{-1} , and D is the rainfall duration in days.

According to this threshold relation for rainfall event with shorter duration such as less than 5 days, rainfall intensity of at least 37 mm day^{-1} is needed to trigger landslide.

On the other hand, an average precipitation of less than 20 mm day⁻¹ is sufficient to cause landsliding if rainfall is continued for more than 31 days.

The equation above suggests that once the intensity-duration of rainfall exceeds the value predicted by the equation, it may provoke slope instability in this area. However Equation (14) is the minimum requirement for triggering landslides in the study area, it may need a higher intensity-duration for a specific slope. This is analogously with coefficient correlation $r^2=0.6082$ presented in the intensity-duration curve (Figure 29 below). The value implies that there is a moderate correlation exists between intensity and duration at failure. The condition can lead to occurrence of both “false positive” (i.e. predicted landslide events that do not occur) and “false negative” (i.e. occurred landslide events that are not predicted) (Z^{ezere et al.}, 2008).

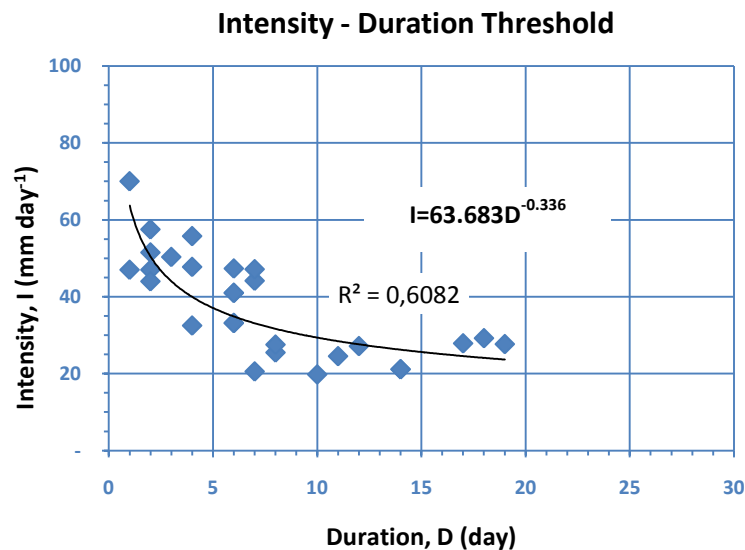


Figure 29: Rainfall intensity – duration thresholds curve for landsliding in Wadas Lintang watershed.

Previous researchers (Van Asch *et al.*, 1999; Glade *et al.*, 2000; Guzzetti *et al.*, 2007; Dahal *et al.*, 2008; Hasnawir *et al.*, 2008; Z^{ezere et al.}, 2008; Sengupta *et al.*, 2009) have done abundant works pertaining rainfall thresholds related with slope instability. All of these works indicate that the threshold varies from one region to the other regions and doesn't follow a general pattern. Moreover, the researchers state that slope movements are usually correlated with distinct hydrological triggering condition that may be influenced by different rainfall intensity – duration, even in a single region.

The Equation (14) is quite lower than rainfall threshold proposed for landslide and debris-flow in Mt. Bawakaraeng, South Sulawesi (Hasnawir *et al.*, 2008), which is ruled by formula $I = 86.517D^{-0.408}$. This relationship indicates that rainfall lasting less than 5 days needs intensity of 44 mm day⁻¹ to trigger landslide and debris flow, while an average

precipitation less than 20 mm day^{-1} is sufficient to trigger landslide and debris-flow if continued for 36 days. When compared with rainfall threshold for triggering landslide in Lisbon (Zezere *et al.*, 2008), the Equation (14) still gives lower value. The rainfall thresholds proposed for this region is $Ri=84.3D^{-0.5}$, hence Ri is rainfall intensity (mm day^{-1}) and D is duration in days. Despite the value of the threshold, the effect of North Atlantic Oscillation also found to play an important role for landslide events around Lisbon.

Nevertheless the proposed value in Equation (14) is based on limited data; this is the only available data that can be used as preliminary early warning for possible slope failure in this area. The proposed value still needs validation through continuous observation of landslide occurrences in the area.

5.4. Effect of Antecedent Rainfall

Antecedent rainfall influences the saturation of soil and groundwater level, thus can be used to determine when landslides are likely to occur (Van Asch *et al.*, 1999; Guzzetti *et al.*, 2007; Sengupta *et al.*, 2009). In combination with soil moisture, antecedent rainfall controls the quantity and duration of critical precipitation to landsliding (Crosta, 1998). Figure 30 below presents rainfall data and landslide events occurring in period of 1 January 2001 to 31 March 2009. The figure indicates that some landslide events correspond to very low rainfall event. Yet, in general the landslide events followed periods of heavy rainfall persisted for several days. This confirms that certain minimum amount of rainfall is required to saturate the ground surface at the slide location. Newer big landslide presented in Figure 20 is an example. At the time of failure, the nearest station recorded total 24 h rainfall of 9 mm, seems unrealistic to cause landsliding, but a total of 309 mm of consecutive previous 18 days regarded to play role for the failure.

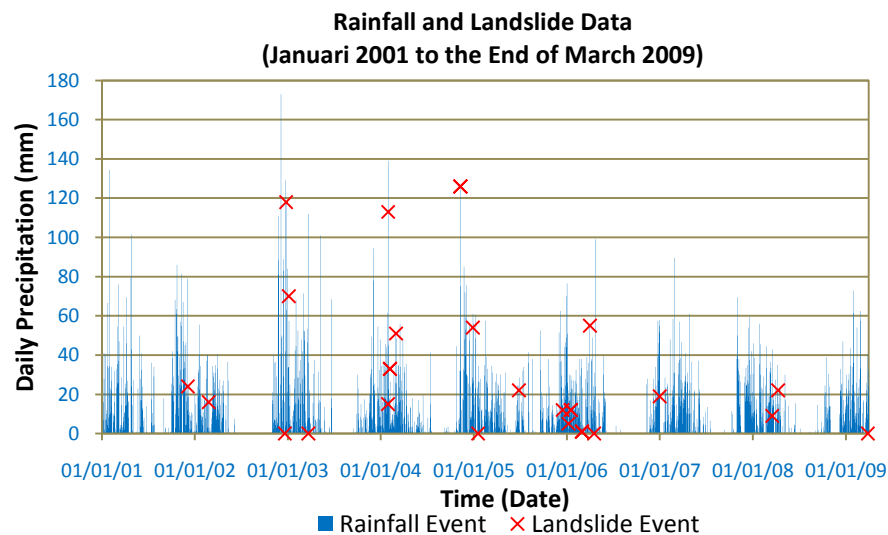


Figure 30: Rainfall and landslide data in Wadaslintang watershed.

To assess the role of antecedent rainfall in triggering landslide in the research site, the antecedent rainfall thresholds were defined. The time durations of the antecedent rainfall taken into consideration in this research were 3, 5, 10, and 15 days. The minimum thresholds for each relationship between landslide and cumulative antecedent rainfall is shown by the orange line used to indicate the lower bound of the threshold. This lower bound is identified visually on the scatter plot of daily rainfall and antecedent rainfall. The blue squares indicate landslide events.

5.6.1. Antecedent 3 Days

The relationship between the landslide occurrences with the daily and 3 days antecedent rainfall (Figure 31) is defined by the equation:

$$T = D_0 + 0.398D_3 - 2.7685 \quad (15)$$

where T is the minimum probable thresholds required for landsliding, D_0 is the daily rainfall measured at the time of failure, and D_3 is the cumulative rainfall of three days before the failure.

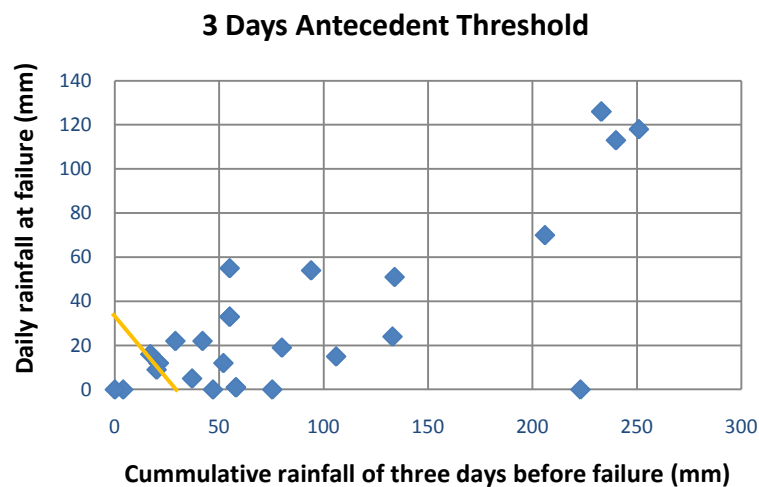


Figure 31: Three Days antecedent rainfall thresholds curve for landsliding in Wadas Lintang watershed.

5.6.2. Antecedent 5 Days

The minimum thresholds of five days antecedent rainfall (Figure 32) needed for triggering landslide can be computed based on the following equation:

$$T = D_0 + 0.3333D_5 - 10.72 \quad (16)$$

where T is the minimum probable thresholds required for landsliding, D_0 is the daily rainfall measured at the time of failure, and D_5 is the cumulative rainfall of five days before the failure.

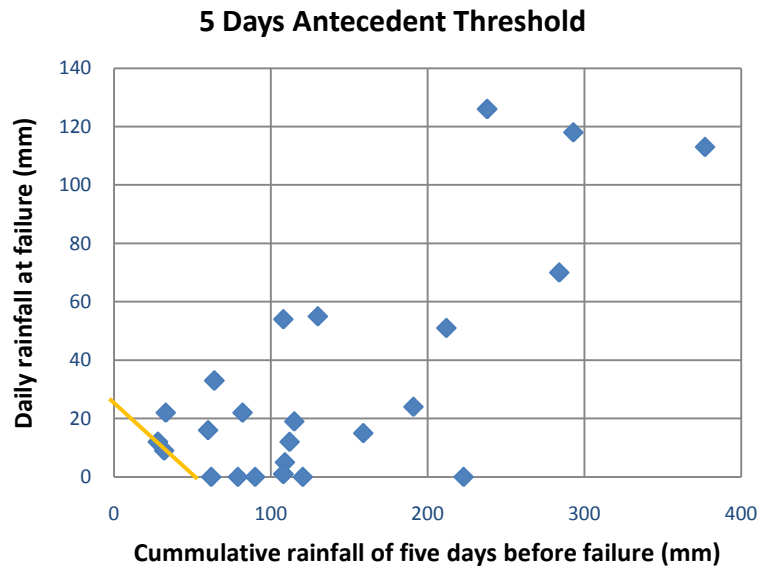


Figure 32: Five Days antecedent rainfall thresholds curve for landsliding in Wadas Lintang watershed

This threshold equation implies that daily rainfall contributes more than the prior cumulative 5 days rainfall. At least 30 mm of prior cumulative 5 days rainfall and around 10 mm of daily rainfall are required to trigger landsliding. Furthermore, at least 64 mm of 5 days antecedent rainfall appears to cause landsliding when combined with 33 mm of rainfall at the day of failure.

5.6.3. Antecedent 10 Days

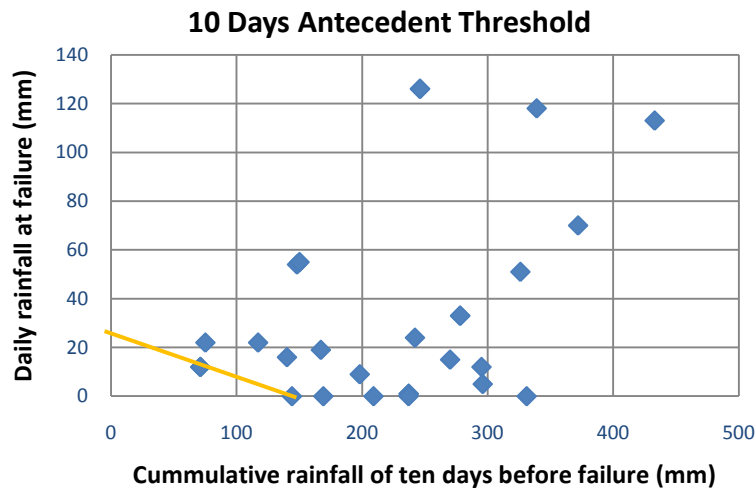


Figure 33: Ten Days antecedent rainfall thresholds curve for landsliding in Wadas Lintang watershed

The minimum basis of the relationship between daily rainfall with ten days antecedent rainfall (Figure 33) is given by the following formula:

$$T = D_0 + 0.182D_{10} - 7.1994 \quad (17)$$

where, T is the minimum probable thresholds required for landsliding, D_0 is the daily rainfall measured at the time of failure, and D_{10} is the cumulative rainfall of ten days before the failure.

5.6.4. Antecedent 15 Days

The minimum threshold for fifteen days of antecedent rainfall (Figure 34) in the study area is defined by the equation below:

$$T = D_0 + 0.1051D_{15} - 0.7320 \quad (18)$$

where, T is the minimum probable thresholds required for landsliding, D_0 is the daily rainfall measured at the time of failure, and D_{15} is the cumulative rainfall of fifteen days before the failure.

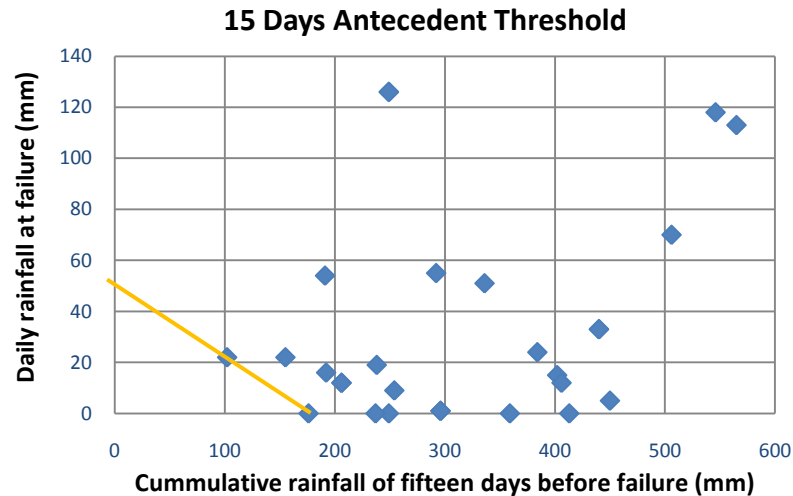


Figure 34: Fifteen Days antecedent rainfall thresholds curve for landsliding in Wadas Lintang watershed

5.6.5. Significance of the antecedent rainfall thresholds

Some researchers (Terlien, 1998; Crozier, 1999; Chleborad, 2003; Aleotti, 2004) found significant influence of rainfall intensity of some periods to govern slope failure. The significance of considered periods of previous rainfall before failure ranges from 3 days to 25 days.

Review of the literatures (Dai *et al.*, 2002; Guzzetti *et al.*, 2007; Sengupta *et al.*, 2009) points out that it's difficult to define the length of period to accumulate the

precipitation. This variability may be affected by several different factors including: (i) diverse lithological, morphological, vegetation, and soil conditions, (ii) different climatic regimes and meteorological circumstances leading to slope instability, (iii) and heterogeneity and incompleteness in the rainfall and landslide data used to determine the thresholds.

On the other hand, the other researchers (Corominas *et al.*, 1999; Aleotti, 2004) didn't find the importance of the antecedent precipitation for the initiation of landslides. They found hydrological properties such as interparticle voids; and presence of large macropores to generate slope failure without significant respect to antecedent precipitation. These two contradictory results lead to debates of whether antecedent rainfall plays a role to trigger slope failure.

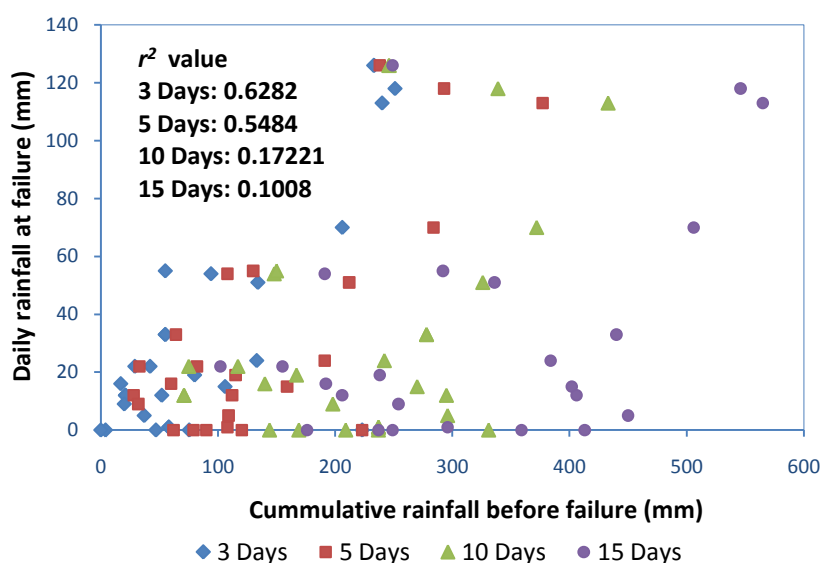


Figure 35: Relationship between daily rainfalls at failure with antecedent rainfall before failure, with correlation coefficient values.

From the data of 28 natural landslide events considered in this study, when the daily rainfall at failure is correlated with the total cumulative rainfall of 3, 5, 10, and 15 days, the scattered population sample data (Figure 35) show the values of relevant correlation coefficients as $r^2=0.6282$, 0.5484, 0.17221, and 0.1008 for 3-, 5-, 10-, and 15-day intervals, consecutively. It exposes that a moderate correlation exists between the antecedent rainfalls of 3 to 5 days and the daily rainfall at the failure. This result is similar to research performed by Rahardjo *et al.*, (2008) in Singapore. His research suggests that under tropical rainfall, antecedent rainfall of maximum 5 days prior to day of failure can influence the stability of slopes.

The influence of antecedent rainfall to landsliding is probably associated with soil texture in the study area. The soil texture in Wadaslintang watershed ranges from clay to loam (Figure 42) with low permeability, and therefore tends to retain water. The soil is saturated after a certain amount of rainfall, and thus influenced by excess water during a rainfall event. Once the soil is saturated and ground water rises up, the debris loses cohesion and starts to flow.

A good correlation is also explained by the type of landslide (deep landslide and creep). As stated by some researchers (Van Asch *et al.*, 1999; Tofani *et al.*, 2006; Z[^]ezere *et al.*, 2008) deep landslide is influenced more by long duration of rainfall. Short duration of excessive rainfall intensity will exceed infiltration rate resulting in higher surface runoff. On the other hand, prolonged moderate rainfall will result in more infiltration that allows the steady rise of the groundwater table reducing the shear strength of affected material.

The mechanism of creep as stated by Bryant (2005) is obviously under presence of expanding clay affected by seasonal inequalities of rainfall. Besides, cohesiveness of clay decreases with increasing moisture content, thus continual creep in clay has its highest rate when the clay is moist for the longest duration.

5.5. Rainfall Recurrence

Rainfall frequency analysis is an analytical method of statistical distribution applied in the study of random hydrological variables such as the annual maximum rainfall. The distribution of rainfall occurrences are estimated by fitting a probability function into observed data. There are two types of uncertainty which exists in such statistical analyses with random variables. The first is associated with the randomness of future rainfall events, and the second is an estimation of suitable relative frequency (Subyani, 2009).

Gumbel distribution, commonly known as extreme value distribution type I, was chosen to be used in this research. This method is one of the most widely used probability density function (pdf) that calculates extreme values in hydrological and meteorological studies which has been applied successfully for the prediction of such meteorological factors both regular-type events (e.g., temperature and vapor pressure) and irregular-type events (e.g., rainfall and wind) (Kotz *et al.*, 2000; Subyani, 2009).

Historical rainfall data (years of 1980 to 2008) from Kaliwiro station was used to derive the rainfall recurrence in the study area. The station is located nearly in the middle of the watershed, thus the data assumed can represent the whole area. Besides, the correlation of mean monthly distribution of the 29-year rainfall data between Wadaslintang and Kaliwiro station is highly correlated ($r^2=0.8502$, the graph is not presented here).

As shown in the Table 3 below, the observed rainfall data is sorted and ranked, then followed by calculation of Left Probability (LP), Right Probability (RP), Time of Recurrence (T), and Y. The calculation employed Equation (1) to (3) to derive the value. The sorted data and Y value then used as X axis and Y axis alternately in following figure to derive the recurrence equation.

The last two ranked data (the most extreme data) in Table 3 are excluded from the data analysis in order to get the equation with higher correlation. According to Kotz *et al* (2000), these extreme data are viewed as independent samples from a homogenous population. Based on the data in Table 3 below and the equation presented in Figure 36, a goodness-of-fit test by means of chi-square (*Chi-test* function in Microsoft Excel 2007) has been done. The test incorporates the sample order statistics (ranked data in the table) and their expected values resulted from the equation. The test gives value of 1.0 assuming that the equation values fit well with the observed data (Kotz *et al.*, 2000; Subyani, 2009).

Table 3: Gumbel Data Analysis Method Based on Kaliwiro Station Data

Year	Rainfall (mm)	Sorted	Rank	Left Probability	Right Probability	TR (Years)	Y
a	b	c	d	$e (=n/(\Sigma n+1))$	$f (=1-e)$	$g (=1/f)$	$h (= -\ln(-\ln(e)))$
1980	97	81	1	0.03	0.97	1.03	-1.22
1981	128	82	2	0.07	0.93	1.07	-1.00
1982	109	86	3	0.10	0.90	1.11	-0.83
1983	90	90	4	0.13	0.87	1.15	-0.70
1984	162	90	5	0.17	0.83	1.20	-0.58
1985	81	94	6	0.20	0.80	1.25	-0.48
1986	115	97	7	0.23	0.77	1.30	-0.38
1987	86	109	8	0.27	0.73	1.36	-0.28
1988	160	109	9	0.30	0.70	1.43	-0.19
1989	140	111	10	0.33	0.67	1.50	-0.09
1990	111	112	11	0.37	0.63	1.58	0.00
1991	118	115	12	0.40	0.60	1.67	0.09
1992	140	115	13	0.43	0.57	1.76	0.18
1993	90	116	14	0.47	0.53	1.88	0.27
1994	115	117	15	0.50	0.50	2.00	0.37
1995	148	117	16	0.53	0.47	2.14	0.46
1996	249	118	17	0.57	0.43	2.31	0.57
1997	215	128	18	0.60	0.40	2.50	0.67
1998	112	137	19	0.63	0.37	2.73	0.78
1999	117	137	20	0.67	0.33	3.00	0.90
2000	140	140	21	0.70	0.30	3.33	1.03
2001	137	140	22	0.73	0.27	3.75	1.17
2002	82	140	23	0.77	0.23	4.29	1.33
2003	117	148	24	0.80	0.20	5.00	1.50
2004	156	156	25	0.83	0.17	6.00	1.70
2005	116	160	26	0.87	0.13	7.50	1.94
2006	109	162	27	0.90	0.10	10.00	2.25
2007	137	215	28	0.93	0.07	15.00	2.67
2008	94	249	29	0.97	0.03	30.00	3.38

Source: Data Analysis, 2009.

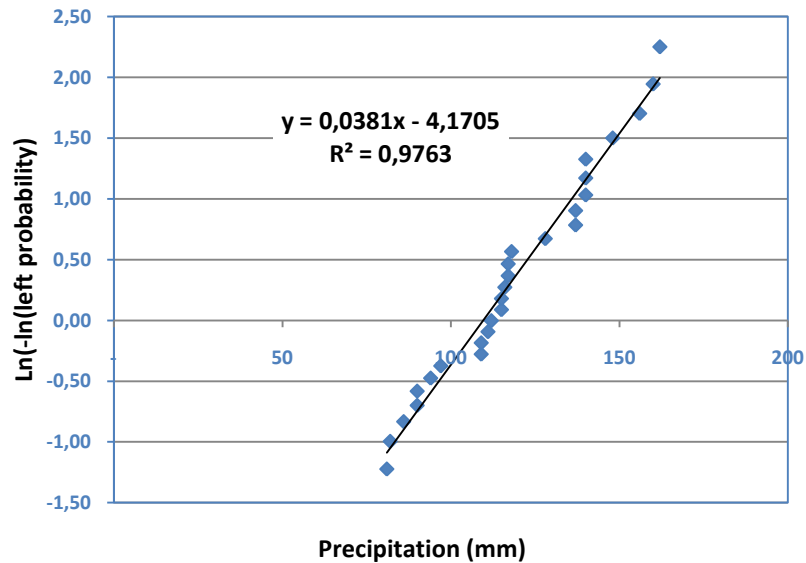


Figure 36: Recurrence Curve, Equation, and coefficient of correlation

To study the recurrence of the rainfall in relation with slope failures, the daily rainfall at day of failure are computed into the equation. Since the data varies, only the data higher than 81 (the lowest data in the ranked data of the Table 3) analyzed for this purpose, as data lower than 81 will give return period of 1 year. The data employed in this analysis are: rainfall of 113, 118, and 126 mm day⁻¹, giving return period respectively of 1.72, 1.94, and 2.42 years. In relation with landsliding, Glade *et al.* (2000), states that temporal changes of such climatic regime (i.e. increased storm frequency with higher magnitude of maximum daily rainfall in a certain year) do not affect the rainfall threshold, but only affect the frequency with which the thresholds is exceeded instead. This will result in a change of the frequency of landsliding.

Another approach was based on the number of yearly rainy days. This approach assumes that longer period of rainy day will result in increment of landslide frequency. The resulted in the equation $Y=0.0316X-4.022$ with r^2 value of 0.9239, and goodness-of-fit value of 0.99. Yearly rainy day years of 2001 to 2008 (reported landslide) are consecutively of 128, 119, 135, 178, 170, 142, 161, and 127 days. The data give return period respectively of 1.6, 1.4, 1.8, 5.5, 4.4, 2.1, 3.4, and 1.6 years. When compared with landslides occurrence in the watershed, rainy day of 178 year⁻¹ and 142 year⁻¹ each recorded 28.57% of the total landslide events, followed by rainy day of 170 year⁻¹ & 119 year⁻¹ each holds 10.71% of the total landslide and the rest rainy days recorded no more than 7%. Based on this data, it implies that year with rainy day more than 110 days year⁻¹ with return period of 1.2 year tends to cause landslide in the study area.

5.6. Terrain Hydrological Condition

5.6.1. Infiltration Rate and Cumulative Infiltration Model

Infiltration rate measurement was done using *double ring infiltrometer* by applying Horton's method. The measurement is done to assess the mechanism of soil saturation affected by rainfall, to determine the infiltration capacity, to determine the constant infiltration rate, and to predict the change of soil moisture content from initial to saturated state.

Mechanism of rainfall-saturated soil is based on assumption that: (i) rainfall intensity is constant; (ii) overland flow occurs after constant infiltration rate is reached; (iii) interception and evapotranspiration are neglected.

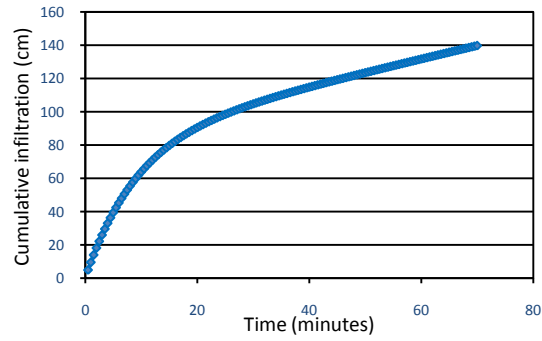
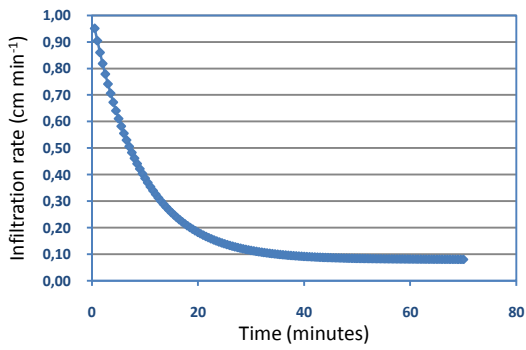
Cumulative infiltration model is defined using Equation (6) based on actual infiltration rate. The model is used to predict soil thickness affected by rainfall infiltration and to determine time interval needed to saturate the soil. Recapitulation of infiltration rate and cumulative infiltration model is presented in Table 4 below. Examples of infiltration rate and cumulative infiltration model of different land use is presented in Figure 37.

Table 4: Recapitulation Infiltration and Cumulative Infiltration Model in the Study Area

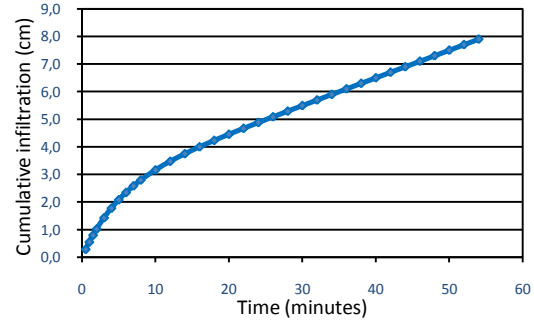
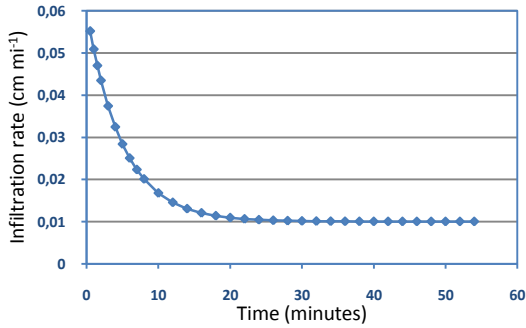
No	Location	Landuse	Eq. of Infiltration Rate (cm/min)	Equation of Cumulative Infiltration (cm/min)	f_0 (cm/min)	f_c (cm/min)	t_{fc} (min)	F_{max} (cm)
1	Penerusan	Mix Garden	$f = 0.150 + 1.250e^{-1.02t}$	$F = 0.150t + 1.230(1 - e^{-1.02t})$	1.400	0.150	26.0	9.33
2	Penerusan	Pine Forest	$f = 0.085 + 0.315e^{-0.14t}$	$F = 0.085t + 2.250(1 - e^{-0.14t})$	0.400	0.085	54.4	82.42
3	Penerusan	Rainfed Ricefield	$f = 0.035 + 0.345e^{-0.51t}$	$F = 0.035t + 0.676(1 - e^{-0.51t})$	0.380	0.035	17.0	17.61
4	Penerusan	Settlement	$f = 0.055 + 0.245e^{-0.25t}$	$F = 0.055t + 0.980(1 - e^{-0.25t})$	0.300	0.055	44.0	43.90
5	Penerusan	Shifting Cultivation	$f = 0.160 + 0.740e^{-0.36t}$	$F = 0.160t + 2.056(1 - e^{-0.36t})$	0.900	0.160	33.5	78.96
6	Tirip	Rainfed Ricefield	$f = 0.025 + 0.075e^{-0.51t}$	$F = 0.025t + 0.147(1 - e^{-0.51t})$	0.100	0.025	20.0	7.97
7	Besuki	Mix Garden	$f = 0.100 + 0.340e^{-0.13t}$	$F = 0.100t + 2.615(1 - e^{-0.13t})$	0.440	0.100	50.0	84.14
8	Besuki	Pine Forest	$f = 0.200 + 0.360e^{-0.81t}$	$F = 0.200t + 0.444(1 - e^{-0.81t})$	0.560	0.200	14.0	54.44
9	Besuki	Settlement	$f = 0.010 + 0.050e^{-0.20t}$	$F = 0.010t + 0.250(1 - e^{-0.20t})$	0.060	0.010	48.0	7.90
10	Gumelar	Settlement	$f = 0.100 + 0.900e^{-0.20t}$	$F = 0.100t + 4.500(1 - e^{-0.20t})$	1.000	0.100	38.0	8.90
11	Gumelar	Rainfed Ricefield	$f = 0.170 + 0.710e^{-0.12t}$	$F = 0.170t + 5.917(1 - e^{-0.12t})$	0.880	0.170	61.5	172.20
12	Kauman	Mix Garden	$f = 0.240 + 0.260e^{-0.36t}$	$F = 0.240t + 0.722(1 - e^{-0.36t})$	0.500	0.240	27.5	78.02
13	Kalialang	Settlement	$f = 0.025 + 0.155e^{-0.14t}$	$F = 0.025t + 1.107(1 - e^{-0.14t})$	0.180	0.025	50.0	25.57
14	Kalibawang	Mix Garden	$f = 0.100 + 0.900e^{-0.29t}$	$F = 0.100t + 3.100(1 - e^{-0.29t})$	1.000	0.100	19.0	5.60
15	Cledok	Settlement	$f = 0.020 + 0.040e^{-0.70t}$	$F = 0.020t + 0.057(1 - e^{-0.70t})$	0.060	0.020	9.0	5.97
16	Medono	Mix Garden	$f = 0.050 + 0.050e^{-1.02t}$	$F = 0.050t + 0.049(1 - e^{-1.02t})$	0.100	0.050	10.0	12.99
17	Medono	Rainfed Ricefield	$f = 0.025 + 0.175e^{-0.20t}$	$F = 0.025t + 0.875(1 - e^{-0.20t})$	0.200	0.025	38.0	27.75
18	Ngadisono	Settlement	$f = 0.025 + 0.055e^{-0.20t}$	$F = 0.025t + 0.275(1 - e^{-0.20t})$	0.080	0.025	25.0	15.00
19	Gambaran	Pine Forest	$f = 0.070 + 0.310e^{-0.15t}$	$F = 0.070t + 2.061(1 - e^{-0.15t})$	0.380	0.070	43.0	62.66
20	Tanjung Anom	Mix Garden	$f = 0.080 + 0.920e^{-0.11t}$	$F = 0.080t + 8.364(1 - e^{-0.11t})$	1.000	0.080	58.5	139.60
21	Kaliwiro	Mix Garden	$f = 0.080 + 0.820e^{-0.14t}$	$F = 0.080t + 5.857(1 - e^{-0.14t})$	0.900	0.080	41.5	93.65

Source: Field data analysis, 2009.

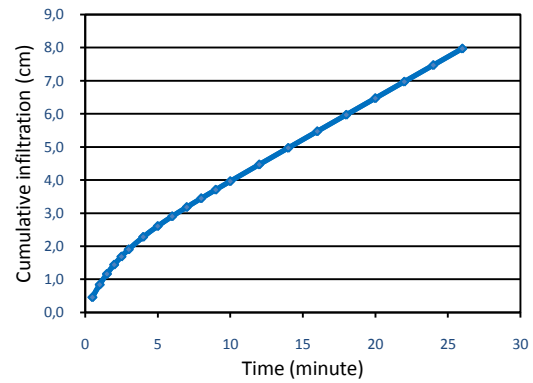
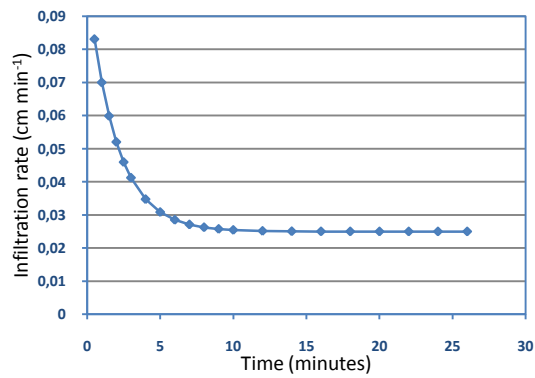
f_0 : initial infiltration rate, f_c : constant infiltration rate; t_{fc} : time interval to reach f_c ; F_{max} : maximum cumulative infiltration.



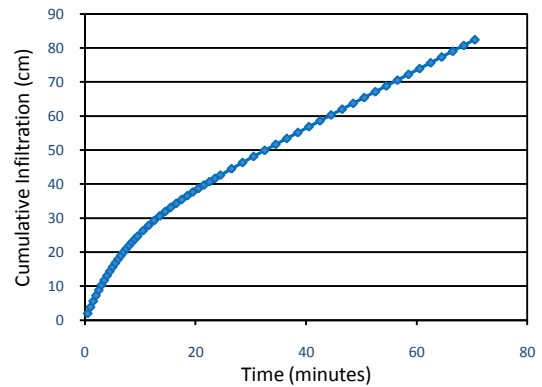
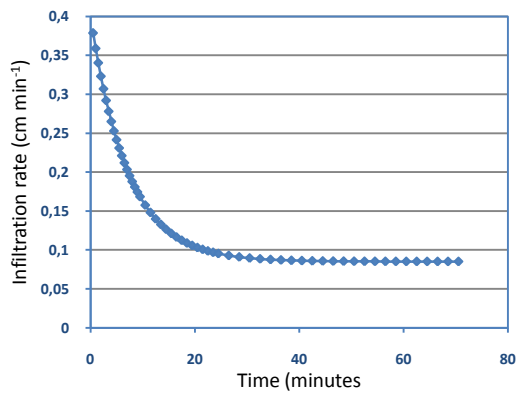
Mix Garden (20)



Settlement (9)



Rainfed Ricefield (6)



Pine Forest (2)

Figure 37: Predicted Infiltration Rate (left side) and Cumulative Infiltration Model (right side) Curves for Various Land Uses in the study area. Number in bracket is the order number of the land use in the Table 4.

The equation of infiltration rate of mix garden shown in Figure 37 above is $f = 0.080 + 0.920e^{-0.11t}$, with $f(t)$ in cm minute^{-1} and t in minute. Based on the equation, infiltration rate's curve is made (upper left most in Figure 37). The curve shows that the maximum infiltration rate is $0.10 \text{ cm minute}^{-1}$ at $t=0$, and the rate decreases sharply until constant rate is reached at $t=61$ minute with constant infiltration rate as $f_c=0.08 \text{ cm minute}^{-1}$. Infiltration rate decline significantly occurring in $t=0$ to $t=20$, and after the $t=20$ the infiltration rate decreases insignificantly until the saturated condition reached, figured by smaller curve gradient compared with previous condition.

Referring to the equation of the infiltration rate, the amount of cumulative infiltrated rainfall can be determined by means of equation of cumulative infiltration illustrating depth of water infiltrated into the soil. Formula of cumulative infiltration model resulted is $F=0.080t+8.364(1-e^{-0.11t})$ and used to build the curve as presented in Figure 37 above (upper right most curve). From the cumulative infiltration curve, it shows that from $t=0$ to $t=20$ minute, the depth of the cumulative infiltrated water is 90.37 cm which increases sharply indicated by wider curve gradient and after the $t=20$ minute, increment of cumulative infiltrated water is slower as soil approaches saturated. At $t=70$ minute, soil reaches saturated condition with cumulative infiltrated water depth equal to 139.60 cm , so that soil thickness affected by cumulative infiltrated rainfall until the saturated condition is as deep as 139.60 cm from the ground surface.

In settlement area, infiltration rate is governed by equation $f=0.010+0.050e^{-0.20t}$. Based on this equation, infiltration rate curve is plotted as presented in Figure 37 (the second left side curve from the top). The curve explains that at $t=0$, maximum infiltration rate of $0.055 \text{ cm minute}^{-1}$ is reached, and the infiltration rate decline rapidly until $t=10$ minute at a rate of $0.016 \text{ cm minute}^{-1}$. Once the $t=10$, infiltration rate recede very slowly as it close to saturated condition. The constant infiltration rate accomplished at $t=54$ with $f_c=0.01 \text{ cm minute}^{-1}$.

Derived from the equation of infiltration rate above, equation of cumulative infiltrated rainfall for the settlement is defined as $F= 0.010t+0.250(1-e^{-0.20t})$ and used to build the curve as shown in figure above. The curve illustrates that at $t=0$, total amount of cumulative infiltrated rainfall is 0.29 cm increasing rapidly until $t=10$ with total amount of 3.16 cm . Following rate increases very slowly as the soil near to saturated condition. When reached saturated condition at $t=54$ minute, depth of cumulative infiltrated rainfall is 8.15 cm meaning that total soil thickness affected by rainfall during infiltration process is 8.15 cm from the surface.

Infiltration rate in rain-fed ricefield is ruled by equation of $f=0.025+0.075e^{-0.51t}$, which is used to draw curve of infiltration rate in this land use. As provided in Figure 37 above (the third left side curve from top), the curve shows that at $t=0$, infiltration rate reaches maximum value equal to $0.083 \text{ cm minute}^{-1}$ and drop sharply to a rate of $0.026 \text{ cm minute}^{-1}$ at $t=8$ minute, as indicated by the wide gradient in the curve. The rate then decreases very slowly until reached saturated condition with f_t of 0.025 at $t=26$ minute.

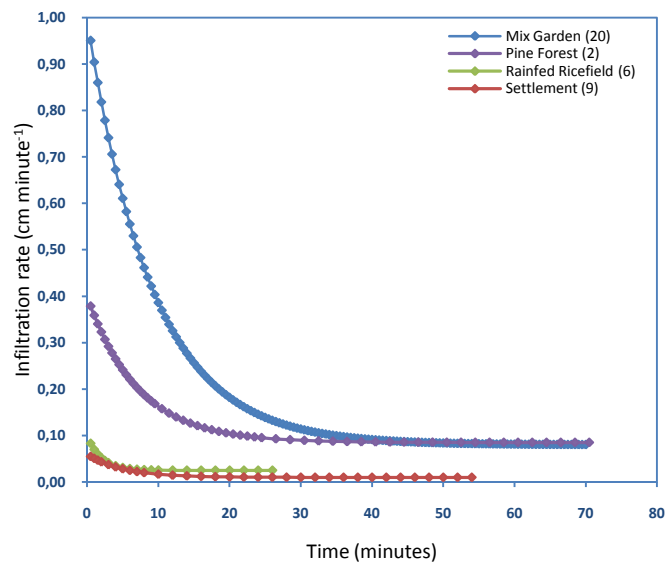
Regarding the equation of infiltration rate above, an equation for cumulative infiltrated rainfall is obtained as $F=0.025t+0.147(1-e^{-0.51t})$. Based on this equation, a curve is built illustrating the relationship of cumulative infiltrated rainfall and time (the third right side curve from the top in Figure 37). The curve shows that the cumulative infiltrated rainfall accumulates rapidly in period of 5 minutes; initially with 0.46 cm at $t=0$ to 2.61 cm at $t=5$ minute. The following accumulation climbs steadily until reaches saturated condition at $t=26$ minute with total cumulative infiltrated rainfall of 7.97 cm . This indicates that the depth of soil influenced by infiltrated rainfall at saturated condition is 7.97 cm below surface.

The left lower most curve in Figure 37 is infiltration rate curve for Pine forest in the study area. The curve drawn based on infiltration rate equation as $f=0.085+0.315e^{-0.14t}$. The curve informs that there is significant fall of infiltration rate in period of 21.5 minutes, from $0.379 \text{ cm minute}^{-1}$ at $t=0$ to $0.101 \text{ cm minute}^{-1}$ at $t=21.5$ minute. The following period shows steady decrease indicated by small curve gradient until it reaches saturated condition at a rate of $0.085 \text{ cm minute}^{-1}$ and $t=71.5$ minute.

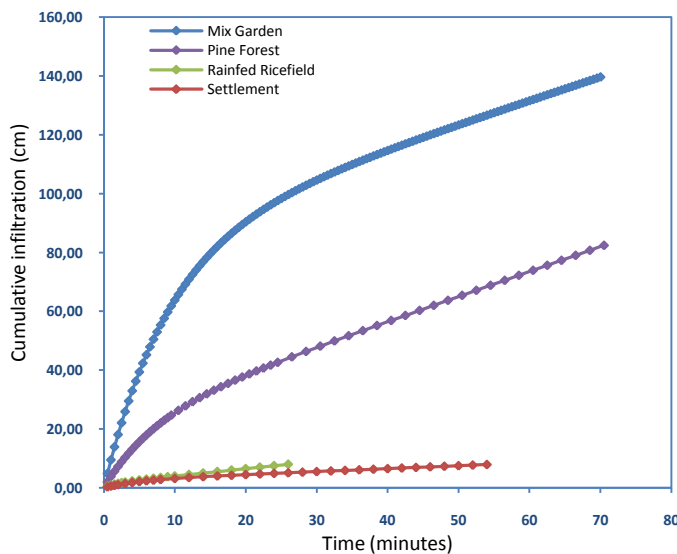
Equation for cumulative infiltrated rainfall model is gotten from the latter equation and defined as $F=0.085t+2.250(1-e^{-0.14t})$. From this equation a curve for cumulative infiltrated rainfall in the Pine forest is built as shown in Figure 37 above (lower left most curve). The curve shows that initial accumulated rainfall is 1.95 cm , then increase sharply until $t=7.5$ minute with total cumulated amount equal to 21 cm . The cumulative infiltrated rainfall climb steadily afterward until reaches saturated condition at $t=70.5$ with depth of water infiltrated 82.42 cm . This means that soil thickness influenced by infiltrated rainfall during infiltration period until saturated condition is 82.42 cm from surface.

To summarize the difference of infiltration rate and cumulative infiltration model among the various landuse types, figure below portrays their rates. The left graph is the infiltration rate and the right graph is the cumulative infiltration model. From the figure, it clearly describes that mix garden has the highest infiltration rate and cumulative infiltration, followed by pine forest, rainfed ricefield, and settlement respectively. The predicted infiltration rate and cumulative infiltration shows that the shortest time to reach

saturated condition is held by rainfed ricefield, then followed by settlement, pine forest, and mix garden consecutively.



Infiltration rate



Cumulative infiltration model

Figure 38: Comparisons of infiltration rate and cumulative infiltration model among the various landuse types.

As presented in Table 4 above, the equations of infiltration rate and cumulative infiltration model involve various k values ranging from 0.11 to 1.02. The values were determined by Equation (5), evaluated experimentally (Lal *et al.*, 2004) through several substitutions into equation of infiltration rate, and chosen which gives the best fit between actual infiltration and predicted infiltration curves. Example evaluations of k values for different land use types shown by Figure 39 below. The r^2 value obtained by comparing

actual and predicted infiltration rate curves in a graph (not presented here), illustrating their correlation.

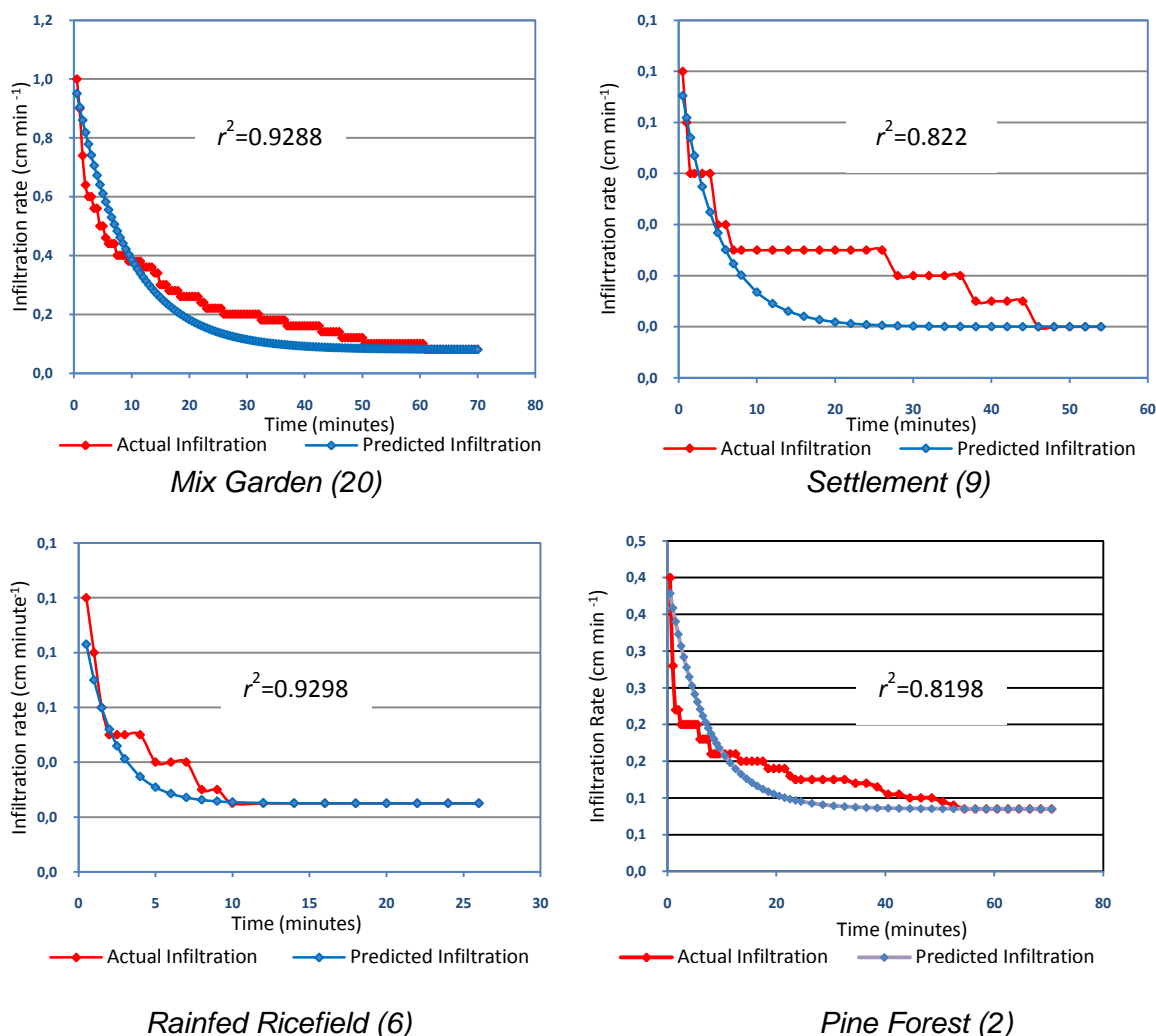
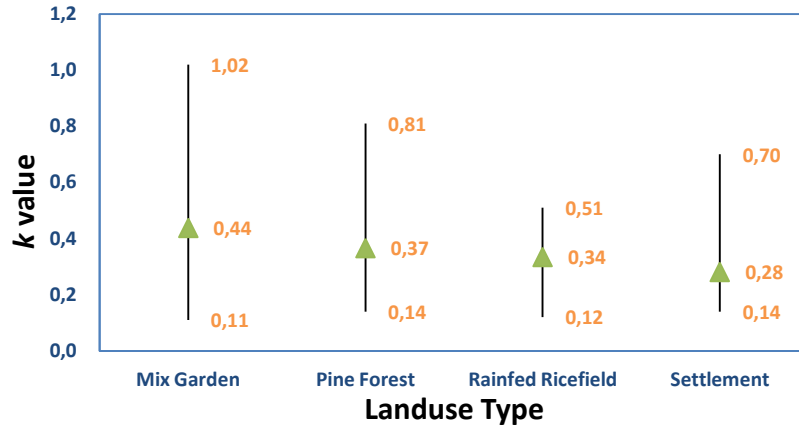


Figure 39: Comparisons of Actual Infiltration Rate and Predicted Infiltration Rate Curves for Various Land Uses in the study area. Number in bracket is the order number of the land use in the Table 4.

To compare the variation of infiltration rate in various land use types, k values involved in this analysis is grouped according to land use type to see the variation in one land use type and to differentiate the variation between land use types. The same treatment also has been done for different land form in the study area.

The k value reflects how quickly the soil pores are filled up, and thus it illustrates rate at which f_0 approaches f_c (Lal *et al.*, 2004), the smaller the value, the shorter the time needed to fill the pores up. Figure below presents variation of k values based on land use type and land form type. The graph gives three values ranging from the highest, mean (assigned by green triangle node), and the lowest value consecutively.

k value based on land use type



k value based on land form unit

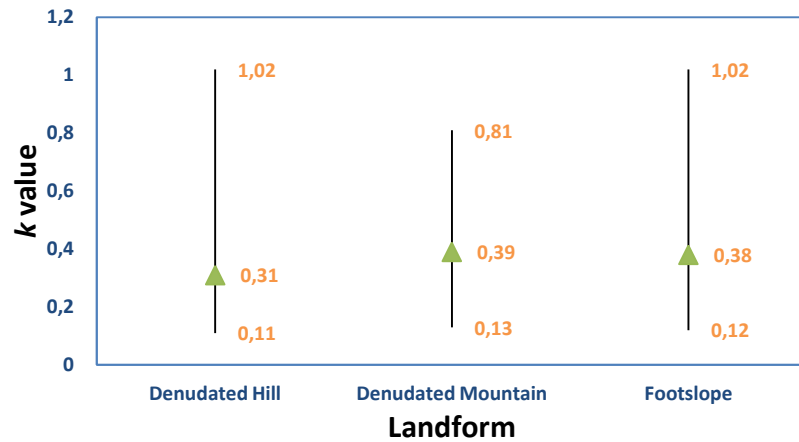


Figure 40: Variation of k values based on land use type and landform unit

As presented in Figure 40 above, range of k value for different land use type varies. The greatest variability is given by mix garden ranging from 0.11 to 1.02; meanwhile the smallest variability is held by rainfed ricefield ranging from 0.12 to 0.51. To summarize the variability between landuse types, it can be assessed based on mean of k value. Of the four main landuse types in the study area, mix garden holds the highest value, followed by pine forest, rainfed ricefield, and settlement consecutively. It means that settlement reaches saturated condition in a shortest duration, meanwhile mix garden saturated longer compared with the three landuse types.

According to Anonymous (2009d), there is a number of factors influencing soil infiltration: texture, crust, compaction, aggregation and structure, water content, frozen surface, organic matter, and pores. Moreover, Tofani *et al* (2006), state that variation distributions of infiltrated rainfall as pore water pressures within the soil are highly variable depending on the hydraulic conductivity, topography, degree of weathering, and fracturing of the soil. In case of differences of k value above, settlement records the lowest average

k value due to compaction as an impact of human activities in this area. Variation of k value in settlement area is probably due to settlement characteristics in which the infiltration test was done: pure settlement (densely populated), gives the lowest value; and clustered settlement (settlement surrounded by landuse types such as mix garden), gives the highest value. For the rainfed ricefield, this landuse type shows lesser variation among the others. The k value for this landuse is influenced by prolonged utilization this area. Ploughing is the main method used for land preparation in growing season. This method influences soil thickness as deep as 30 cm, below this depth; soil is undisturbed creating a compacted zone (plowpan) (Anonymous, 2009d) which restricts water to seep into the deeper zone.

Among the four landuse types, mix garden performs the highest average k value meaning that it needs longer period to achieve saturated condition. The existence of Sengon (*Albazia falcataria*) tree as the main crop considered affecting this condition. Sengon is integrated in *Mimosacea* botanical family which has nodules in their rooting system as result of symbiosis process with *Rhizobium* bacterium. These nodules are very helpful in altering soil porosity and improving soil aeration system that increases soil fertility (Anonymous, 2009a). Besides, during field observation I found that the area consists of very loose material which makes it difficult to take soil sample using ring soil sample. Variation of k value among this landuse type influenced by low-lying crops combined with the Sengon; short-term crops such as cassava gives higher value than long-term crops such as coffee and banana.

Although naturally forest supposed to give higher value, the forest in the study area holds lower value than of mix garden. This also is affected by compaction on soil surface in the area due to pine resin tapping (bark incision method). Almost all the trees in the area were incised to extract their resin and track networks for collecting the harvested resin found throughout the area. PT Perhutani, a state-owned forestry company, managed and applied this forest management type in the area, especially in Java since 1980s for conservatory purpose.

Based on landform unit, denudated hill gives the lowest average value; meanwhile the rest two landforms have almost similar value. The lowest average value of denudated hill is probably caused by its position in the low-lying area resulting in relatively high soil moisture content. The value variability within the landform is resulted from variety of landuse types. The same condition is performed by landform of foot slope which has higher average value. The value variability within the landform is assumed due to landuse differences combined with variability in topography (Tofani *et al.*, 2006). On the other

hand, the denudated mountain landform tends to have small difference in k value due to uniformly topography on which the landform is located.

Infiltration plays a key role in slope instability, hence lead to slope failure (Casagli *et al.*, 2006; Rahardjo *et al.*, 2008). Infiltration of rainfall will reduce the shear strength due to loss of matric suction, generation of positive water pressure as well as increase in unit weight (Tsao *et al.*, 2005; Jeong *et al.*, 2008; Dahal *et al.*, 2009; Damiano *et al.*, 2009; Újvári *et al.*, 2009). Based on constant infiltration rates, presented in Table 4 above, the infiltration rates in the study area are categorized in range of low to medium rate (Anonymous, 2009e). According to Dahal *et al.* (2009), the lower the rate, the more prone the slope to landslide.

5.6.2. Model of Rainfall-Saturated Soil

Model of process of soil saturation due to rainfall is developed based on initial soil moisture and soil moisture content at constant infiltration rate. In this research, initial moisture is measured in laboratory on undisturbed soil samples taken from field; meanwhile the maximum soil moisture content is estimated based on soil texture from Soil Water Characteristics software version 6.02.74 provided by USDA Agricultural Research Service in cooperation with Department of Biological Systems Engineering Washington State University. Assumptions to develop the mechanism of soil saturation are: (i) at the constant infiltration rate the maximum soil moisture content is reached, and thus soil moisture content would not increase more, (ii) the rise of soil moisture content and the infiltration rate are identical but in inverse curve model.

Table 5: Recapitulation of soil moisture content equation and the developed relationship of soil moisture content - infiltration rate.

No.	Location	Landuse	Soil Moisture Equation	θ_0 (%)	θ_s (%)	t_{bs} (min)	Soil moisture content - infiltration rate relationship	
							Equation	r^2
1	Penerusan	Mix Garden	$\theta = 47.0-35.95e^{-1.02t}$	11.50	47.0	6.0	$f = -0.0348\theta + 1.7842$	1
2	Penerusan	Pine Forest	$\theta = 52.1-39.79e^{-0.14t}$	12.31	52.1	48.5	$f = -0.0079\theta + 0.4975$	1
3	Penerusan	Rainfed Ricefield	$\theta = 50.2-38.12e^{-0.51t}$	12.08	50.2	14.0	$f = -0.0091\theta + 0.4893$	1
4	Penerusan	Settlement	$\theta = 47.3-35.93e^{-0.25t}$	11.37	47.3	28.0	$f = -0.0068\theta + 0.3775$	1
5	Penerusan	Shifting Cultivation	$\theta = 48.6-35.47e^{-0.36t}$	13.13	48.6	18.5	$f = -0.0209\theta + 1.1739$	1
6	Tirip	Rainfed Ricefield	$\theta = 47.0-31.62e^{-0.51t}$	15.38	47.0	9.0	$f = -0.0024\theta + 0.1365$	1
7	Besuki	Mix Garden	$\theta = 47.0-29.13e^{-0.13t}$	17.87	47.0	44.0	$f = -0.0117\theta + 0.6486$	1
8	Besuki	Pine Forest	$\theta = 45.4-26.29e^{-0.81t}$	19.11	45.4	8.0	$f = -0.0137\theta + 0.8217$	1
9	Besuki	Settlement	$\theta = 55.5-37.66e^{-0.20t}$	17.84	55.5	34.0	$f = -0.0013\theta + 0.0837$	1
10	Gumelar	Settlement	$\theta = 56.1-41.00e^{-0.20t}$	15.10	56.1	36.0	$f = -0.0220\theta + 1.3315$	1
11	Gumelar	Rainfed Ricefield	$\theta = 48.7-33.89e^{-0.12t}$	14.81	48.7	54.5	$f = -0.0210\theta + 1.1903$	1
12	Kauman	Mix Garden	$\theta = 59.2-50.11e^{-0.36t}$	9.09	59.2	19.0	$f = -0.0052\theta + 0.5472$	1
13	Kalialang	Settlement	$\theta = 47.4-38.17e^{-0.14t}$	9.23	47.4	48.0	$f = -0.0041\theta + 0.2175$	1
14	Kalibawang	Mix Garden	$\theta = 46.7-37.14e^{-0.29t}$	9.56	46.7	19.0	$f = -0.0242\theta + 1.2317$	1
15	Cledok	Settlement	$\theta = 49.5-41.26e^{-0.70t}$	8.24	49.5	9.0	$f = -0.0010\theta + 0.0680$	1
16	Medono	Mix Garden	$\theta = 58.4-49.77e^{-1.02t}$	8.63	58.4	10.0	$f = -0.0010\theta + 0.1087$	1
17	Medono	Rainfed Ricefield	$\theta = 59.3-51.77e^{-0.20t}$	7.53	59.3	38.0	$f = -0.0034\theta + 0.2255$	1
18	Ngadisono	Settlement	$\theta = 47.0-33.96e^{-0.20t}$	13.04	47.0	25.0	$f = -0.0016\theta + 0.1011$	1
19	Gambaran	Pine Forest	$\theta = 56.4-50.31e^{-0.15t}$	6.09	56.4	46.0	$f = -0.0062\theta + 0.4175$	1
20	Tanjung Anom	Mix Garden	$\theta = 58.0-49.76e^{-0.11t}$	8.24	58.0	56.5	$f = -0.0185\theta + 1.1523$	1
21	Kaliwiro	Mix Garden	$\theta = 55.1-48.42e^{-0.14t}$	6.68	55.1	41.5	$f = -0.0169\theta + 1.0131$	1

Source: Data Analysis, 2009.

Table 5 above presents the recapitulation of soil moisture content equation, initial moisture (θ_0), maximum soil moisture content (saturated condition) (θ_s), time needed to reach saturated condition/ponding time ($t_{\theta s}$), and the relationship between soil moisture content and infiltration rate. The examples of Rainfall Saturated Soil Model curve of soil moisture change in respect to time for various landuse types in the study area are presented in Figure 41.

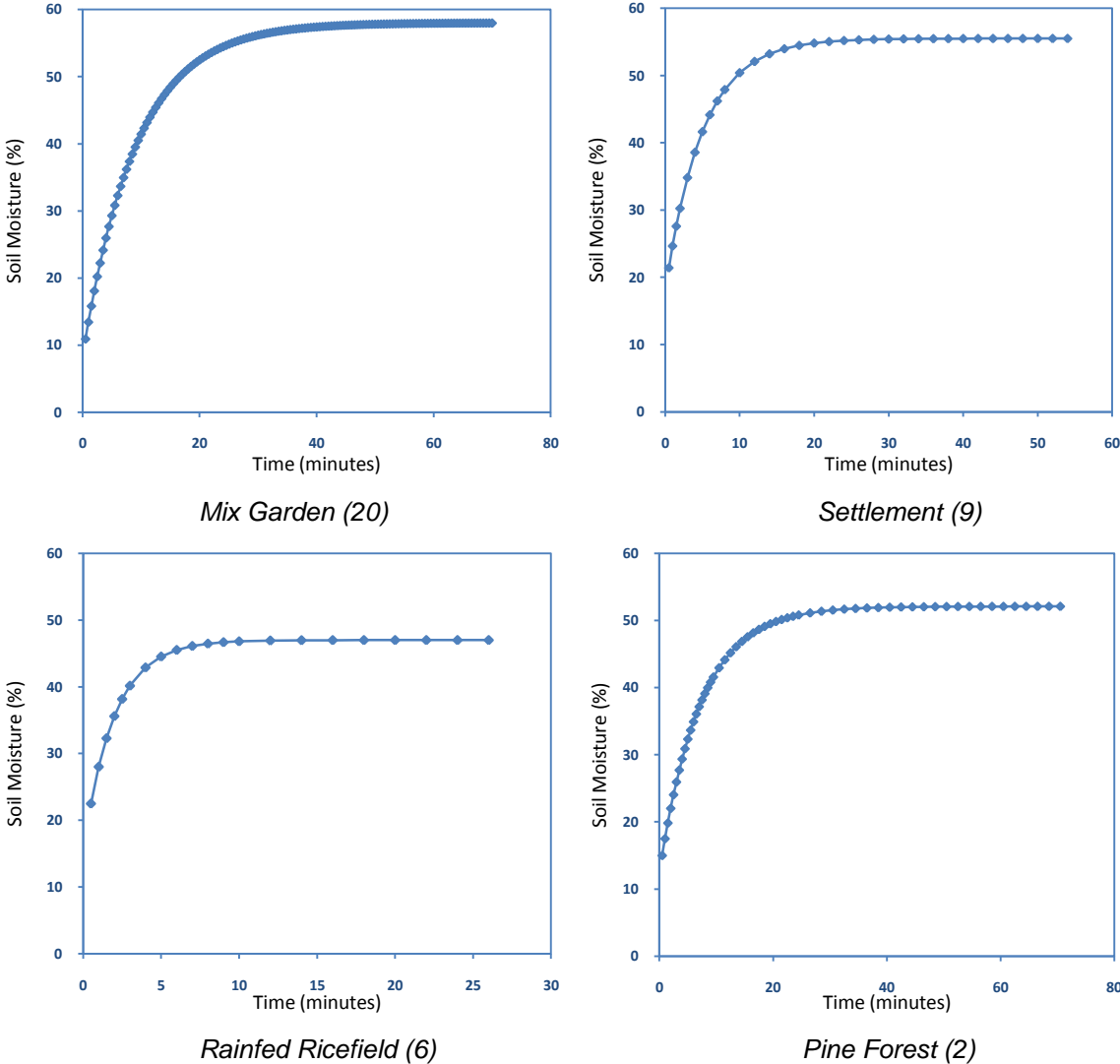


Figure 41: Curves of Soil Moisture Change in Respect to Time for Various Land Uses in the study area. Number in bracket is the order number of the land use in the Table 5.

Based on the figure above, equation of soil saturation for mix garden due to increase in soil moisture is ruled by $\theta = 58.0 - 49.76e^{-0.11t}$, with θ in percentage (%) and t in minutes. The model is arranged from infiltration measurement with initial soil moisture equal to 8.24% and maximum soil moisture (saturated condition) of 58.0%. Time interval needed to

reach the saturated condition, known as ponding time, is 56.5 minutes. Soil moisture change in this period is 49.76%, and at this time, soil moisture would not increase anymore assumed to be constant. Overland flow estimated occurs when approach 56.5 minutes under conditions of: rainfall intensity is equal or more than constant infiltration rate ($0.08 \text{ cm minute}^{-1}$ or 48 mm hour^{-1}) and cumulative rainfall as 1,396 mm.

Soil moisture change for settlement is governed by equation $\theta = 55.5 - 37.66e^{-0.20t}$, with θ in percentage (%) and t in minutes. Initial moisture before the infiltration measurement is 17.84 % and the moisture content at saturation state is 55.5% which reached in period of 34 minutes. During the period, there is a 37.66% increase in soil moisture, and regarded as the maximum soil moisture content. Afterward, rainfall will be either ponding or overland flow as long as the rainfall intensity is equal of more than constant infiltration rate ($0.01 \text{ cm minute}^{-1}$ or 6 mm hour^{-1}) and cumulative rainfall as 79 mm.

Mechanism of soil saturation in rainfed ricefield is determined by mathematical formula $\theta = 47.0 - 31.62e^{-0.51t}$. This equation is based on initial moisture content (15.38%) before infiltration measurement done and the maximum soil moisture content (47.0%) derived from Soil Water Characteristic software. The saturation process needs 9 minutes resulting soil moisture change as 31.62%. Water ponding or overland flow occurs after 9 minutes if the rainfall intensity is the same or more than constant infiltration rate ($0.025 \text{ cm minute}^{-1}$ or 15 mm hour^{-1}) and cumulative rainfall as 79.7 mm.

Saturation model in Pine forest as due to soil moisture rising is $\theta = 52.1 - 39.79e^{-0.14t}$. θ is in percentage and t in minute. The model is developed from infiltration measurement in which initial soil moisture content is 12.31% and the moisture content at saturated condition is 52.1%. This maximum moisture content is reached in 48.5 minutes performing soil moisture enhancement as 39.79%. Once the maximum moisture content is accomplished, soil moisture becomes constant and forces water ponding or overland flow at rainfall intensity is equal or more than $0.085 \text{ cm minute}^{-1}$ or 51 mm hour^{-1} (constant infiltration rate) and cumulative rainfall as 82.4 mm.

5.6.3. Model of Soil Moisture-Infiltration Rate Relationship

Model of correlation between soil moisture and infiltration rate is defined based on equations of infiltration rate measurement and soil moisture content. Their relationship models are developed for the 21 locations where soil moisture content (%) acts as affecting variable and infiltration rate (cm minute^{-1}) as affected variable. The model is used to estimate infiltration rate at various soil moisture content (predictor) ranging from initial moisture content (θ_o) to saturated soil moisture content (θ_s). The maximum soil moisture

content used as predictor is the soil moisture content at saturated condition (θ_s) assumed that at the saturated condition the soil moisture content would not increase anymore and thus the predicted infiltration rate is constant.

As presented in Table 5 in the two right-most columns, the correlation of soil moisture content and infiltration rate in all locations are very high ($r^2=1$). The correlation is negative meaning that the higher the soil moisture content, the slower the infiltration rate. Based on the coefficients of determination are equal to one meaning that all the equations have very high significance. All the equations are showing relationship between soil moisture content and infiltration rate to be linier.

5.6.4. Soil Texture

To obtain the soil texture in the whole study area, the soil samples were taken in the same locations in which soil infiltration test were performed. The soil samples were brought to laboratory to be analyzed. Based on laboratory analysis, soil texture in the study area ranges from clay to clay loam (Figure 42) showing similarity in the three landform types. Based on the figure below, the clay content of soil in the study area is relatively high (around 30 – 70%). The clay content determines the susceptibility of the soil to landslide. The higher the clay content, the more prone the soil to landslide (Picarelli *et al.*, 2006; Yalcin, 2007). When clay is saturated with water, it has very low strength parameter (Yalcin, 2007). Jeong *et al.* (2008), revealed that slope safety factor increases rapidly at clay content less than 10%, beyond that it follows with a more gradual increase or flattens as the clay content increases.

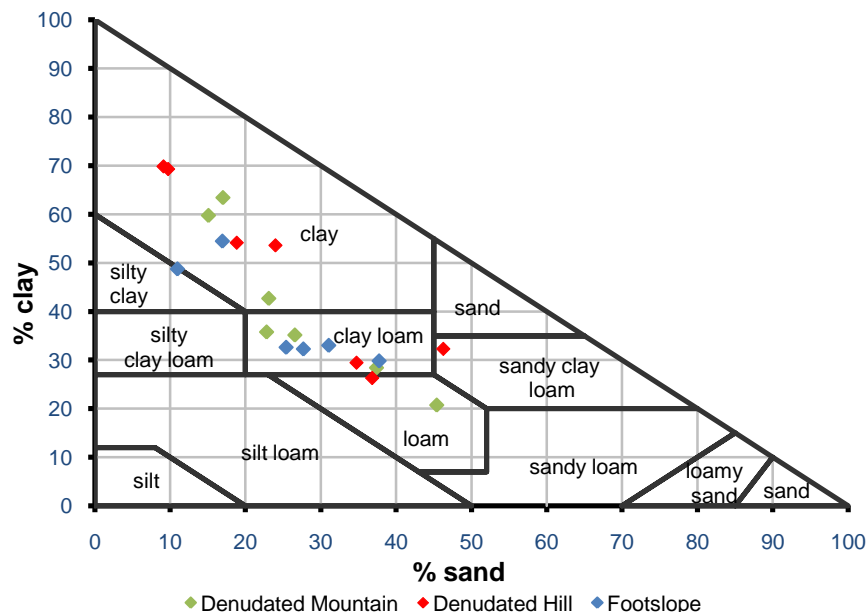


Figure 42: Soil Textures in the Study Area

5.6.5. Slope Stability Assessment

The advance in GIS application now days can readily modeling the slope stability analysis, as various intensive data can be easily integrated and manipulated in it. However, to obtain the precise model which simulates spatial and temporal of the slope failure likely to occur is highly data depending and time consuming. Besides, a part the area being studied is underdeveloped that instrumentation and regular data collection is difficult. A very little available data collection also hampers intensive modeling in the area. Therefore, an application of GIS incorporating a simple steady-state hydrological model and slope stability parameters is applied to assess the slope stability in the Wadasintang watershed.

5.6.5.1. Landslide Point Map

SINMAP requires landslide point map to evaluate condition where landsliding has occurred (Pack et al., 1998). As one of the main data input, accurate positioning of the initiation locations of known landslides is an essential element for a successful SINMAP calibration (Deb et al., 2009). Landslide point map used in this research is based on verified reported landslide locations done during the fieldwork. All the landslide locations mapped using hand-held GPS receiver and the geographic positions of the head scarp of the landslides are tallied as points in GIS. Figure 25 presents complete landslide inventory map in the study area.

Table 6: Classes of slope stability based on value of the Stability Index (*SI*).

Condition	Class	Predicted state	Parameter range	Possible influence of factors not modeled	Reclassified predicted state
$SI > 1.5$	1	Stable slope zone	Range cannot model instability	Significant destabilizing factor are required for instability	Safe area
$1.5 > SI > 1.25$	2	Moderately stable slope zone	Range cannot model instability	Moderate destabilizing factors are required for instability	Low-to-medium susceptibility
$1.25 > SI > 1.0$	3	Quasi-stable slope zone	Range cannot model instability	Minor destabilizing factors are required for instability	
$1.0 > SI > 0.5$	4	Lower threshold slope zone	Pessimistic half of range required for instability	Destabilizing factors are not required for instability	High susceptibility
$0.5 > SI > 0.0$	5	Upper threshold slope zone	Optimistic half of range required for instability	Stabilizing factors may be responsible for stability	Very high susceptibility
$0.0 > SI$	6	Defended Zone	Range cannot model instability	Stabilizing factors are required for stability	

Source: Deb et al. (2009)

5.6.5.2. Topographic Data

Topographic data of the study area is shown in Figure 16. In this SINMAP analysis, 10-m, 15-m, and 20-m DEMs of the study area are used alternately to observe DEM giving the best performance. The DEM derived from digital topographic map provided by

Bakosurtanal scale of 1:25,000 and contour interval of 12.5 m. Once the DEM added, SINMAP prompts to process the DEM as follows: fit-filling, slope, flow direction, and specific catchment area.

5.6.5.3. Slope Stability Index

The SINMAP model for the study area was run under the default parameter values of gravity (9.81 m s^{-2}), soil density ($2,000 \text{ kg m}^{-3}$), water density ($1,000 \text{ kg m}^{-3}$), T/R ratio ($2,000 - 3,000 \text{ m}$), cohesion ($0 - 0.25$), and soil friction angle ($30^{\circ} - 45^{\circ}$). A single calibration region was used to calibrate the model parameters, since there was no comprehensive soil mapping or geomorphology had been done in the area.

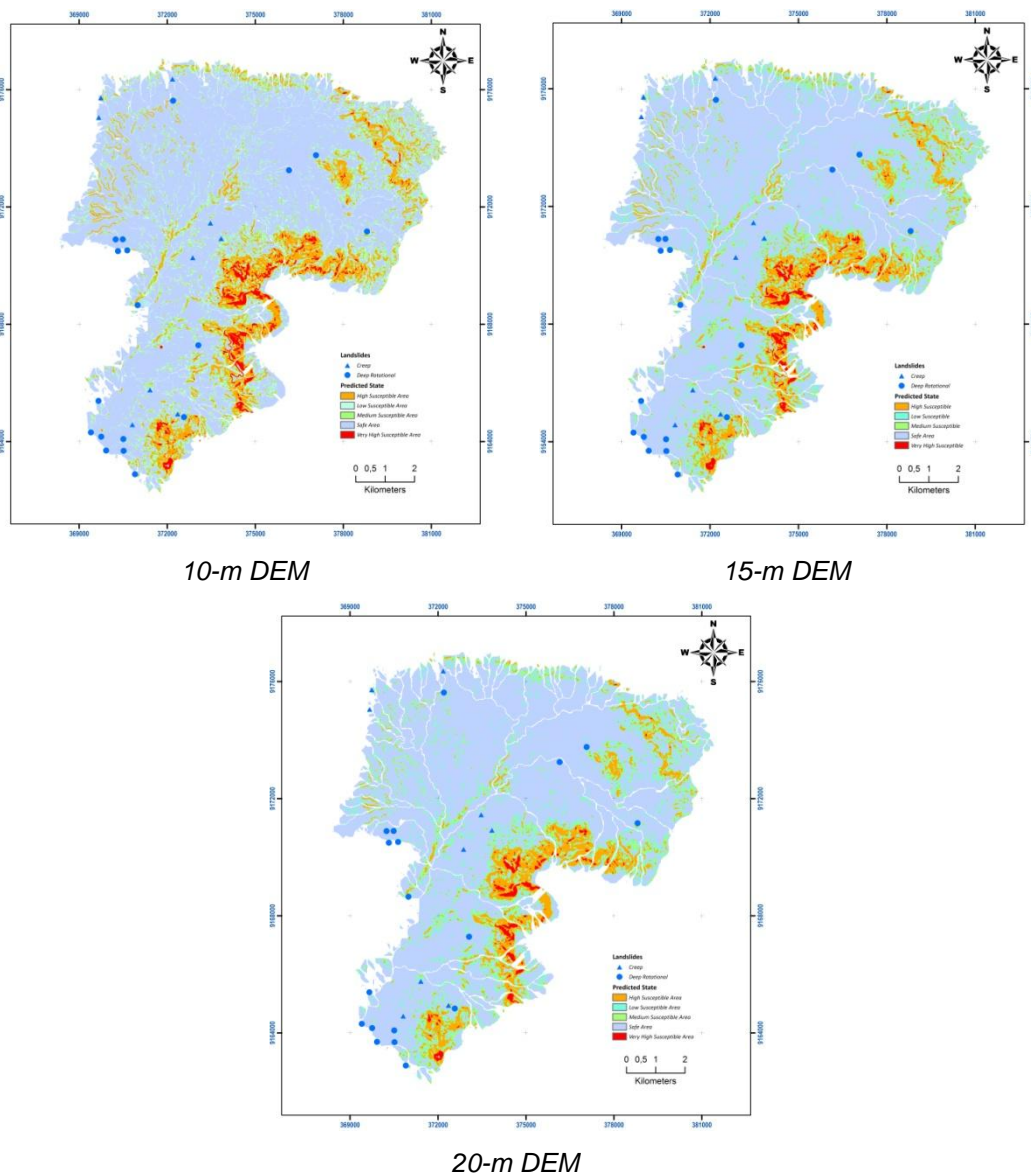


Figure 43: Comparison of SINMAP Modeling Results for Various DEM Resolutions

Result of stability index in terms of predicted state modeled by SINMAP presented in Figure 43 above. The three results based on DEM variety show similarity in predicting the spatial distribution of the regions stability. However, comparison of the result shows that the 10-m resolution DEM quantified best in modeling the stability of the watershed. The 10-m, 15-m, and 20-m DEM successfully predict stability 90.74, 88.80, and 87.19 percentages respectively of the total area. Based on the result, the 10-m DEM is used for subsequent analysis.

According to the model of 10-m DEM, 66.4% of the total area is classified as stable, whereas 19.4% of the area ranges from moderately to quasi stable. 12.3 % of the area has probability to fail less than 50%, and 1.6% of the area tends to fail with the probability more than 50%. The model also classifies 0.2% of the area as “defended” that the model cannot explain the causes of the failures if occur in this zone.

Interestingly, the model implies that all the landslides occurred in the stable slope zone (see Figure 45) with the density of 0.3 km⁻². This result validates the applicability and limitation of the SINMAP that the model only capable of predicting shallow translational landsliding and does not applicable for deep-seated instability including deep earthflows and slumps (Pack *et al.*, 1998). Apart from this result, unreported big landslide presented in Figure 24 (assumed to be debris flow) is calculated by the model to be in “upper threshold slope zone”. Although this model is impractical for the recorded landslide occurrences in the study area, it exposes the nature of slope stability that may be worse (unstable) if inappropriate or careless landuse practices applied in the study area, especially in the low-to medium susceptibility level (moderate to quasi stable). For areas lie in the high to very high susceptibility level, the certain landuse practices, such as settlement, mix garden, shifting cultivation and ricefield should be restricted in order to minimize the landslide risk to lowering the future damages and losses.

By implementing the level of susceptibility as proposed by Deb *et al.*, (2009) in Table 6, the model was combined with the landuse map to localize the susceptibility for the whole catchment. The result is presented in Table 7 below, showing the extent of each landuse in every state of susceptibility (Ha), the ratio of the classified landuse to the total landuse (% LU), and the ratio of the classified landuse to the total extent of the level of susceptibility (% State).

Table 7: Predicted State for Various Landuse in the Study Area

Predicted State Landuse	Very High Susceptibility			High Susceptibility			Low to Medium Susceptibility			Stable Area		
	Ha	% LU	% State	Ha	% LU	% State	Ha	% LU	% State	Ha	% LU	% State
Bush	65.48	6.26	34.39	280.27	26.81	22.17	244.22	23.36	12.51	455.48	43.57	6.66
Shifting Cultivation	47.45	3.58	24.92	294.31	22.23	23.28	396.44	29.94	20.31	585.77	44.24	8.56
Forest	59.22	8.78	31.10	211.07	31.29	16.70	193.18	28.64	9.90	211.12	31.30	3.09
Mix Garden	17.91	0.39	9.41	434.69	9.36	34.39	932.46	20.08	7.77	3,258.14	70.17	47.63
Ricefield	0.35	0.02	0.18	35.83	2.38	2.83	126.82	8.43	6.50	1,340.94	89.16	19.60
Settlement	0.00	0.00	0.00	7.81	0.74	0.62	58.85	5.58	3.01	988.77	93.68	14.46

Source: Data Analysis, 2009.

Based on the Table 7 above, the level of susceptibility is grouped into 2 groups: High to very high levels and other levels, to portray the degree of susceptibility of each landuse in the level according to ratio between classified landuse and total area of the landuse, and extent of each landuse and total area of the susceptibility level (see Figure 44 below). Figure 44 reveals that mix garden contributes the biggest area in the high to very high susceptibility region followed by bush and shifting cultivation, then by forest. The degree of contribution performed by these landuse types is influenced either by location or total extent of the landuse, or both. For instance, mix garden giving 31.12% to the total of the susceptibility area since the landuse occupies 44.04% of the whole catchment. Such contribution is more influenced by the total extent of the landuse as only around 10% of its total area located in this region. Meanwhile, contribution determined by location is shown by bush, shifting cultivation, and forest. Their contributions are almost similar (23.77%, 23.50%, and 18.58% respectively) although their total extents compared with total catchment area are less than 15%. The ratios of their area within this susceptibility region and their total area range from 25 to 40%. These imply that their areas are located relatively more within this susceptibility region than the other landuse types.

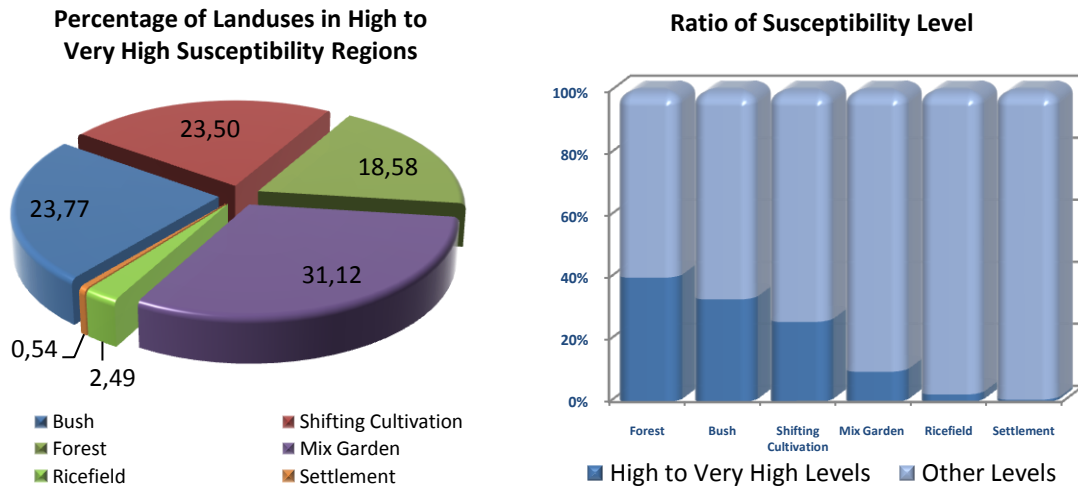


Figure 44: Contribution of landuse types in high to very high susceptibility regions and ration of susceptibility level for various landuse types.

The Figure 44 above also implies the landuse management applied in this area. Since the high to very high susceptibility region located on the steeper slope, the development conducted in this area has to appropriate or be adjusted with the local setting. As stated previously, forest area in this maintained for conservancy purposes due to the steep slopes. The trees would not be cut down and the grower/farmer can exploit the other products of the trees, such as resin, fallen branches for firewood, etc. Besides, the farmer can grow low-lying crops among the main crops (forest). Bush areas in this region situated in abandoned land including abandoned garden due to infertile soil. The areas also positioned on the steeper slopes with shallow soil thickness. Mix garden holding around 9% ratio of the susceptibility level and its total area. It can be inferred that this condition is controlled by several things: the area is dominated by forest and bush (around 47%) that hard or cannot be converted into the other landuse types; the selling process of the main product of the mix garden, logs of Sengon tree, that will be cut down at minimum age of 5 years, will be impeded by the steeper slopes in case of transporting the product.

The Figure 44 exhibits that ricefield and settlement give the smallest area both in percentage to the susceptibility region and the ratio between two groups of the susceptibility level. This suggests that the region is unsuitable for ricefield due to the limited water. In the dry season, the ricefield is used to grow seasonal crops, such as corn, watermelon, and beans/peanut. The small proportion of settlement in the area also influence by the location of the region on the remotely steeper slope. The people prefer to live near the street to facilitate them to transport and sell their crop yields. The

settlement located in the region is occupied by the farmers who tap the pine resin in the area and utilize the other landuse types in the area.

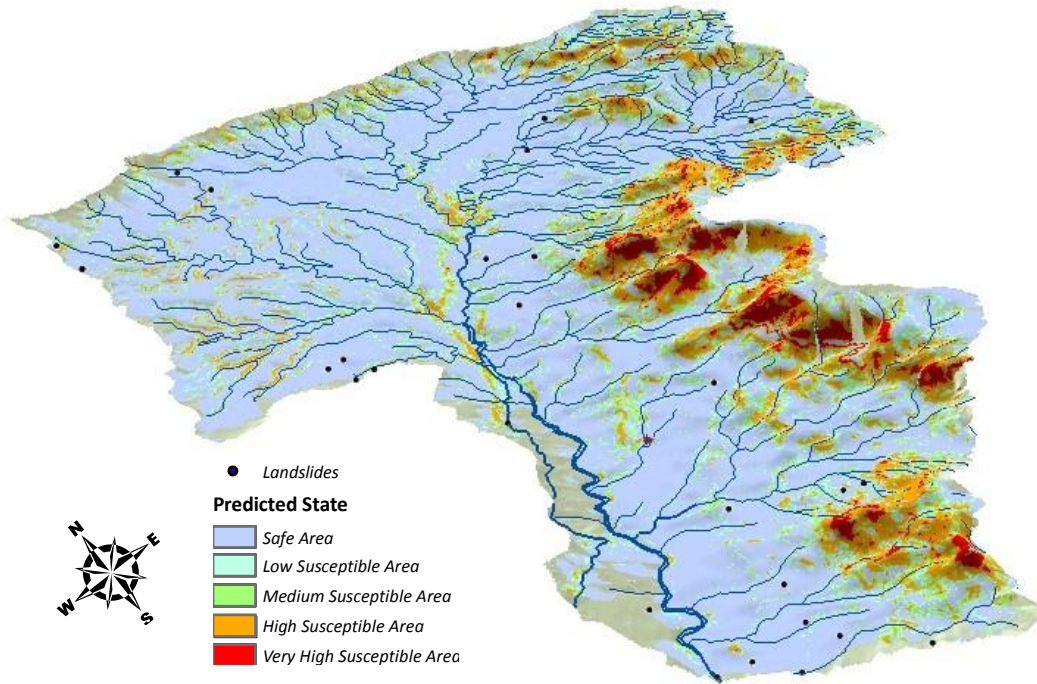


Figure 45: 3D View Plotting Distribution of Susceptibility Levels and Landslide Locations (not scaled)

Referring to Figure 44, it can be concluded that forest, bush, and shifting cultivation are the landuse practices that are more susceptible to landsliding. This based on quantitative assessment on both charts that the three landuses occupy 65% of the total area of high to very high susceptibility level, and then their areas located in this region range from 25% to 40% of their total areas.

6. CONCLUSIONS, LIMITATIONS, AND RECOMMENDATIONS

6.1. Conclusion

Conclusions of data analysis in this research are addressed to answer the research objectives and research questions. Conclusion for each research objective is presented below preceded by research objective in italic letter:

The main objective of this research is *to determine rainfall thresholds for landslide initiation in Wadas Lintang Watershed - Wonosobo, Central Java Province*. Based on threshold analysis, the relationship between rainfall intensity and duration for landsliding in the study area is defined by formula: $I=63.683D^{-0.336}$, where I is the rainfall intensity in mm day^{-1} , and D is the rainfall duration in days. According to this threshold relation for rainfall event with shorter duration such as less than 5 days, rainfall intensity of 37 mm day^{-1} is sufficient to trigger landslide, meanwhile an average precipitation of less than 20 mm day^{-1} seems necessary to cause landsliding if rainfall continued for more than 31 days.

The second objective is *to determine the influence of rainfall prior to the day of landslide occurrence*. The landslide occurrences in the study area are affected also by antecedent rainfall of 3 to 5 days before the day of failure. Analysis result shows that a moderate correlation exists between the antecedent of 3 to 5 days and the daily rainfall at the failure with correlation coefficient of $r^2=0.6282$, and 0.5484 respectively.

The third objective is *to determine the return period of excessive rainfall events which trigger landslides*. Recurrence of excessive rainfalls causing landsliding in this study area ranges from 1 to 2.42 years, based on computation using extreme value distribution type I. It implies that the excessive rainfalls causing landsliding occur every year in this area.

The fifth objective is *to study the terrain hydrological properties in the study area*. Terrain hydrological properties in this area include infiltration rate, soil moisture content, soil texture and slope stability index. Data analysis result shows that infiltration rate varies both among the landuse types and among landforms in the study area, and generally, the infiltration rate ranges from slow to medium rate which is more prone to landslide. The analysis outcome also illustrates that correlation between soil moisture content and infiltration rate is very high, thus the infiltration rate can be estimated based on soil moisture content. Soil texture analysis shows that clay content rounds at 30 – 70% implying that the soil is prone to landsliding. Slope stability of the study area as result of SINMAP model reveals that 66.4% of the area is classified as stable, 19.4% ranges from

moderately to quasi stable, 12.3% as lower threshold, 1.6% as upper threshold, and 0.2% is classified as defended slope.

The last objective is *to assess the land use types which are susceptible to landsliding*. The result of SINMAP model exposes the extent of susceptibility level in the study area. The model calculates that **forest, bush, and shifting cultivation** are the landuse practices that are more susceptible to landsliding. This is based on quantitative assessment on both charts that the three landuses occupy 65% of the total area of high to very high susceptibility level, and that their areas located in this region range from 25% to 40% of the total areas.

6.2. Research Limitations

There are several limitations in this research. The limitations are mainly related with data used. The limitations are as follows:

- a. This research involves limited use of landslide causative factors. Since rainfall is regarded as the main triggering factor for landslide in the study area, the other triggering factor, such as earthquake, was not taken into account.
- b. Landslide data used in this research was obtained from Badan Kesbanglinmaspol of Wonosobo District. The data might be different from the actual landslide occurrence in this area because no specific authority was mentioned responsible for recording landslide events in this area. Limitation in rainfall data also exists. The available rainfall data are only 24-hour data and no hourly data, thus the analysis was done under duration in days. The event-rainfall data on the day of failure were obtained from the nearest station.

6.3. Recommendations

Although the proposed values of rainfall-landslide thresholds in this study are based on limited data; this is the only available data that can be used as predictive tool for landslide early warning in this area, but need considerable care when they are actually used. The proposed values give first approximation for the area and still need validation through continuous observation of landslide occurrences in the area.

The result of SINMAP model cannot be validated due to data absence. Nevertheless, the result can be utilized as identification tool for hazardous and safe zones in this study area. The SINMAP prediction may be further improved by conducting extensive study of soil properties for its parameter inputs.

REFERENCES

- Aleotti, P., 2004. *A warning system for rainfall-induced shallow failures*. Engineering Geology **73** (3-4): 247-265.
- Anonymous, 2008. *Wonosobo Profile*. Wonosobo Government. Retrieved 15 May, 2009, from www.wonosobokab.go.id.
- Anonymous, 2009a. *Budidaya Sengon* Retrieved 14th November, 2009, from www.lablink.or.id
- Anonymous, 2009b. *Data Bencana Alam Kabupaten Wonosobo Tahun 2001 - 2009*. Badan Kesbanglinmaspol Kabupaten Wonosobo Provinsi Jawa Tengah.
- Anonymous, 2009c. *Kompas*. Retrieved 16th May, 2009, from www.kompas.com.
- Anonymous, 2009d. *Soil Quality Indicators: Infiltration*. Soil Quality Information Sheet. USDA Natural Resources Conservation Service. Retrieved 15th November, 2009, from <http://soils.usda.gov>.
- Anonymous, 2009e. *Texas Agricultural Experiment Station*. Texas Precise Agriculture. Retrieved 11th November, 2009, from http://txprecag.tamu.edu/warez/HMUA_Guide.pdf.
- Aspinall, R. J. and Hill, M. J., (Eds.), 2008. *Land Use Change Science, Policy and Management*. New York, CRC Press, Taylor & Francis Group, 232p. ISBN-13: 978-1-4200-4296-2
- BNPB, 2009. *Indonesian Disaster Data and Information*. Badan Penanggulangan Bencana Nasional (National Disaster Management Agency) Retrieved 21th May, 2009. <http://dibi.bnpb.go.id/>
- Bryant, E., 2005. *Natural Hazards: Second Edition*. Cambridge University Press, The Edinburgh Building, Cambridge, UK. ISBN: 978-0-511-08022-7
- Casagli, N., Dapporto, S., Ibsen, M. L., Tofani, V. and Vannocci, P., 2006. *Analysis of The Landslide Triggering Mechanism During The Storm of 20th–21st November 2000, in Northern Tuscany*. Landslides **3** (Springer-Verlag): 13-21. DOI: 10.1007/s10346-005-0007-y
- Chleborad, A. F., 2003. *Preliminary Evaluation of a Precipitation Threshold for Anticipating the Occurrence of Landslides in the Seattle, Washington, Area*. USGS Open-File Report 03-463. USGS. 12
- Corominas, J. and Moya, J., 1999. *Reconstructing recent landslide activity in relation to rainfall in the Lobregat River basin, Eastern Pyrenees, Spain*. Geomorphology **30** (1-2): 79-93.
- Crosta, G., 1998. *Regionalization of rainfall thresholds: an aid to landslide hazard evaluation*. Environmental Geology **35** (2-3): 131-145.
- Crozier, M. J., 1999. *Prediction of rainfall-triggered landslide: a test of antecedent water status model*. Earth surface processes and landforms **24**: 825-833.
- Cruden, D. M., 1991. *A Simple Definition of a Landslide*. Bulletin International Association of Engineering Geology **43**: 27-29
- Daag, A. S., 2003. *Modelling the Erosion of Pyroclastic Flow Deposits and the Occurrences of Lahars at Mt. Pinatubo, Philippines*. Ph.D Dissertation. ITC, Enschede, The Netherlands
- Dahal, R. K. and Hasegawa, S., 2008. *Representative Rainfall Thresholds for Landslide in the Nepal Himalaya*. Geomorphology **100**: 429-443. 10.1016/j.geomorph.2008.01.014
- Dahal, R. K., Hasegawa, S., Yamanaka, M., Dhakal, S., Bhandary, N. P. and Yatabe, R., 2009. *Comparative Analysis of Contributing Parameters for Rainfall-triggered Landslides in the Lesser Himalaya of Nepal*. Environmental Geology **58** (Springer-Verlag): 567-586. DOI: 10.1007/s00254-008-1531-6
- Dai, F. C., Lee, C. F. and Ngai, Y. Y., 2002. *Landslide risk assessment and management: an overview*. Engineering Geology **64** (1): 65-87.
- Damiano, E. and Olivares, L., 2009. *The Role of Infiltration Processes in Steep Slope Stability of Pyroclastic Granular Soils: Laboratory and Numerical Investigation*. Natural Hazards (Springer Science). DOI: 10.1007/s11069-009-9374-3
- Deb, S. K. and El-Kadi, A. I., 2009. *Susceptibility Assessment of Shallow Landslides on Oahu, Hawaii, under Extreme-rainfall Events*. Geomorphology **108** (Elsevier): 219-233. DOI:10.1016/j.geomorph.2009.01.009

- Glade, T., Anderson, M. and Crozier, M., (Eds.), 2005. *Landslide Hazard and Risk*. West Sussex, England., John Wiley & Sons Ltd., ISBN 0-471-48663-9
- Glade, T., Crozier, M. and Smith, P., 2000. *Applying Probability Determination to Refine Landslide-triggering Rainfall Thresholds Using an Empirical "Antecedent Daily Rainfall Model"*. *Pure and Applied Geophysics* **157** (Birkhauser Verlag, Basel): 1059–1079. DOI: 0033–4553:00:081059–21
- Guzzetti, F., Peruccacci, S., Rossi, M. and Stark, C. P., 2007. *Rainfall thresholds for the initiation of landslides in central and southern Europe*. *Meteorology and Atmospheric Physics* **98** (3-4): 239-267. 10.1007/s00703-007-0262-7
- Hack, R., 2000. *Geophysics for slope stability*. *Surveys in Geophysics* **21**: 423-448.
- Hasnawir and Kubota, T., 2008. *Analysis of Critical Value of Rainfall to Induce Landslides and Debris-Flow in Mt. Bawakaraeng Caldera, South Sulawesi, Indonesia*. *Journal of the Faculty of Agriculture Kyushu University* **53** (2): 523-527.
- Highland, L. M. and Bobrowsky, P., 2008. *The Landslide Handbook - A Guide to Understand Landslide*. US Geological Survey Circular 1325, Reston, Virginia. 129p.
- Jeong, S., Kim, J. and Lee, K., 2008. *Effect of Clay Content on Well-graded Sands due to Infiltration*. *Engineering Geology* **102** (Elsevier): 74-81. DOI:10.1016/j.enggeo.2008.08.002
- Karsli, F., Atasoy, M., Yalcin, A., Reis, S., Demir, O. and Gokceoglu, C., 2008. *Effects of Land-use Changes on Landslides in a Landslide-prone Area (Ardesen, Rize, NE Turkey)*. *Environmental Monitoring and Assessment* (Springer Science). DOI: 10.1007/s10661-008-0481-5
- Kotz, S. and Nadarajah, S., 2000. *Extreme Value Distributions : Theory and Applications*. Imperial College Press, London. ISBN: 00-039667
- Kuthari, S., 2007. *Establishing Rainfall Thresholds for Landslide Initiation along with Slope Characterisation Using GIS-based Modeling*. M.Sc. Thesis. ITC Enschede - IIRS India,
- Lal, R. and Shukla, M. K., 2004. *Principles of Soil Physics*. Marcel Dekker, Inc. New York - Basel ISBN: 0-203-02123-1
- Marfai, M. A., King, L., Singh, L. P., Mardiatno, D., Sartohadi, J., Hadmoko, D. S. and Dewi, A., 2008. *Natural hazards in Central Java Province, Indonesia: an overview*. *Environmental Geology* (Springer-Verlag). DOI: 10.1007/s00254-007-1169-9
- Pack, R. T., Tarboton, D. G. and Goodwin, C. N., 1998. *SINMAP: A Stability Index Approach to Terrain Stability Hazard Mapping. User's Manual*.
- Pack, R. T., Tarboton, D. G. and Goodwin, C. N., 2001. *Assessing Terrain Stability in a GIS using SINMAP*. The 15th Annual GIS Conference: GIS 2001. 19-22 February, 2001. Vancouver, British Columbia.
- Picarelli, L., Urciuoli, G., Mandolini, A. and Ramondini, M., 2006. *Softening and Instability of Natural Slopes in Highly Fissured Plastic Clay Shales*. *Natural Hazards and Earth System Sciences* **6** (European Geosciences Union): 529-539.
- Rahardjo, H., Leong, E. C. and Rezaur, R. B., 2008. *Effect of Antecedent Rainfall on Pore-water Pressure Distribution Characteristics in Residual Soil Slopes under Tropical Rainfall*. *Hydrological Processes* **22** (Wiley InterScience): 506-523. DOI: 10.1002/hyp.6880
- Sengupta, A., Gupta, S. and Anbarasu, K., 2009. *Rainfall thresholds for the initiation of landslide at Lanta Khola in north Sikkim, India*. *Natural Hazards and Earth System Sciences* (Springer). DOI: 10.1007/s11069-009-9352-9
- Smith, K. and Petley, D. N., 2008. *Environmental Hazards: Assessing Risk and Reducing Disaster, Fifth Edition*. Routledge, London, 414p. ISBN 0-203-88480-9
- Subyani, A. M., 2009. *Hydrologic Behavior and Flood Probability for Selected Arid Basins in Makkah area, Western Saudi Arabia*. *Arab J Geosci* (Springer). DOI: 10.1007/s12517-009-0098-1
- Terlien, M. T. J., 1998. *The determination of statistical and deterministic hydrological landslide-triggering thresholds*. *Environmental Geology* **35** (2-3): 124-130.

- Tofani, V., Dapporto, S., Vannocci, P. and Casagli, N., 2006. *Infiltration, Seepage and Slope Instability Mechanisms during the 20–21 November 2000 Rainstorm in Tuscany, Central Italy*. *Natural Hazards and Earth System Sciences* **6** (European Geosciences Union): 1025-1033.
- Tsao, T. M., Wang, M. K., Chen, M. C., Takeuchi, Y., Matsuura, S. and Ochiai, H., 2005. *A Case Study of The Pore Water Pressure Fluctuation on The Slip Surface Using Horizontal Borehole Works on Drainage Well*. *Engineering Geology* **78** (Science Direct): 105-118. DOI:10.1016/j.enggeo.2004.11.002
- Újvári, G., Mentés, G., Bányai, L., Kraft, J., Gyimóthy, A. and Kovács, J., 2009. *Evolution of a Bank Failure Along the River Danube at Dunaszekcső, Hungary*. *Geomorphology* **109** (ScienceDirect): 197-209. DOI:10.1016/j.geomorph.2009.03.002
- Van Asch, T. W. J. and Van Beek, J. B., L.P.H. , 1999. *A View on Some Hydrological Triggering Systems in Landslides*. *Geomorphology* **30** (Elsevier Science): 25-32.
- Van Westen, C., Kerle, N., Damen, M., Alkema, D., Lubszynska, M., Kingma, N., Parodi, G., Rusmini, M., Woldai, T., McCall, M. and Montoya, L., 2009. *Multi-hazard Risk Assessment: Guide Book*, Enschede, The Netherlands. United Nations University - ITC School on Disaster Geo-information Management (UNU-ITC DGIM). Unpublished Work. www.itc.nl
- Wanielista, M., Kersten, R. and Eaglin, R., 1997. *Hydrology: Water Quantity and Quality Control, 2nd Edition*. John Wiley & Sons, Inc., New York.
- Wilson, E. M., 1969. *Engineering Hydrology*. Mac Millan & Co Ltd, London, UK.
- Yalcin, A., 2007. *The Effects of Clay on Landslides: A Case Study*. *Applied Clay Science* **38** (Science Direct): 77-85. DOI:10.1016/j.clay.2007.01.007
- Zêzere, J. L., Trigo, R. M., Fragoso, M., Oliveira, S. C. and Garcia, R. A. C., 2008. *Rainfall-triggered Landslides in the Lisbon region over 2006 and Relationships with the North Atlantic Oscillation*. *Natural Hazards and Earth System Sciences* **8**: 483-499.

Appendixes

Appendix 1: Landslide Documentation



Deep Seated Rotational Slide.
(Dotted line shows the head of the scarp)



Creep.
(Dotted line shows the house's original foundation level)



Creep.
(Note the window blades do not fit to their frames anymore)



Creep.
(Dotted line shows the house's original foundation position)



Creep.
(Arrow shows the movement direction)



Deep Seated Rotational Slide.
(Dotted line shows the head of the scarp)

Appendix 2: Soil Texture Data



UNIVERSITAS GADJAH MADA
FAKULTAS PERTANIAN
JURUSAN ILMU TANAH

Bulaksumur, Yogyakarta, 55581 Telp. 0274-548414

Hasil Analisis Tanah Order Sdr. Emba Tampang Allo
Sebanyak 21 Contoh

Kode	Kadar Lengas %	Tekstur %			
	2 mm	Lp	Db	Ps	Kelas
1	19,46	32,64	41,93	25,42	Geluh Lempungan
2	26,32	42,69	34,20	23,11	Lempung
3	30,27	35,79	41,39	22,81	Geluh Lempungan
4	18,87	29,84	32,39	37,77	Geluh Lempungan
5	28,95	33,04	35,88	31,08	Geluh Lempungan
6	24,52	49,01	40,11	10,88	Lempung
7	72,09	28,44	34,16	37,40	Geluh Lempungan
8	52,43	20,77	33,84	45,39	Geluh
9	24,01	48,77	40,24	10,99	Lempung
10	22,66	54,49	28,55	16,96	Lempung
11	19,74	32,30	39,99	27,71	Geluh Lempungan
12	28,46	69,31	20,94	9,76	Lempung Berat
13	23,79	29,49	35,75	34,76	Geluh Lempungan
14	35,90	26,33	36,83	36,84	Geluh
15	23,52	35,17	38,26	26,57	Geluh Lempungan
16	24,20	59,74	25,15	15,11	Lempung Berat
17	28,10	69,85	21,01	9,15	Lempung Berat
18	34,29	32,33	21,39	46,28	Geluh Lempungan Pasiran
19	27,58	54,16	26,98	18,86	Lempung
20	27,65	63,41	19,56	17,03	Lempung Berat
21	27,90	53,62	22,38	24,00	Lempung

Mengetahui,
Ketua Jurusan Ilmu Tanah,

ttd

Dr. Ir. Abdul Syukur, SU.

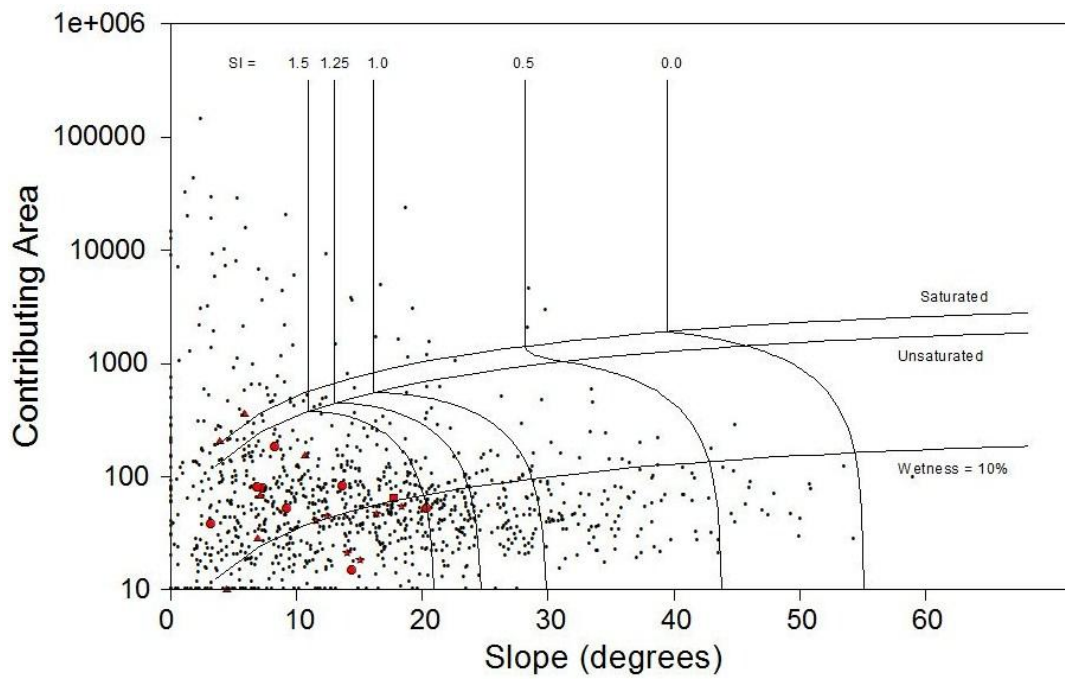
Yogyakarta, 1 Oktober 2009
Ketua Komisi Pengabdian Masyarakat,

ttd

Dr. Ir. Benito H. Purwanto, M.Sc.

Appendix 3: SINMAP Result

Statistical Summary for Dem							
	Stable	Moderately Stable	Quasi-Stable	Lower Threshold	Upper Threshold	Defended	Total
Region 1							
Area (km ²)	68.1	9.8	10.2	12.6	1.7	0.2	102.6
% of Region	66.4	9.5	9.9	12.3	1.6	0.2	100.0
#Landslides	22	0	0	0	0	0	22
% of Slides	100.0	0.0	0.0	0.0	0.0	0.0	100.0
LS Density (#/km ²)	0.3	0.0	0.0	0.0	0.0	0.0	0.2



SINMAP Summary